Centro Internacional de Agricultura Tropical
Desde 1967 / Ciencia para cultivar el cambio

Project

Climate change vulnerability in the agricultural sector in Latin America and the Caribbean

Funded by
Inter-American Development Bank (IADB)

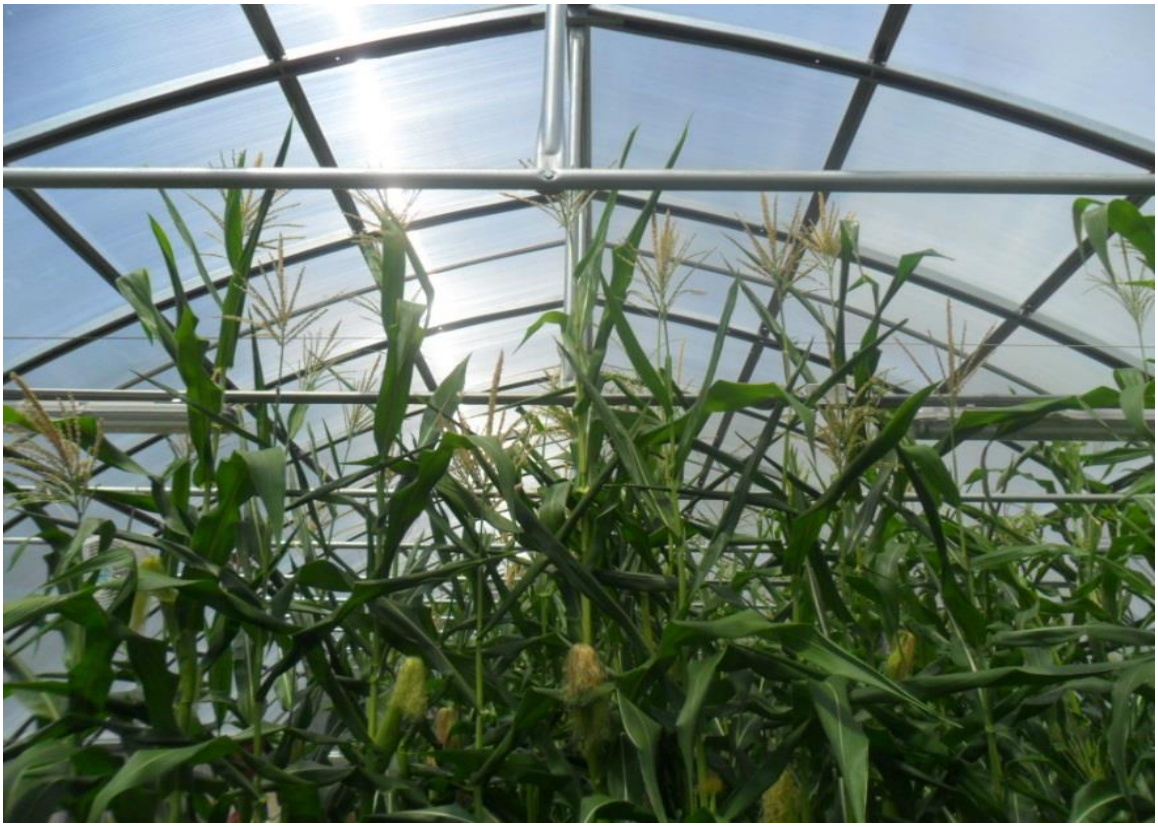

Final report:

Modeling of present-day and future agricultural yields for regionally important crops.

International Center for Tropical Agriculture (CIAT)

November 2015

Sharon Gourdji, Jeison Mesa, Patricia Moreno, Carlos Navarro, Diego Obando, Myles J. Fisher, and Julian Ramirez-Villegas

Contents

List of Tables

List of Figures

Appendix

1 Introduction

Agriculture plays an important role in the economy of Latin America and the Caribbean (LAC), accounting for approximately 5% of the region's gross domestic product (GDP) in 2012 (Vergara et al. 2014), and roughly 20% of the total employment (World Bank, 2014). In addition, Latin America is expected to help ensure global food security in the coming decades due to large tracts of arable land and ideal growing conditions in many areas (Alexandratos & Bruinsma, 2012; Zabel et al. 2014).

Therefore, the net impact of long-term progressive climate change on crop yields is a key area of concern for both farmers and policy-makers at the local, national, and regional level and this remains a highly active area of scientific research (see Porter et al. 2014). Process-based crop models can help to estimate the net effect of climate changes on crop yields, while niche-based models estimate changes in suitability under future climate conditions (Estes et al. 2013). Many modeling studies have been undertaken specifically to assess the potential impacts of climate change on crop production, many of which are included in the Intergovernmental Panel on Climate Change (IPCC) assessments (White et al. 2011; Magrin et al. 2014; Porter et al. 2014).

Climate change could impact crop production through many different mechanisms (see Hatfield et al. 2011, Lobell & Gourdji, 2012, and Porter et al. 2014 for reviews). Some of the most important of these are shorter crop durations (Eyshi et al., 2014), increased heat stress at flowering (Teixeira et al 2013; Lobell et al. 2013; Asseng et al. 2014), increased water stress due to less frequent and more intense precipitation and higher evapotranspiration (Alexander et al. 2006; Sheffield and Wood, 2008; Dai 2013; Cook et al. 2014), and the CO_2 fertilization effect (Ainsworth and Long 2005; Long et al. 2006; Leakey et al. 2009). Increased levels of atmospheric CO_2 affect crop production through two key mechanisms: first, an increase in photosynthesis rates for C_3 crops, but also an increase in water-use efficiency for both C_3 and C_4 crops because of reductions in stomatal conductance (Ainsworth and Long 2005; Markelz et al 2011; Leakey et al. 2009). Process-based models attempt to simulate the interacting effects of all of these processes (Asseng et al. 2014; Ruane et al. 2014; Ewert et al. 2002).

This study aims to contribute to a better understanding of the effects of near-term climate change (to the 2030's) on the productivity of key crops in the Latin American and Caribbean region through the use of both process-based and niche-based crop models. A two-tiered approach is used, taking advantage of state-of-the-art global and regional datasets and crop models and covering a wide range of crops, to produce regional-level projections of climate change impacts on agriculture in LAC. More specifically, yield impacts are estimated for a first group of crops (i.e. maize, rice, wheat, dry bean and soybean) using the Decision Support System for Technology Transfer (DSSAT) mechanistic crop model (Jones et al. 2003). For a second group of crops, namely banana, cassava, potato, coffee (robusta and arabica), sugarcane, and yam, the EcoCrop niche-based model (Ramirez-Villegas et al. 2013) is used to estimate crop suitability changes rather than yield. The net production values across Latin America and the Caribbean for these crops, along with other economically important crops, are shown in Figure 1.

Yield changes are estimated with the DSSAT model under current conditions and for the near-future under a 'no adaptation' scenario. The crop varieties and input use are kept at their historical values, although realistically these are known to change with technology and improved access to knowledge and inputs. Crop cultivation areas are also fixed at their current distribution for the DSSAT simulations,

although changing climatic suitability, crop profitability and ongoing deforestation are also likely changing the distribution of cultivated areas over the course of a half-century. Therefore, the simulated yield changes presented here can be taken as a worst-case scenario, or what would happen in the absence of any technological and management changes or shifts in crop cultivation areas. This scenario allows identifying geographic disparities in relation to climate change impacts, and as such helps prioritizing adaptation efforts (Porter et al. 2014; Lobell 2014; Lobell et al. 2008).

The changes in crop yield and suitable area due to near-term climate change simulated for this study can hopefully help to guide agricultural decision-makers in the identification, design, and execution of adaptation measures to confront anticipated impacts and minimize risks for Latin American agricultural production in the decades to come (e.g. Zabel et al. 2014; Olmstead and Rhode 2011).

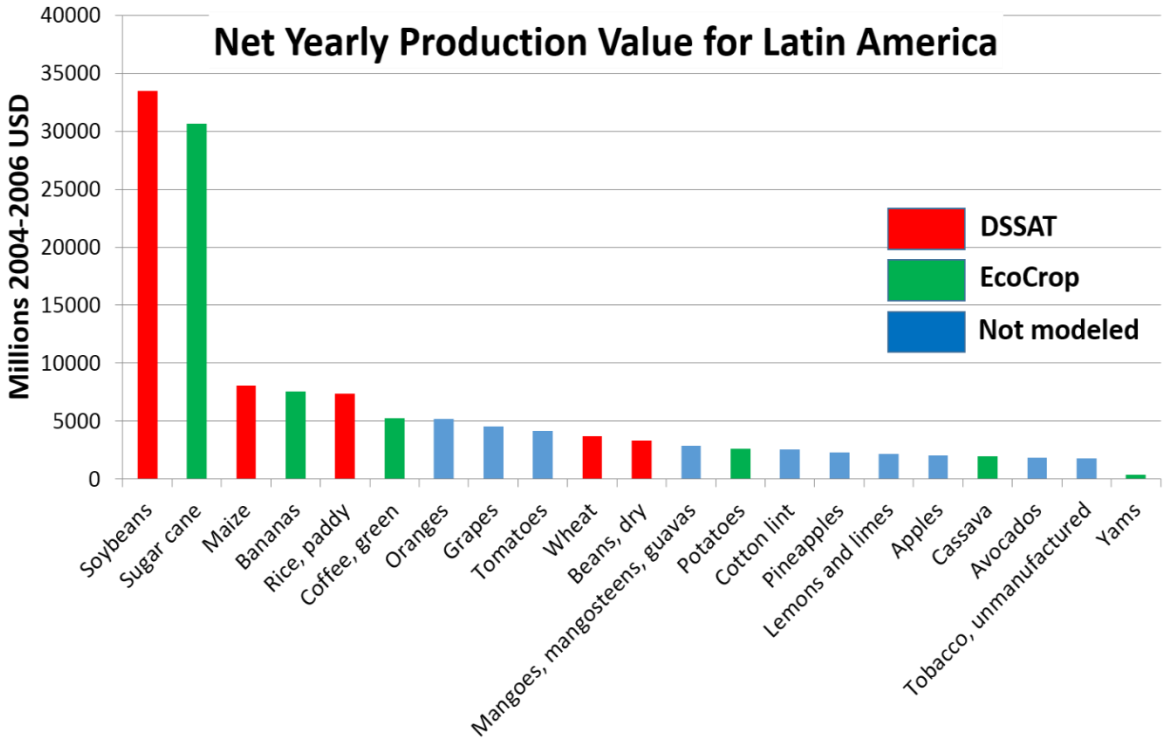

Figure 1. Net yearly production value for key crops in the Latin America and Caribbean region, averaged from 2009 to 2013. The 20 crops with the highest production value are shown in order, while also including yam (44th in production value). Bar colors indicate whether (red, green) or not (blue) the crop was modeled in this study, as well as the type of model used: DSSAT (red) and EcoCrop (green) (Source: FAOSTAT).

2 Methodology

This section describes the modelling strategy as a whole, starting with a general description of the crop models (Section 2.1), followed by a description of input datasets: climate (Section 2.2), DSSAT model inputs (Section 2.3), and EcoCrop parameters (Section 2.4). Finally, the section provides a description of the simulations conducted and the analysis strategy.

2.1 Description of crop models

As stated above, in this study, two types of crop models are used to evaluate the potential impacts of progressive climate change on crop production: 1) process-based mechanistic crop models that simulate crop development, water, nutrient and carbohydrate balances and final yields, and (2) niche-based models that assess climatic suitability for crop cultivation. The first type of model simulates the processes of plant growth and development, using daily weather data as well as additional environmental (e.g. soil) and management factors (e.g. fertilizer applications) in order to simulate daily crop growth dynamics and, ultimately, crop yields. The second type of model is less complex, and considers changes in monthly temperature and precipitation in order to determine crop suitability (see below and Section 2.4 for a definition), for a given location. Unfortunately, process-based crop simulation models are available for only a limited number of crops (e.g. 18 crops simulated in DSSAT v4.5; Hoogenboom et al., 2010) and are very data-intensive in terms of their inputs and parameterization (Stack & Kafatos, 2013; Iglesias et al., 2011; Rosenzweig et al. 2013). Therefore, in order to take advantage of state-of-the-art modeling tools and datasets, a process-based crop simulation model (DSSAT, or the Decision Support System for Agrotechnology Transfer) was run to simulate projected yield changes for five crops previously identified as having high priority for the region: soybeans, maize, rice, dry beans and wheat. For a second set of (6) crops, a process-based model did not exist, was not robust, or the necessary input data was not available. Therefore, the niche-based model EcoCrop was used in order to evaluate changes in suitable area for these other economically important crops.

The DSSAT suite of crop models has been under development for at least three decades, and has been used by crop modeling researchers worldwide in numerous climate change simulation studies (Jones et al., 2003). In fact, in a review of 221 climate change impact studies using crop models (White et al. 2011), roughly a third used the DSSAT sub-models CERES, CROPGRO, and SUBSTOR. These crop sub-models simulate in detail the daily development of a crop, from planting to harvest, integrating the effects of the biophysical elements of the crop system (for example, crop, soil, weather, and management options) to simulate yield outcomes. Crop growth is represented using production functions which are applied in each component of the cropping system, that is, canopy photosynthesis and light interception, carbon balance, water balance, vegetative and reproductive development, nitrogen balance, etc. The basic structure of the models, including the underlying differential equations, has been previously documented in several publications (Wilkerson et al. 1983; Boote et al. 1989; Jones et al. 2003; Hoogenboom et al. 2010; Lizaso et al. 2011).

Most climate change mechanisms that affect crop growth are currently incorporated in process-based crop simulation models such as DSSAT, albeit sometimes in a basic way, with the simulation of CO_2 effects remaining highly uncertain (White et al, 2011; Elliott et al. 2014a; Ainsworth et al. 2008). In addition, more work needs to be done to incorporate the effect of extreme heat at flowering, and

improve the energy balance and simulation of canopy temperatures (Jarvis et al. 2011; Rotter et al. 2011; White et al. 2011). Although research is ongoing to improve these mechanisms in crop models (especially in the Agricultural Model Inter-comparison and Improvement, i.e. AgMIP, community, www.agmip.org; Asseng et al. 2013a, 2014; Rosenzweig et al. 2013), the models are currently sufficient to give a general sense of the direction of crop yield changes and the mechanisms that can explain simulated changes (Rosenzweig et al. 2014; Elliott et al. 2014).

EcoCrop is a relatively simple yet robust crop niche prediction model aimed at simulating crop suitability. Suitability of a species is referred to as the degree to which the physiological and ecological requirements of a species are met at a site. In other words, suitability is a measure of whether a species can thrive at a given site. Suitability can also be interpreted as the probability of occurrence (Soberón and Nakamura, 2009; Wiens et al., 2009). Climatic suitability is thus used to refer to the solely climate component of suitability –since there may be soil and ecosystem components to it. EcoCrop is based on the Food and Agriculture Organization EcoCrop database (FAO, 2007; Ramirez-Villegas et al. 2013). The model was originally developed by CIAT with the support of Bioversity International and the International Potato Centre (CIP)[1]. The model exists in its original implementation in the software DIVA-GIS (Hijmans et al. 2005), as well as in more flexible implementations in the R software for statistical computing. The basic model uses ecological ranges of temperature and precipitation based on the literature, data-based calibration and expert advice, as inputs to determine the main environmental niche of a crop. The precipitation and temperature of each location are compared with the optimal and marginal ranges of the crop; if the location is within the optimal range, the suitability will be 100% but if not, climatic suitability is estimated through a series of rule-based non-linear equations (see Section 2.4). The model estimates suitability separately for temperature and precipitation, to then compute overall crop suitability as the interaction (i.e. product) of suitability temperature and precipitation suitability (for more details, see Ramirez-Villegas et al. 2013). The model has been used previously to study climate change impacts for beans (Beebe et al., 2011), cassava (Ceballos et al., 2011; Jarvis et al., 2012), potato (Schafleitner et al., 2011), sorghum (Ramirez-Villegas et al. 2013), maize (Challinor et al. 2015), banana and plantains (Ramirez et al., 2011), among others.

2.2 Climate data

The Watch Forcing Dataset (WFD, Weedon et al. 2011) was used to reconstruct historical weather conditions in growing areas across Latin America from 1971 to 2000. WFD is a global dataset of daily weather data derived via extensive calibration and bias correction of the European Center for Medium Range Weather Forecasts (ECMWF) 40+ year Reanalysis (ERA-40). The dataset is of comparable quality to others used in regional-scale crop and water resources modeling (Sheffield et al. 2006; Elliott et al., 2014b; Ruane et al., 2015). For a complete description and analysis of the dataset, the reader is referred to Weedon et al. (2011). Daily data at a resolution of 0.5 x 0.5º were downloaded from the WFD official website (https://gateway.ceh.ac.uk/home, accessed 15th June 2013).

For the future period from 2020 to 2049, daily general circulation model (GCM) outputs from nine models were gathered from the Climate Model Inter-Comparison Project 5 archive at

[1] Original description in the DIVA-GIS manual at: http://www.diva-gis.org/docs/DIVA-GIS_manual_7.pdf

https://pcmdi9.llnl.gov/esgf-web-fe/ (CMIP5, 2015; Taylor et al. 2012). Raw (i.e. uncorrected) climate model output was regridded to a 0.5º resolution and bias-corrected with the historical WFD dataset. A detailed description of this re-gridding and bias correction process is provided in the climate data section of the immediately previous report. The nine selected GCMs (Table 1), were selected as having the best performance for the region (Watterson et al. 2014), while including only one version per climate modeling institution. This strategy maximizes the coverage of the CMIP5 uncertainty envelope while reducing the computational burden of the gridded crop models (cf. Rosenzweig et al. 2014; Elliott et al. 2014b).

For the 30 years in the historical (WFD) and future periods (GCMs), daily maximum and minimum temperatures, solar radiation and precipitation were extracted for use in DSSAT. For EcoCrop, daily maximum and minimum temperatures and precipitation were aggregated to the monthly timescale for use in the analysis. In DSSAT, atmospheric CO_2 concentrations were fixed at 380 ppm for both the historical and future periods in order to disentangle the projected impacts of changes in climate variables from the more uncertain impacts of changes in CO_2 (cf. Lobell et al. 2015).

Table 1. List of GCMs used in the modeling simulations.

GCM name	Institute	Country
BCC-CSM1	Beijing Climate Center, China Meteorological Administration	China
BNU_ESM	Beijing Normal University	China
CCCMA_CANESM2	Canadian Centre for Climate Modelling and Analysis	Canada
GFLD_ESM2G	NOAA Geophysical Fluid Dynamics Laboratory	United States
INM-CM4	Russian Institute for Numerical Mathematics	Russia
IPSL-CM5A-LR	Institut Pierre Simon Laplace	France
MIROC-MIROC5	University of Tokyo, National Institute for Environmental Studies, and Japan Agency for Marine-Earth Science and Technology	Japan
MPI-ESM-MR	Max Planck Institute for Meteorology	Germany
NCC-NORESM1-M	Norwegian Climate Centre	Norway

2.3 DSSAT inputs

DSSAT is an input data-intensive crop model designed to simulate crop growth and development dynamics at the field scale. In addition to daily weather data, DSSAT simulations require detailed information on soils, crop variety, planting dates and rules, applications of fertilizers and irrigation, and other management-type information such as planting density and row spacing. In any given model simulation, all this input information is stored in or linked to other files from an experiment file (referred to in DSSAT jargon as the 'X-FILE'). Examples for the model runs performed here are shown in Figures A1 to A5 in the appendix. Given that DSSAT is run at a 0.5° spatial resolution for pixels across Latin America and the Caribbean, it is therefore required to have input databases at this same scale

in order to parameterize crop model runs for each pixel. These input databases are described in further detail in the following sections.

2.3.1 Soils data

The DSSAT model requires information on the water-holding characteristics of different soil layers. It needs a root weighting factor that accommodates the impact of several soil factors on root growth in different soil layers, such as soil pH, soil impedance, and salinity. Additional soil parameters are needed for computing surface runoff, evaporation from the soil surface, and drainage (Ritchie, 1998). Soil information was extracted for each pixel from the Harmonized World Soil Database (HWSD; FAO et al., 2012), processed into DSSAT format using the method of Hoogenboom et al. (2009). For about 10% of pixels with missing data from HWSD, we instead used generic soil profiles from Koo and Dimes (2013) (also referred to as HC27), where soil type is a simple combination of soil organic carbon content, soil rooting depth and major constituent (sand/ loam/ clay). HWSD can be freely downloaded at http://www.fao.org/soils-portal/soil-survey/soil-maps-and-databases/harmonized-world-soil-database-v12/en/, whereas the Koo and Dimes (2013) dataset can be found at http://harvestchoice.org/labs/hc27-genericprototypical-soil-profiles.

2.3.2 Crop presence and water management

In order to identify current cultivation areas for each crop, physical area estimates were used from the Spatial Production Allocation Model (SPAM) 2005 v2.0 database (You et al. 2014), freely available at http://mapspam.info. These data were aggregated from their native resolution of 5 arc-minutes to 0.5º for all crops used in the study. Because DSSAT was run in a separate mode for irrigated and rain-fed production, the SPAM database was also used to separately identify irrigated and rain-fed cultivation areas.

2.3.3 Planting windows and initial conditions

Approximate sowing dates for rain-fed and irrigated production were taken from the MIRCA 2000 dataset (i.e., the Monthly Irrigated and Rain-fed Crop Areas in year 2000, Portman et al. 2010), freely available at https://www.uni-frankfurt.de/45218023/MIRCA. The planting windows in the MIRCA2000 dataset were estimated by incorporating data from national agricultural census statistics and national reports, and global databases, like that from the Food & Agriculture Organization (FAO). The MIRCA2000 dataset is of comparable quality to other crop calendar datasets (e.g. Sacks et al. 2010; Waha et al. 2012, Elliott et al. 2014b) and has been used in recent crop modeling studies (Rosenzweig et al. 2014; Osborne et al. 2013).

For rain-fed simulations, the automatic planting option was used in DSSAT, whereby the model chooses the exact planting date within a specified window when the soil water reaches a specified threshold. Here, the window was set to start at the middle of the planting month from MIRCA2000 and continue for 6 weeks afterwards to maximize the probability of finding favorable conditions for sowing within the window. The threshold for sowing was set to 50% of total soil-available water. The simulation was started 15 days before the start of the window, with the soil water initialized at the permanent wilting point for each layer from the soils database. This allows two weeks for the soil water balance to be equilibrated before the planting window begins. Typically, farmers are able to

adjust their sowing dates with the arrival of the rains, but they have limited flexibility to shift dates due to other adjoining cropping seasons. Therefore, if the available soil water never reaches this threshold (50%) during the planting window, the model assumes that the crop season fails for that pixel and hence stops the simulation.

For irrigated simulations where sowing can take place whenever irrigation is applied, the planting date was specified as the middle of the planting month from MIRCA2000. The simulations were also started on the same day as sowing, with the soil water initialized at field capacity for each layer.

Since the soil N balance module was turned on in all simulations (cf. Webber et al. 2015), initial soil NH_4 and NH_3 concentrations had to be specified. Both NH_4 and NH_3 concentrations were initialized at the soil organic carbon (SOC) values for each layer from the soils database. In the absence of other spatially-distributed information for these parameters, SOC values represent a reasonable proxy for soil nitrogen concentrations (K. J. Boote and C. H. Porter, personal communication; Webber et al. 2015).

2.3.4 Fertilizer

Gridded nitrogen fertilizer application data were taken from a dataset developed by the Global Gridded Crop Model Inter-comparison (GGCMI; Elliott et al. 2014b), a joint initiative between the Agricultural Model Inter-comparison and Improvement Project (AgMIP) and the Inter-Sectorial Impacts Model Intercomparison Project (ISI-MIP). This dataset, which is freely available at http://esg.pik-potsdam.de and at https://www.rdcep.org/research-projects/ggcmi, contains a single yearly value (in kg ha^{-1} $year^{-1}$) per pixel and crop. The dataset was separated into values for irrigated and rain-fed systems by scaling the value according to the percent of irrigated and rain-fed area in each pixel, and assuming that nitrogen applications in irrigated systems are roughly double those in rain-fed systems. Then, high-input systems were defined for each crop using thresholds of seasonal nitrogen application defined from the literature and expert advice (Table 2). For high-input systems, the total amount of nitrogen applied was divided into two applications at sowing and a crop-specific number of days after sowing. As there are no data that disaggregate fertilizer by crop cultivar, we assume that fertilizer rates do not vary across cultivars.

2.3.1 Crop cultivars

For the DSSAT model runs, crop cultivars were selected for each crop, pixel and irrigated / rain-fed combination from among those already calibrated in DSSAT. The cultivar parameters are for all crops available with the official model release, which can be downloaded or free at http://www.dssat.net. Calibrated cultivars in the DSSAT release used in this study have been extensively calibrated and evaluated in multiple locations across the globe and provide state-of-the-art model parameters for realistic crop varieties (Rosenzweig et al. 2014; Elliott et al. 2014b; Ahmed et al. 2015). The cultivars differ in terms of their growing degree-day requirements and other genetic coefficients, and generally reflect typical, widely-adapted improved varieties and hybrids grown across Latin America and the Caribbean. Despite the wide adaptability of these varieties, it is likely that differences in latitude (hence day-length) and climate across the region make region and altitude-specific varieties a more realistic option. Therefore, cultivars were selected for crop-specific latitude and altitude combinations based on the analysis done for Rosegrant et al. (2014) by the consultant Dr. Myles

Fisher. For the present study, Dr. Fisher also ran this same analysis to identify cultivars among those calibrated in DSSAT for wheat and dry bean (not included in the Rosegrant et al. report). The cultivars used for each latitude-altitude, crop and rain-fed / irrigated combination are shown in Table A1 in the Appendix.

Table 2. Fertilizer application rules used to separate high and low input systems for each crop, as described in Section 2.3.4. Below the threshold, the entire quantity is applied at sowing in the DSSAT simulations. Above the threshold, 50% of the fertilizer is applied at sowing, and the other 50% is applied at the indicated days after sowing (DAS).

Crop	System	Kg N ha^{-1}	1.DAS	%	2.DAS	%
Maize	Low input	<120	0	100	*NA*	*NA*
	High input	>120	0	50	40	50
Rice	Low input	<75	0	100	*NA*	*NA*
	High input	>75	0	50	30	50
Wheat	Low input	<120	0	100	*NA*	*NA*
	High input	>120	0	50	30	50
Dry bean	Low input	<40	0	100	*NA*	*NA*
	High input	>40	0	50	20	50
Soybean	Low input	>0	0	100	*NA*	*NA*
	High input	>0	0	100	*NA*	*NA*

2.4 EcoCrop input parameters and robustness checks

Crop-specific parameters are needed in EcoCrop in order to define precipitation and temperature optima and growing limits, and ranges of possible durations in days. In order to define these parameters, the calibration procedure includes the initial adoption of values chosen from a literature review (see Table 3) and the FAO EcoCrop database (FAO, 2007). Second, the suitability maps, generated using the initial set of parameters, are compared visually with the distribution of physical area for each crop from the SPAM database (Figure A6 in the Appendix). This comparison is made considering climatic suitability for both temperature and rainfall for rain-fed systems, whereas for irrigated systems, suitable areas are evaluated on the basis of temperature suitability alone. Finally, for those crops for which we do not have previous studies using EcoCrop, experts (primarily crop breeders) were consulted in order to corroborate the parameters and the current distribution of crop cultivation areas. Table 3 shows the sources used to select parameters for each crop, while Table 4 shows the actual parameters chosen.

In the absence of expert opinion for all crops, an additional consistency check of the model output was developed, which involves comparing the simulated with reported presence and absence of each crop. This is a typical procedure to determine the performance of niche-based species distribution models (Liu et al. 2005, 2013a). For EcoCrop, it provides an indication of the level of agreement between the model prediction and the known distribution of the crop (as reported in SPAM 2005), with the remark that low levels of agreement are not necessarily a result of poor model performance. Lack of agreement can also be a product of data sparseness, non-climatic drivers limiting the actual

distribution of the crop (Ramirez-Villegas et al. 2013). The methodology of Rippke (2014) was followed, in which the reported presence of physical cultivation areas in SPAM (for rain-fed areas) for each crop is compared with the simulated suitability (excluding forested areas, e.g. in the Amazon).

Table 3. Crop-specific calibration procedure. Based on Rippke (2014).

Crop	Calibration procedure	Expert(s)	Literature
Banana	Adopted from literature	NA	Ramirez et al. (2011)
Yam	CIAT database	Dr. Antonio Lopez-Montes (International Institute of Tropical Agriculture, IITA), Dr. Alexandre Dansi (University of Abomey-Calavi, Benin)	Rippke (2014)
Cassava	Adopted from literature	NA	Ceballos et al. (2011)
Coffea arabica	CIAT-CENICAFÉ unpublished research	Juan Carlos García (Centro Nacional de Investigaciones de Café en Colombia, CENICAFÉ)	NA
Coffea robusta	Adopted from literature	NA[†]	Bunn et al (2015) FAO (2007)
Potato	Adopted from literature	NA	Schafleitner et al. (2011)
Sugarcane	Adopted from literature	NA	AVA (2013); Quintero (1995)

[†]NA= Not Applicable

Table 4. Ecological parameters used to run the EcoCrop model. Minimum and maximum growing duration in days (Gmin, Gmax); killing temperature (Tkill); absolute range of the monthly maximum and minimum temperature (Tmax, Tmin); optimum range of the monthly maximum and minimum temperature (Topmax and Topmin); absolute range of the maximum and minimum precipitation during the growing season (Rmax, Rmin); and optimum range of the maximum and minimum precipitation during the growing season (Ropmax, Ropmin). All temperatures are in ˚C, and precipitation values in mm. Parameters were derived from the sources shown in Table 3.

Crop	Gmin	Gmax	Tkill	Tmin	Topmin	Topmax	Tmax	Rmin	Ropmin	Ropmax	Rmax
Banana	365	365	10	16	24	27	35	700	1,000	1,300	5,000
Yam	210	210	12	20	25	34	40	750	1,100	1,400	2,000
Cassava	240	240	0	15	22	32	45	300	800	2,200	2,800
Coffea arabica	365	365	0	15	17.6	22.7	24.7	750	1,400	2,300	4,200
Coffea robusta	365	365	0	12	19	27	33	900	1,700	3,000	4,000
Sugarcane	365	365	0	10	25	32	45	800	843	1,439	2,500
Potato	120	120	-0.8	3.75	12.4	17.8	24	150	251.2	326.5	785.5

The area under the receiver operating characteristic (ROC) curve is used to compare EcoCrop predictions and SPAM observations (Peterson et al. 2008; Freeman and Moisen 2008). To this aim, an analysis of the fractions of true positives (sensitivity) and true negatives (specificity) is first conducted (Worster et al. 2006; Rippke, 2014; Liu et al. 2013a). A true positive occurs when the model predicts

the presence of the crop and the reference distribution confirms this to be true; similarly, a true negative is when the model predicts absence, which is confirmed by the reference distribution. The ROC curve constructed by plotting "1 – specificity" on the x-axis against sensitivity on the y-axis (Figure 2). The area under the ROC curve (AUC) summarizes the overall accuracy of the model, i.e. its ability to correctly discriminate presences and absences. An AUC of 0.5 indicates random guessing, and 1.0 would represent a perfect fit (Liu et al. 2013a; Peterson et al. 2008). A high AUC value is a sign of the model's ability to distinguish correctly between locations where a crop is present or absent in the benchmark database, and values over 0.7 are considered to have a reasonable correspondence (Rippke, 2014; Peterson et al. 2008; Pearson, 2010). In this study, the curve was constructed for the average 30-year suitability in the baseline period (1971-2000) across all pixels for a given crop with the *PresenceAbsence* package in R.

As stated above, it should be noted that high values of physical area in SPAM should correspond to high climatic suitability as calculated by EcoCrop, but the converse is not necessarily true. For example, low values of physical area for a given crop may still have high climatic suitability, given that other non-climatic factors (economic and social pressures, non-suitable soils, pest and disease pressure among others) may make other land-uses more profitable. A high rate of false positives (climatically suitable areas without physical area) would shift the ROC curve to the right and reduce the AUC. Therefore, EcoCrop AUC values are unlikely to ever reach 1.0.

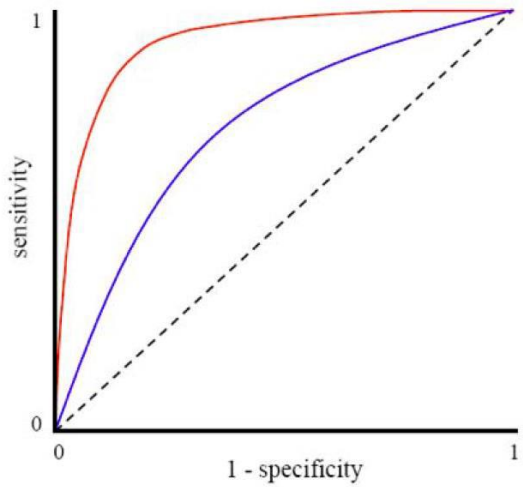

Figure 2. Example of an ROC curve. The broken line represents random predictive ability. The red line shows better model performance than the blue line (Pearson, 2010).

2.5 Crop simulation and analysis strategy

The DSSAT and EcoCrop models are both run yearly for a historical period (1971 to 2000) and a future period (2021 to 2049) at a 0.5° spatial resolution across Latin America and the Caribbean in current and potential cultivation areas (excluding currently forested regions), respectively. The historical

period corresponds to the availability of observational data from the Watch Forcing Dataset (described in Section 2.2), and the future period represents the near-term scenarios of climate change, for which uncertainty in radiative forcing and hence in emissions trajectories is of minor importance (Hawkins and Sutton 2009, 2011; Knutti and Sedlacek, 2012). Due to inter-annual and decadal climate variability, a 30-year period is standard for establishing realistic climate conditions in each simulated period, i.e. capturing the transient climate for the period. In addition, by simulating 30 cropping seasons in the historical and future periods with DSSAT, changes in inter-annual yield variability over time can also be assessed (cf. Porter et al. 2014).

For both the DSSAT and EcoCrop model runs, R scripts were written to create model input files, automate the model runs, and analyze output. Yields and suitability values were estimated yearly for each of the 30 years in the historical and future periods and for each GCM in the future period. This resulted in 300 [30*(1+9)] simulations for each pixel and crop (and irrigated / rain-fed combination with DSSAT), resulting in millions of simulations in total (the exact number depends on how extensively the crop is grown throughout LAC). Mean yield and suitability were then calculated across the 30 years in each period, and across the GCM's in the future period. In the case of DSSAT, the yield coefficient of variation was also computed using the 30 simulated years, as a measure of interannual variability. We therefore assessed how long-term mean yields might change, but also their inter-annual variability, which is critical for rain-fed crops and for market stability.

In addition to calculating changes in mean suitability, to evaluate changes in suitability for each crop between the historical and future periods, suitable areas were defined as having suitability values greater than a threshold of 50% (see Liu et al. 2005, 2013a). A similar approach was employed by Ramirez-Villegas and Thornton (2015) and CGIAR (2015) to ease interpretation and improve usefulness of EcoCrop predictions. Five categories were defined to identify changes in suitable area between current (***cs***) and future suitability (***fs***).

- *Becomes unsuitable (suitability drops from above to below 50%)*:

$$(cs \geq 50\%) \cap (fs < 50\%) \cap (|fs - cs| > 5)$$

- *Less but still suitable (suitability drops, but remains above 50%)*:

$$(cs \geq 50\%) \cap (fs \geq 50\%) \cap (fs - cs < 0) \cap (|fs - cs| > 5)$$

- *Remains suitable (suitability above 50% with no significant change):*

$$(cs \geq 50\%) \cap (fs \geq 50\%) \cap (fs - cs < 0) \cap (|fs - cs| \leq 5)$$

- *More suitable (suitability above 50% and goes up):*

$$(cs \geq 50\%) \cap (fs \geq 50\%) \cap (fs - cs \geq 5)$$

- *Becomes suitable (suitability formerly below 50% and now above)*:

$$(cs < 50\%) \cap (fs \geq 50\%) \cap (fs - cs \geq 5)$$

Categorical changes are only considered as percentage changes larger than a threshold of 5%, in order to avoid identifying very marginal changes as a change in category.

Modeling results are compared at the pixel level and also at two aggregated spatial scales (Figure 3). The first scale is the Food Production Unit (FPU) from the IMPACT model (Rosegrant et al. 2014), with 41 across Latin America and the Caribbean. The second scale are five sub-regions based on groups of FPUs and defined as Mexico (MEX), Central America and the Caribbean (CEN), the Andean region (AND), Brazil and Amazonia (BRA), and the Southern Cone of South America (SUR). These regions are defined somewhat similarly to Lobell et al. (2008), with a few modifications. The physical areas by region for the five crops simulated with DSSAT are shown in Table 5.

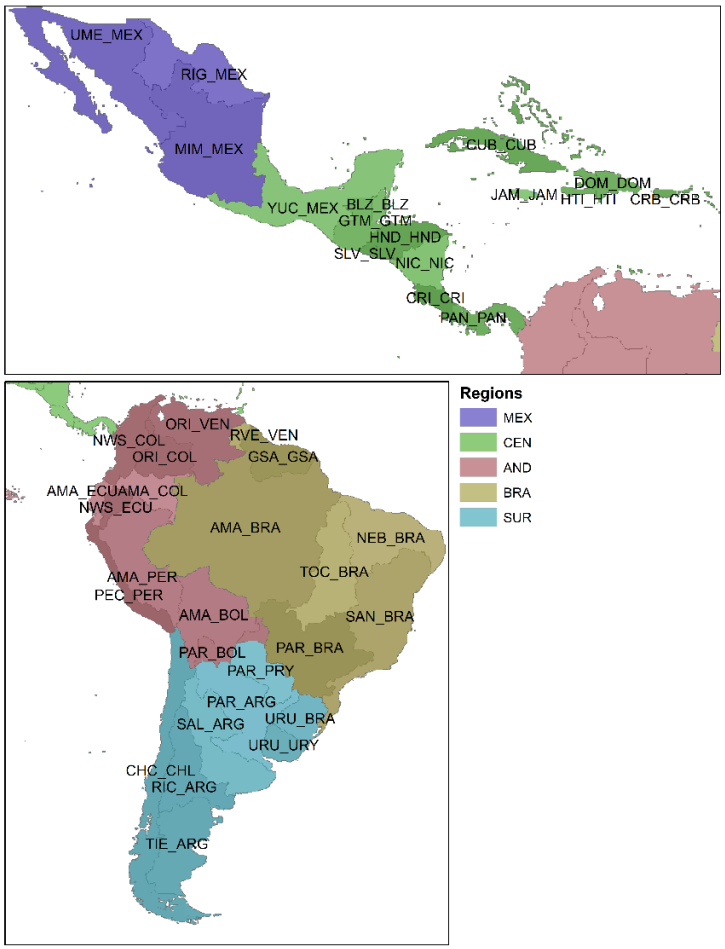

Figure 3. Regions of Latin America and the Caribbean used to aggregate modeling results. Central and northern Mexico (MEX), Central America and the Caribbean (CEN), the Andean countries (AND), Brazil and northern South America (BRA), and the Southern Cone (SUR). Regions are groupings of Food Production Units (Rosegrant et al. 2014), also shown here, and are loosely based on regions defined in Lobell et al. (2008).

Table 5. Physical area (in thousands of km^2) for each cropping system simulated by DSSAT. Areas are shown by region and for all Latin America and the Caribbean (LAC). (Source: SPAM 2.0; You et al. 2014)

	Maize		Rice		Wheat		Dry bean		Soybean	
	Irrigated	Rainfed	Irrigated	Rainfed	Irrigated	Rainfed	Irrigated	Rainfed	Irrigated	Rainfed
MEX	834	3,650	24	1	447	0	216	1032	0	0
CEN	468	3,530	363	195	1	3	28	930	0	4
AND	454	1,762	851	511	0	229	45	188	0	941
BRA	92	9,772	298	2,207	1	1,250	81	3,214	44	16,906
SUR	185	4,520	1,022	262	48	5,871	6	328	58	18,584
LAC	2,033	23,234	2,558	3,176	497	7,353	376	5,692	102	36,435

3 Results

The interpretation of future climates based on GCM output requires careful consideration. Climate models capture both changes in mean climate conditions (e.g., changes in long-term mean temperatures) as well as changes in other statistical features of the local or regional climates, e.g. frequency of daily extremes, the annual cycle, and inter-annual variability (Sillmann et al. 2013; Cook et al. 2015; Kharin et al. 2013). Particular attention needs to be paid to the fact that even-though multi-model mean results are often presented, climate models simulate future climate in different ways, providing a range of potential futures. Thus, due to their very nature, climate change simulations provide projections (i.e. equally-plausible realizations of the future of the climate system), rather than predictions (i.e. competing attempts to prescribe a future reality) (Knutti and Sedlacek 2012; Taylor et al. 2012). It is the job of the scientist to interpret their outcomes appropriately.

Long-term progressive climate change is not only an increase in average temperatures, but also more regional changes in solar radiation and the timing and magnitude of precipitation, all of which have the potential to affect crop production (Chavez et al. 2015; Trnka et al. 2014; Porter et al. 2014). In the following sections, the results of the climate models themselves are addressed, and then, through the lens of the crop modeling results, the potential impacts of these changes on crop production in Latin America and the Caribbean are considered.

3.1 General information

The countries of Latin America cover from 32°N to 52°S latitude (ignoring Tierra del Fuego), ranging from warm temperate in northern Mexico, through tropical in Central America, to equatorial in northern Brazil, Colombia, Ecuador, Peru and Venezuela and back through the sequence of tropical to warm temperate to cool temperate as one goes southward towards Argentina and southern Chile. Overlaying this latitudinal range are wide variations in geography. The Köppen-Geiger classification provides a convenient broad classification of the climates (Peel et al., 2007) (Figure 4).

The widely differing climates have different patterns and amounts of rainfall, which interacted with the geology to give different soils over many thousands of years. Soil characteristics, mainly the amount of clay, interact with the pattern and amount of rainfall to determine the water climate of any crop (Adiku et al. 1996; Suleiman and Ritchie 2001). Irrigated crops are not so dependent on soil characteristics, although they are a dominant factor in the water management.

Crops differ physiologically, particularly between those with the C3 and C4 pathways of photosynthesis and between legumes, which are all C3s, and non-legumes. Soybean, dry bean, potato, wheat and rice are C3 crops, while maize, sorghum and millet are C4s. Moreover, crops differ in the temperature optima of their biochemistry and physiology, which influences their suitability for different temperature environments. For example, wheat is a temperate crop that originated in Mesopotamia, while rice is a tropical crop that originated in East Asia. This is reflected in their global distribution: rice is the main crop of the tropics while wheat is the main crop of the temperate zone. In contrast, maize is more broadly adapted and is thus more widely distributed (Monfreda et al. 2008; Ureta et al. 2012; Cairns et al. 2013). The crops simulated in this study will therefore respond differently depending on the countries' geography and the distribution of climatic zones within each (Porter and Semenov 2005).

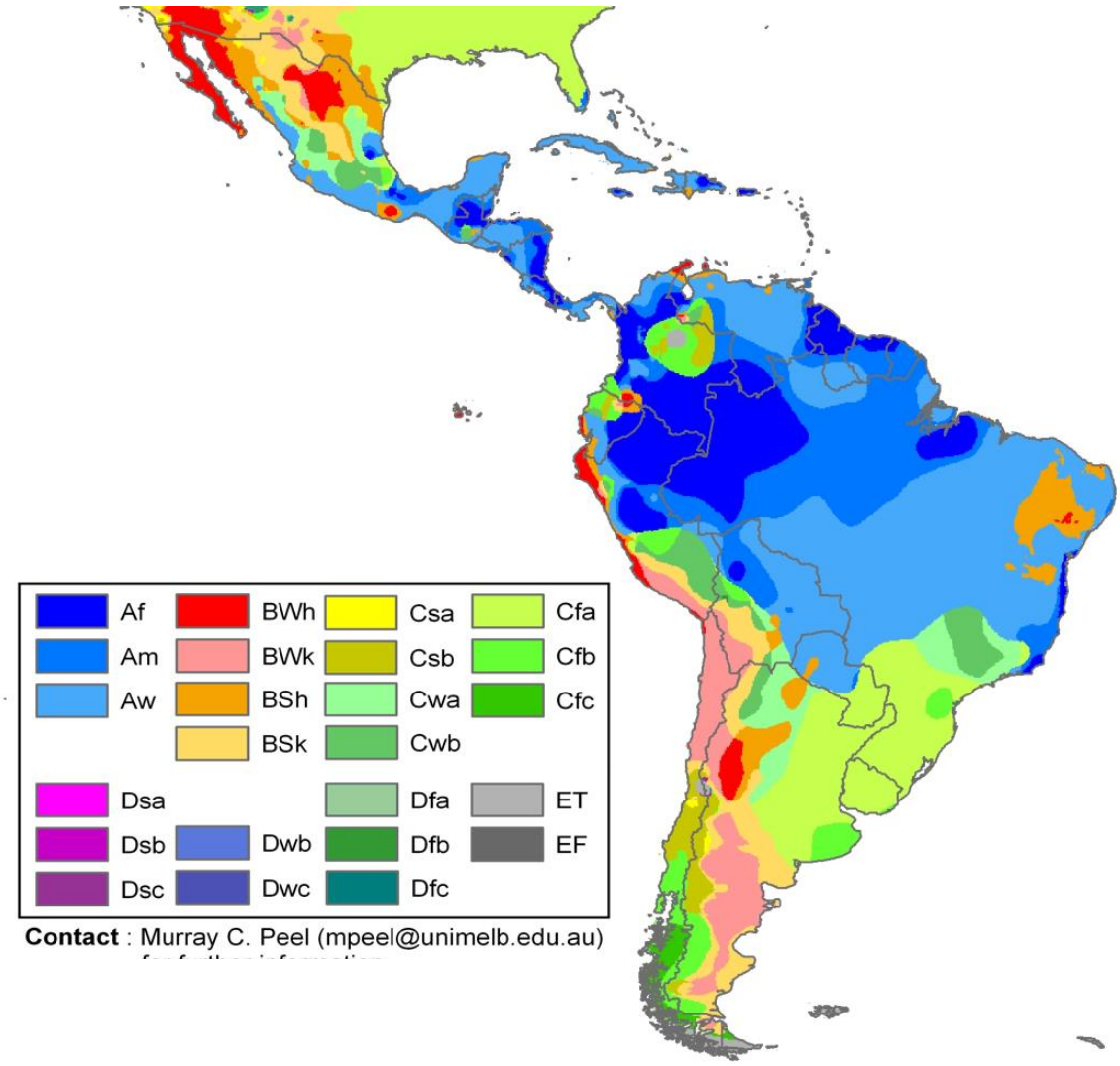

Figure 4. Köppen-Geiger climate classification of Latin America and the Caribbean Source: Peel et al. (2007). Names of climate classes are as follows: Group A: Tropical rainforest climate (Af); Tropical monsoon climate (Am); Tropical wet and dry or savanna climate (Aw); Group B: Desert climate BW: Hot desert (BWh), Cold desert (BWk); Steppe climate (Semi-arid) BS: Hot steppe (BSh), Cold steppe (BSk); Group C: Dry-summer or Mediterranean climates (Csa/Csb); Humid subtropical climates (Cwa,Cfa); Maritime temperate climates or Oceanic climates (Cwb, Cwc,Cfb, Cfc); Temperate highland tropical climate with dry winters (Cwb, Cwc); Maritime subarctic climates or subpolar oceanic climate (Cfc); Dry-summer maritime subalpine climate (Csc) Group D: Hot summer continental climates (Dsa, Dwa, Dfa); Warm summer continental or hemiboreal climates (Dsb, Dwb, Dfb); Continental subarctic or boreal (taiga) climates (Dsc, Dwc, Dfc); Continental subarctic climates with extremely severe winters (Dsd, Dwd, Dfd); Group E: Tundra climate (ET); Ice cap climate (EF).

Some crops have sharp cutoffs in their temperature ranges, while other crops are less affected (Sanchez et al. 2014). This affects their distribution. In southern Colombia, for example, rice is grown successfully at Jamundí at 1000 m at 3.3°N latitude, but not at Popayan 100 km south at 1700 m at 2.5°N. Despite the relatively short distance, the temperature difference between the two sites, calculated on the adiabatic lapse rate (change of temperature with elevation), is 4°C and is sufficient that rice is not a viable crop at Popayan. In contrast, rice grain sterility increases by 10% per degree above 30°C at anthesis (when the plant flowers and fertilization of the seeds occur) (Horie, 1993; Kim

et al., 1996; Matsui et al., 1997; Satake and Yoshida, 1978; Peng et al. 2004). The effect of climate change of 2°C could lead to substantial increase in the area of land currently not hot enough for rice, but to yield losses in hotter areas where rice currently grows (see e.g. Li et al. 2015). These effects also occur in other crops (see Asseng et al. 2014; Teixeira et al. 2013; Hawkins et al. 2013). Geographical differences in prevailing climatic conditions and differences in crop eco-physiology are the reason why climate change will not affect all crops the same and why changes in yields of the same crop will differ within and between countries.

The distribution of the climates within and between countries are important determinants of crop yield potential (van Ittersum et al. 2013). Farmers' management is an overarching consideration. The more truly that farmers apply the optimum agronomy for a particular crop (sowing time, seeding and fertilizer rates, which are broadly location-specific) the more closely they will approach the yield potential of their crop (Lobell et al. 2009; Cassman 1999).

We provide this information so that the reader can understand how changing climate will affect crop growth and yield, especially through higher temperatures and reduced precipitation. In the sections that follow, we have sought only to identify the differences and how they might be affected by future climates. For readers seeking further information on the interaction between climate and crop ecology in general, we refer them to Evans (1996) and Connor et al. (2011).

3.2 Projected climate changes

Given that projected climate changes may differ throughout the year, and that cropping systems are only sensitive to the changes that occur during their growing seasons, projected changes are shown by 3-month seasons (Figure 4) for four agriculturally relevant climate variables: precipitation, daily maximum and minimum temperatures and solar radiation. These changes represent averages across the 9 GCMs for the future period (2020-2049) relative to the baseline climate data in the historical period (1971-2000). Figures A9 to A13 in the Appendix show the same seasonal changes for each variable, but individually for each GCM in order to show the range of projected changes.

Projected changes in rainfall are varied and complex, with mean changes ranging from -30 to +30% across the continent, although with strong variability across GCMs (Figures A9-A13 in the appendix). On average, LAC is projected to become drier in the period between June and November, but become wetter in the period December-May. The Amazonian region shows decreases of up to 30% from June to November, and drying throughout the year is also evident in northern South America, parts of Mexico, central Chile and southern Argentina. In Central America and the Caribbean, rainfall is projected to decline at the start and middle of the rainy season (MAM and JJA). In contrast, the Andes of South America show increases in precipitation throughout the year, and Uruguay and eastern Argentina show increases in the austral fall and spring seasons. Generally, in the wetter areas, precipitation is likely to increase in both magnitude and frequency, while frequency is expected to decline elsewhere.

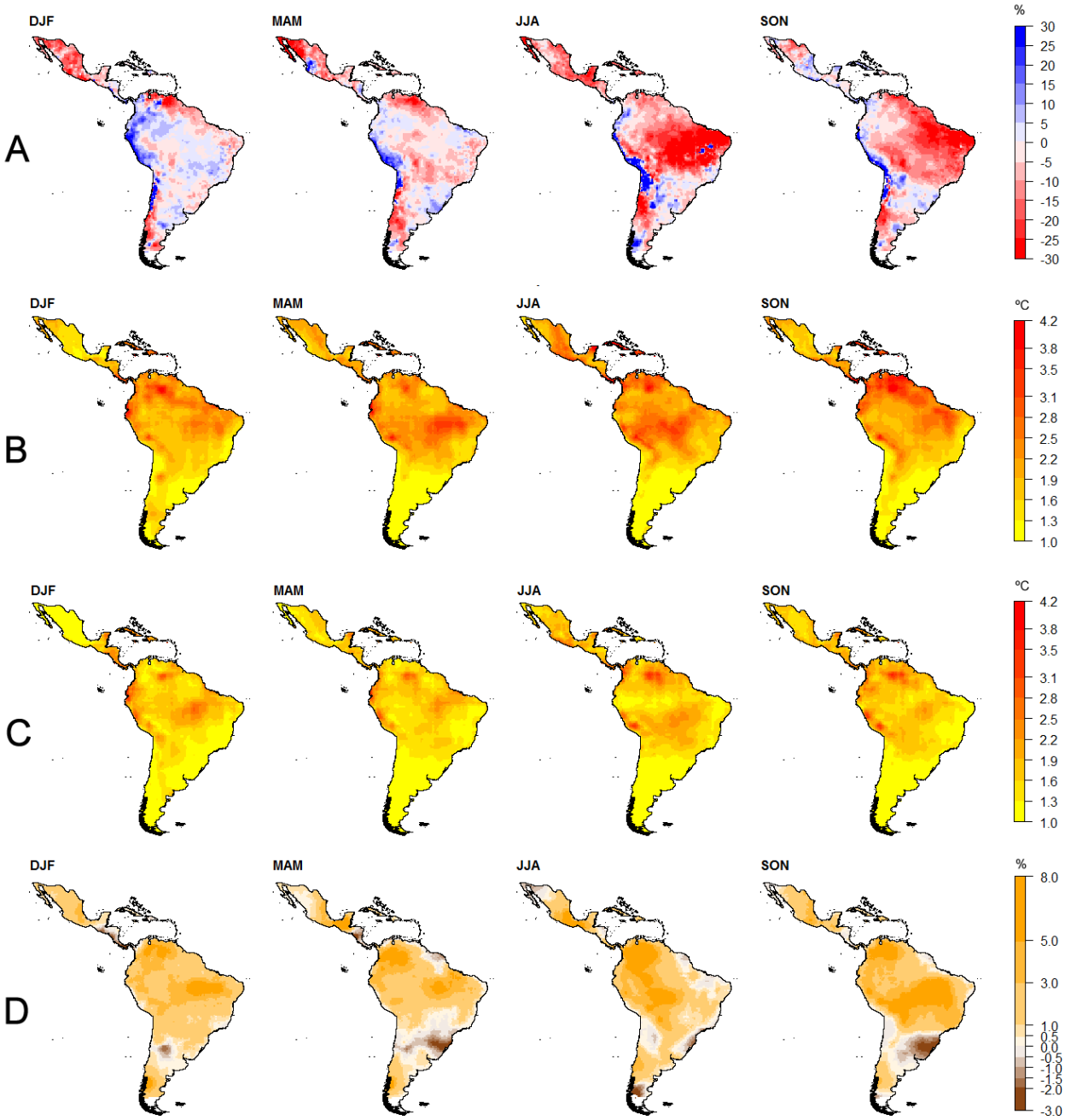

Figure 5. Changes in accumulated rainfall (A), mean maximum temperature (B), mean minimum temperature (C) and solar radiation (D) for four seasons, as follows, December-January-February (DJF), March-April-May (MAM), June-July-August (JJA), and September-October-November (SON).

Overall, seasonal maximum temperatures are projected to increase by 1–4°C across the Latin American and Caribbean region, and minimum temperatures by 1-3°C, with tropical South America projected to warm at higher rates than the more temperate areas of Mexico and the southern Cone. Increases in maximum temperatures are generally higher than increases in minimum temperatures,

due to projected drying and less frequent precipitation in many areas. This larger rate of change for maximum temperature is likely to exacerbate evapotranspiration losses in areas of low air moisture (i.e. high vapor pressure deficit) (Lobell et al. 2013; Cook et al. 2015).

Increases in solar radiation are evident almost everywhere throughout the year, with the strongest increases in the tropical latitudes of South America. Decreases in radiation are limited to southern Brazil, Uruguay and Argentina, especially in MAM and SON, the austral autumn and spring, when precipitation increases are projected in these areas. The observed changes in downwards shortwave solar input (Figure 5D) have a number of causes, some of which are subject of ongoing research in climate science (e.g. Allen et al. 2013; Andrews et al. 2012). In general, we note that changes in solar radiation, reflect the GCMs predicted changes in cloudiness with future climates.

Increases in maximum temperatures accompanied by decreases in precipitation are likely to increase the risk of agricultural droughts. Rain-fed crops will be confronted with less reliable start of the rainy season and, possibly, the risk of desertification will increase (also see Cook et al. 2015; Sheffield et al. 2012; Dai 2013). The most affected regions in Latin America are likely to be mainly in Mexico, Central America and the Caribbean, Venezuela, northern Colombia, northeast Brazil and most of Amazonia.

3.3 Results of DSSAT crop model simulations

This section details the main results and findings from the spatially-explicit DSSAT simulations for five crops, namely, maize, soybean, rice, wheat and dry bean. Results are presented in four sections: first, historical and future yield simulations are presented (Section 3.3.1), and secondly, a section that provides results for other model prognostic variables is provided (Section 3.3.2). Section 3.3.2 helps to disentangle the projected yield changes. However, we note that due to the complexity of the crop simulation models used, the fact that for each climate scenario we conducted a single set of simulations with all stresses acting simultaneously, and the scale and multi-crop nature of the work presented, explaining fully the yield change drivers is not feasible. Such an undertaking is difficult even in country-level or site-specific studies for single crops (see e.g. Ramirez-Villegas 2014; Lobell et al. 2013, 2015; Asseng et al. 2013a). This section presents results at the FPU (Section 3.3.3) and at the sub-region (Section 3.3.4) scales.

3.3.1 Simulated spatially-explicit historical yields and future projected yield changes

Average simulated yields in the historical period are shown in Figure 6 for rain-fed and irrigated production for all crops. As expected, average yields are generally higher for irrigated compared to rain-fed simulations. Geographical differences in simulated yields are a product of resource availability for plants (e.g. nutrients, water, solar radiation) and the potential of the different crops to capture and efficiently use such resources (Lobell et al. 2009; Cassman 1999; van Ittersum et al. 2013). Maize yields are highest in central Mexico and southern Brazil for both irrigated and rain-fed production; in these regions, the values higher than 9000 kg ha^{-1} are similar to those reported in SPAM 2005 (You et al., 2014), where the climate and soils are more favorable. Rain-fed maize has relatively low yields throughout northern Mexico, north-east Brazil, Bolivia, Peru and northern Argentina, mostly because these areas have lower annual rainfalls (Magrin et al. 2005; Rosenzweig et al. 2014).

Irrigated rice shows high yields in Cuba, Uruguay and southern Brazil, Ecuador, Colombia, Panama, Venezuela y Guatemala, whereas rain-fed rice shows a similar spatial pattern but with yields less than a third of irrigated rice in many coincident areas. The Brazilian savannah region shows low rain-fed rice, mostly as a result of terminal and reproductive drought stress (see Heinemann et al. 2015).

Wheat yields are highest for both irrigated and rain-fed production in eastern Argentina (Asseng et al. 2013b), Uruguay, the mountainous region of Mexico and the south of Chile. Low yields for rain-fed production (<2000 kg ha^{-1}) are principally found in Bolivia and the north of Argentina, which is consistent with SPAM 2005 (You et al., 2014).

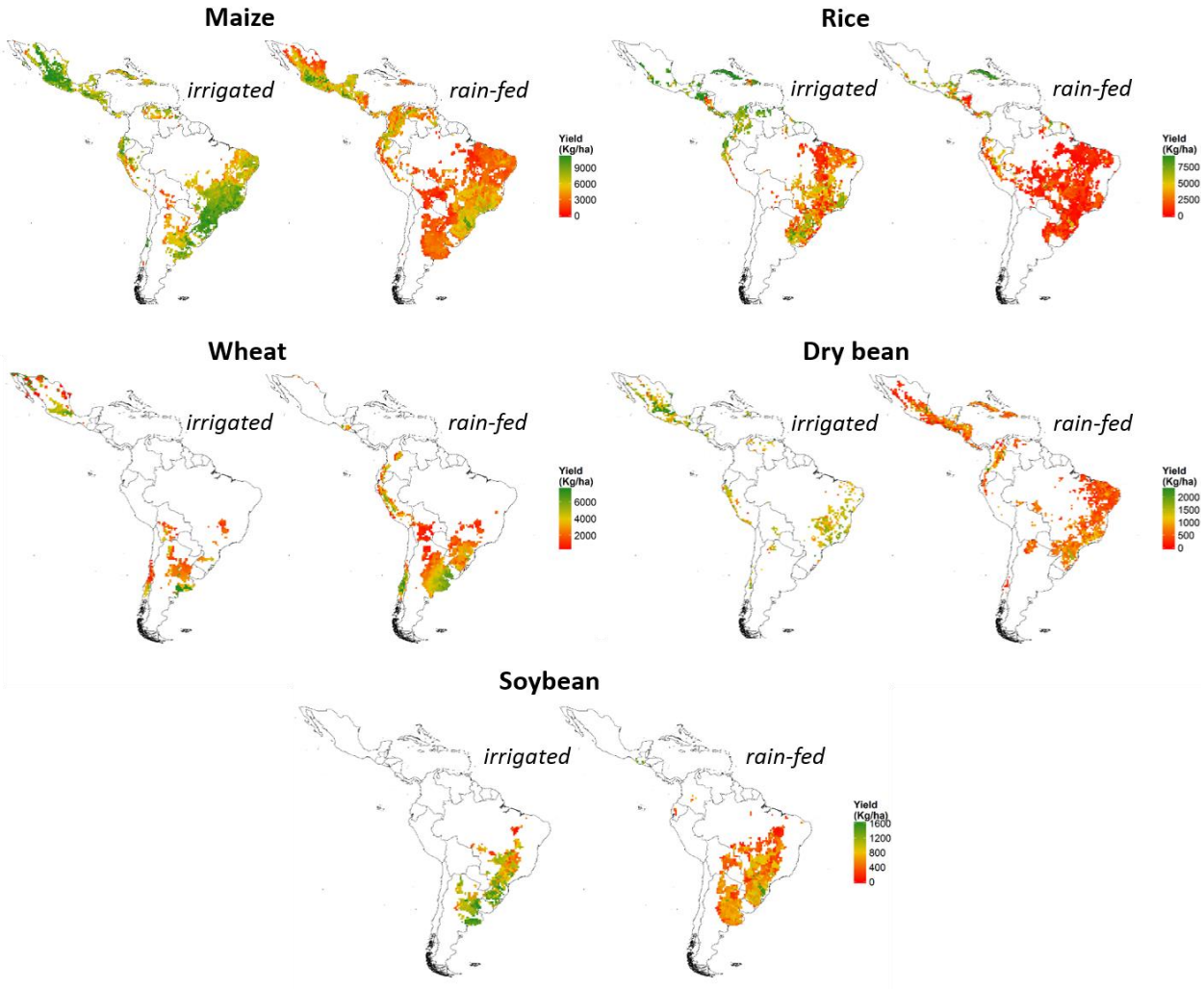

Figure 6. Average yields in the historical period (1971-2000).

Irrigated bean yields are about 2000 kg ha^{-1} for the majority of simulated areas, whereas irrigated soybean has similarly high yields in Argentina and southern Brazil. Rain-fed dry bean and soybean yields are nearly a third and half of irrigated yields, respectively. Rain-fed dry bean and soybean yields

are low in the north of Brazil, but relatively high in the southeast Brazilian regions of Rio Grande do Soul, Sana Catarina and Paraná, which is at least in part a result of the impact of drought stress (also see Heinemann et al. 2016). Rain-fed dry bean yields are also low throughout Central America, the Caribbean and northern South America.

Spatially-explicit projected average yield changes (in percent) between the historical and future periods are shown in Figure 7, whereas regional-level (LAC) average values are shown in Table 6. Generally, relative yield changes are stronger in magnitude for rain-fed as compared to irrigated systems for all crops, due to lower historical mean yields as well as to a higher exposure to drought (Challinor et al. 2015; Lesk et al. 2016; Iizumi et al. 2014). Among the five crops, maize shows the most severe declines for rain-fed production, and especially so in central Mexico, the Yucatan and northern South America, which is consistent with earlier findings (Challinor et al. 2014; Rosenzweig et al. 2014). Irrigated wheat also shows severe declines in northern Mexico and northern Argentina, while rain-fed dry bean shows similar declines in southern Mexico and Guatemala, Colombia, Venezuela and northeastern Brazil. These hotspots for yield declines in rain-fed production are associated with projected decreases in rainfall from the GCMs, pointing to the importance of increasing water stress as a threat to rain-fed production across Latin America and the Caribbean (Elliott et al. 2014; Liu et al. 2013b; Jones and Thornton 2003). Yield decreases in rain-fed systems under future climate conditions are also associated with a higher risk of crop failures, that is the crop dies as a result of drought without giving any yield (Figure A15 in the appendix).

Other cropping systems show yield increases under future climate change conditions. Both rain-fed and irrigated rice show yield increases throughout Brazil, Uruguay, Bolivia, Peru, Ecuador and Nicaragua (also see Rosenzweig et al. 2014). While these increases were seen to be somewhat sensitive to the choice of variety in sensitivity tests (with less strong increases and even declines with other varieties), the increases seen here show that it should be possible to benefit from changing climate conditions with the right genetic material for some cropping systems, as has been shown earlier (Challinor et al. 2014; Beebe et al. 2011; Gourdji et al. 2013). Other systems with projected yield increases include irrigated dry bean in Mexico, rain-fed and irrigated soybean in Brazil, and rain-fed soybean in eastern Argentina and Ecuador (also see Magrin et al. 2014; do Rio et al. 2015; Asseng et al. 2013b).

The range of yield changes for all crops across climate modeling scenarios is shown in the appendix (i.e. the 10^{th} & 90^{th} percentiles from bootstrapped confidence intervals, Figures A14 & A15). Areas with insignificant changes (where the sign changes from positive to negative, or vice-versa) include irrigated and rain-fed soybean in Brazil, rain-fed maize and soybean in eastern Argentina, and rain-fed dry bean in parts of central Mexico, eastern Brazil and Ecuador. However, in most areas, the sign of the projected yield changes remains the same, implying that the results shown are robust towards the choice of GCM. These findings are consistent with the global modelling study of Rosenzweig et al. (2013), and with the global meta-analysis presented in the last IPCC report (Porter et al. 2014; Challinor et al. 2014).

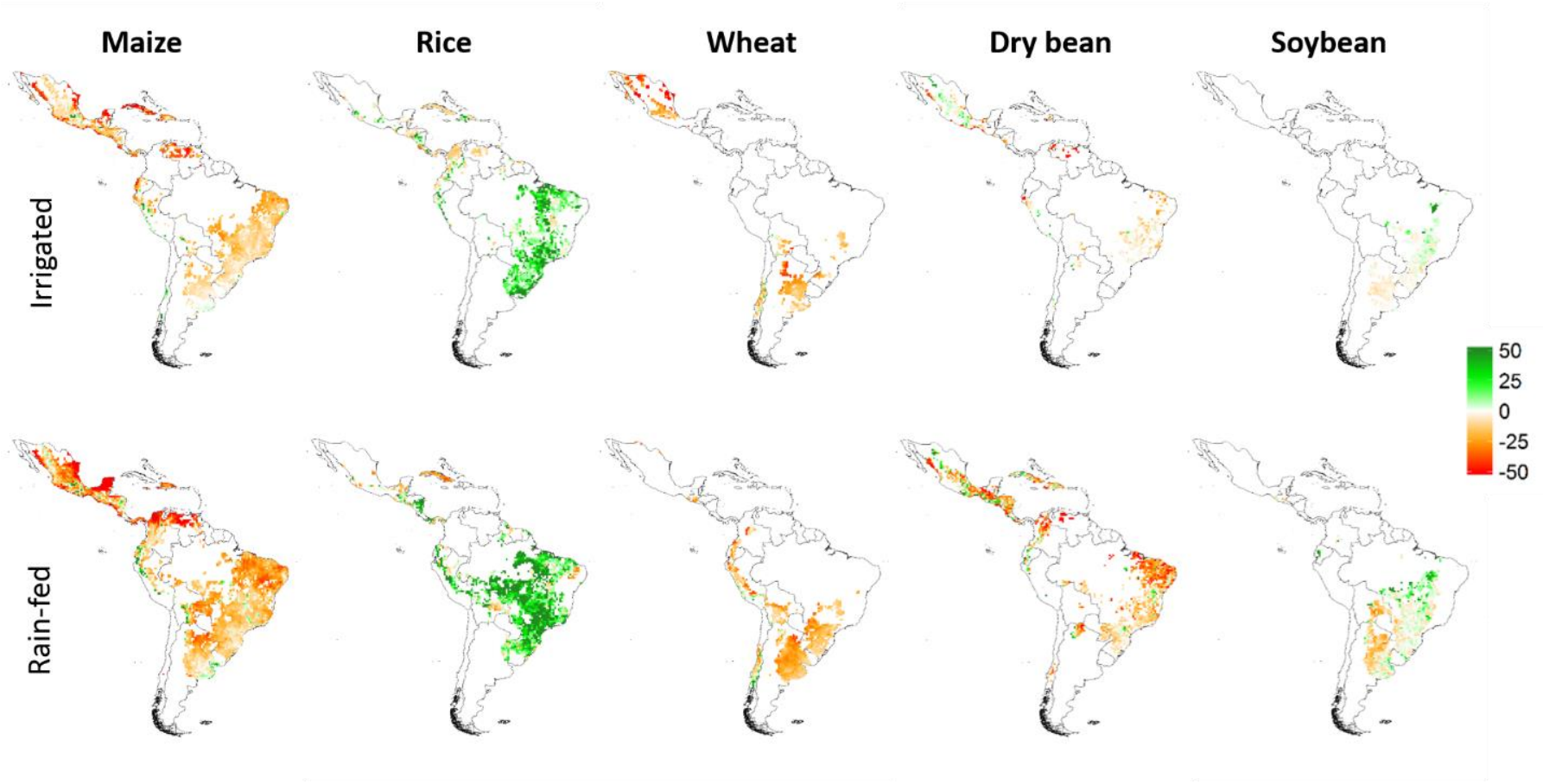

Figure 7. Mean percentage changes in yield of five crops between the historical period (1971-2000) and as simulated based on the projections nine GCMs for 2020–2049.

Table 6. Average yields and % changes for rain-fed and irrigated maize, rice, and soybean, aggregated to the Latin American and the Caribbean scale for all cultivation areas. Yields are first averaged across the 30-year period per pixel, from 1971−2000 (for the baseline period) or 2021−2048 (for the future period). Then, pixel-scale yields are spatially averaged across all cultivation areas in Latin America, weighting by the physical area per pixel. Finally, multi-model means are calculated across all 10 GCM simulations for the future period. Percent change was calculated between the mean yields in the future period (averaged across GCMs) and the historical period. The confidence intervals on the percent change metric were calculated by bootstrapping results across GCMs 500 times, and then selecting the 2.5 and 97.5 percentiles. Significant percent changes between the historical and future periods are shown in bold.

	Maize: irrigated	Maize: rainfed	Rice: irrigated	Rice: rainfed	Soybean: irrigated	Soybean: rainfed
Historical baseline (t/ha): 1971−2000	7.2	5.3	5.7	4.4	1.4	0.9
Multi-model mean (t/ha): 2020−2049	7.4	5.1	5.7	4.2	1.4	0.9
% change (in multi-model mean relative to baseline)	**2.1**	**-4.5**	**-1.0**	**-5.5**	-1.1	**-4.3**
95% confidence intervals (of % change)	1.3 to 3.0	-7.1 to -2.2	-2.0 to -0.1	-8.5 to -2.2	-2.2 to 0.2	-5.7 to -2.8

3.3.2 Changes in non-yield variables and relationship with simulated yield changes

In this section, we show baseline levels and changes for non-yield variables that are output by DSSAT, namely, crop duration and seasonal water and nitrogen stress indices, aimed at explaining the simulated yield changes. This choice follows basic crop physiology principles (Evans 1996) as well as previous studies of our own and of other authors in which these variables are usually the main drivers of crop yield changes (Ramirez-Villegas 2014; Heinemann et al. 2015, 2016; Webber et al. 2015; Rosenzweig et al. 2014; Elliott et al. 2014; Lobell et al. 2008, 2013; Asseng et al. 2013a). We present results for these variables for rain-fed production only, given that results for irrigated production look similar although with less severe changes under future climate conditions.

Water and nitrogen control fundamental aspects of crop growth and yield (Ritchie, 1998; Godwin and Singh, 1998). This study used DSSAT version 4.5.1.023. Examination of the Fortran code of DSSAT version 4.5.1.023 shows that the indices of 'water stress' and 'N stress' are indicators of resource demand to availability. More specifically, the 'water stress factor' is the amount of water transpired by the plant as fraction of the potential transpiration. It is calculated daily, averaged over the life of the plant and expressed as a stress factor 0-1, where 0 is no stress. An 'N stress factor' is calculated for each day as the ratio of the actual plant N concentration to standard values for the particular crop. As for water, the values are expressed as a stress factor 0-1, where 0 is no stress. The water- and N-stress indices are applied to reduce the efficiency of different processes of plant growth (e.g. photosynthesis, leaf growth) each day of the crop.

Crops differ in their ability to yield under conditions of water or nitrogen stress. Legumes in particular are able to obtain N from the atmosphere by virtue of symbiotic nitrogen fixation by bacteria that invade their

roots. Moreover, equilibrium soil N concentrations depend on soil organic matter content, management of crop residues and precipitation. All are variable nationally and regionally.

Crop duration is a crop species characteristic and can vary widely between cultivars (Evans, 1996: 119-120). Optimum crop duration varies with latitude and altitude and can affect crop yield. In general, the life cycle of particular crop becomes longer at lower temperatures. All other things being equal, shorter crop durations reduce crop yields because they reduce the time for capturing resources (e.g. light interception) (Fuhrer 2003; Porter and Semenov 2005). Farmers in different countries use crop cultivars that are broadly suited to the agricultural climatology of where they farm (see e.g. Marteau et al. 2011). This selection leads to national and regional differences in mean crop duration (van Bussel et al. 2015).

Mean crop durations are shown for the historical baseline period in Figure 8. Generally, crop durations are longer for rice and wheat (about 140 and 130 days respectively), and shorter for dry bean and soybean (about 100 days for both). Maize durations are intermediate between the other crops, but vary strongly by environment, with durations of about 170 days in eastern Argentina and the highlands of Mexico, and about 100 to 120 days in most other locations.

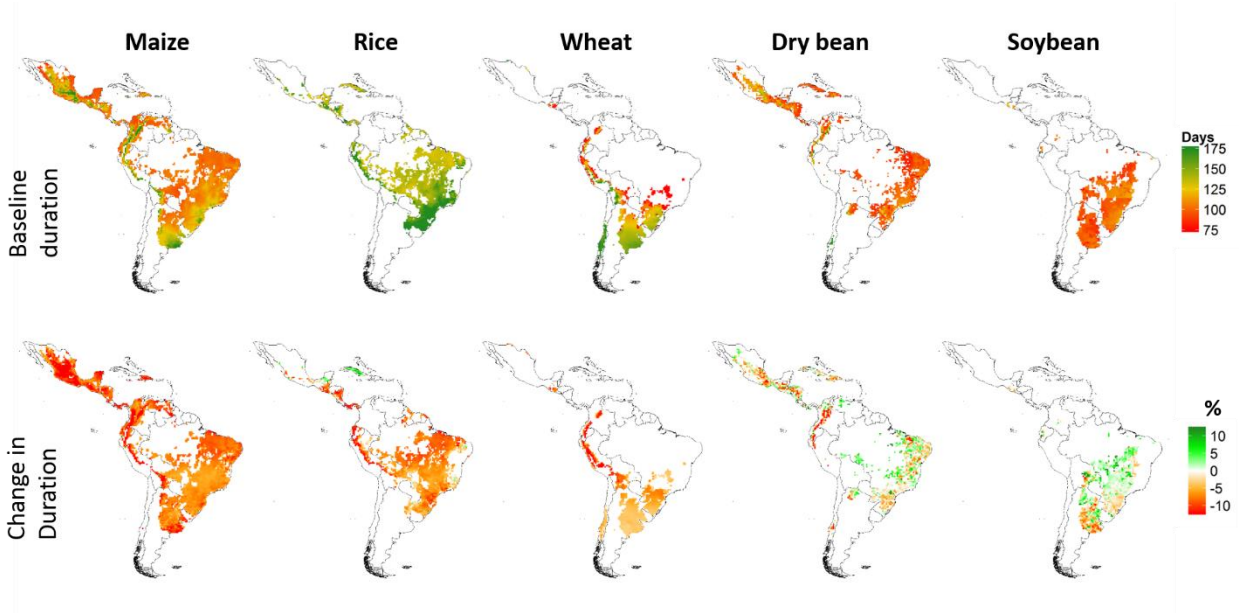

Figure 8. Mean crop durations for rain-fed simulations. Actual values in the historical period (top row) and percent change in duration between historical and future periods (bottom row).

For most crops, higher temperatures imply faster development and shorter crop duration and can reduce yield (Bassu et al. 2014; Li et al. 2015; Asseng et al. 2013a, 2014). As expected, reductions in crop durations by about 10% are seen under future climate conditions for maize, rice and wheat, and in some areas for dry bean and soybean (Figure 8). However, durations are shown to increase by about 5% in many areas for dry bean and soybean, principally in Brazil, Argentina and Venezuela. For soybean, in particular, there is high correspondence between areas of yield increases and of duration increases, indicating that the lengthening of the crop cycle is mostly responsible for the projected yield increases (see Figure 7).

Baseline historical values of the seasonal water stress index (on a scale of 0 to 1) for rain-fed production are shown in the top row of Figure 9. Across the five crops, rain-fed rice and soybean have the lowest values of water stress, whereas values higher than 0.3 (relatively stressed) are shown for maize in

northern Mexico, Ecuador and parts of north-eastern Brazil, and for wheat in Bolivia, northern Argentina, and central Chile. Intermediate values of the water stress index are seen for dry bean in growing areas throughout Mexico, Central America, Venezuela and northeastern Brazil (also see Heinemann et al. 2016; Beebe et al. 2011).

Increases in the water stress index under future climate conditions (bottom row of Figure 9) are seen for all crops in almost all growing locations, indicating an increasing prevalence of drought stress. This increasing stress is seen to be most severe for rain-fed maize, with increases of 0.1 or higher in central Mexico and the Yucatan, Haiti and the Dominican Republic, and northern Colombia and Venezuela, and with intermediate increases in most other growing areas with the exception of Ecuador. Other areas with strong increases in water stress are rice in Cuba, wheat in Argentina and Uruguay, and dry bean in Venezuela and northeast Brazil. The finding of widespread intensification of drought stress is consistent with previous research on crop production and hydrology globally and regionally (Elliott et al. 2014; Jones and Thornton 2003; Thibeault et al. 2010; Dai 2013).

Reductions in water stress are seen in only a few localized areas, for maize in Ecuador and small parts of Brazil, for wheat in Peru, and for dry bean in Ecuador, Cuba and parts of southern Mexico and El Salvador, mostly as a result of low rates of warming and seasonal precipitation increases (see Figure 5).

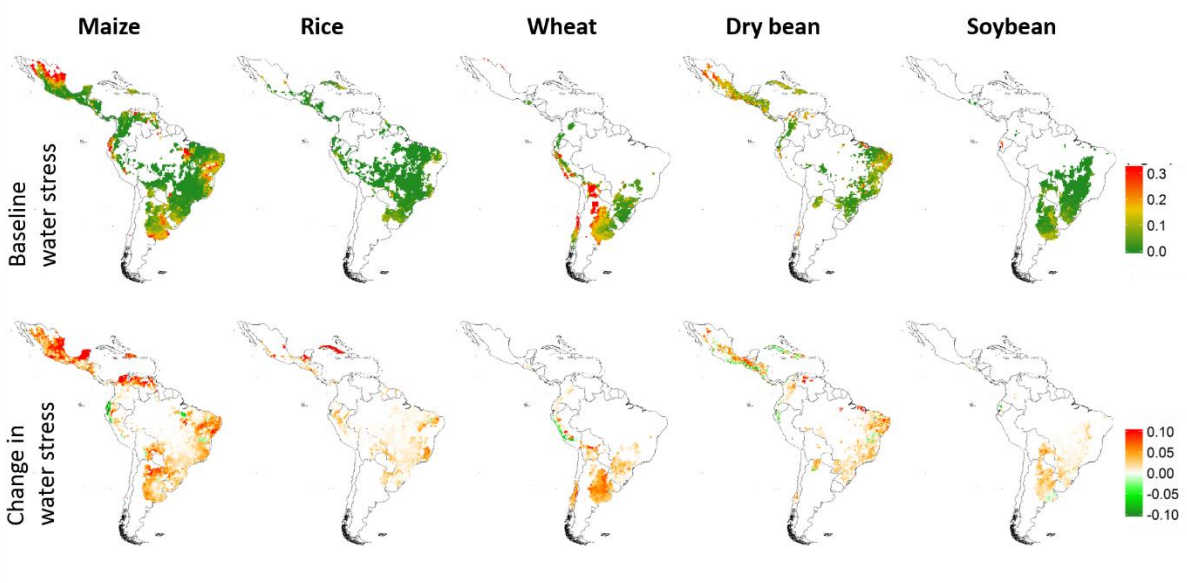

Figure 9. Water stress indices for rain-fed simulations. Actual indices in the historical period (top row) and mean changes in absolute values of index between historical and future periods (bottom row).

Baseline values of nitrogen stress (Figure 10) are shown to be high (> 0.3) across most production areas for rain-fed production of the five crops, with the exception of maize in Ecuador, Colombia, Venezuela and Mexico, rice in Cuba, wheat in Argentina and Uruguay, dry bean in parts of Brazil and Cuba, and soybean in Argentina and southern Brazil. Areas of low nitrogen stress roughly coincide with areas of high historical yields (see Figure 6).

Future climate conditions are projected to bring a decrease in nitrogen stress for almost all growing areas, with especially strong reductions for maize and dry bean, likely due to their nitrogen-fixing capacity (cf.

Fuhrer 2003; Vitousek et al. 2013). The other crops show modest reductions, and even small increases in stress in southern Brazil for rice and Argentina for wheat, implying that the high baseline nitrogen stress will remain in many areas, especially for rice and soybean in Brazil, without the addition of more N inputs to the system. The reductions in nitrogen stress shown here may be related to more vigorous growth earlier in the season, along with shortened durations and reduced stress at the end of the season (cf. Rosenzweig et al. 2014; Webber et al. 2015). These reductions may also be associated with reduced losses from leaching and runoff, due to drying and less frequent precipitation in many areas.

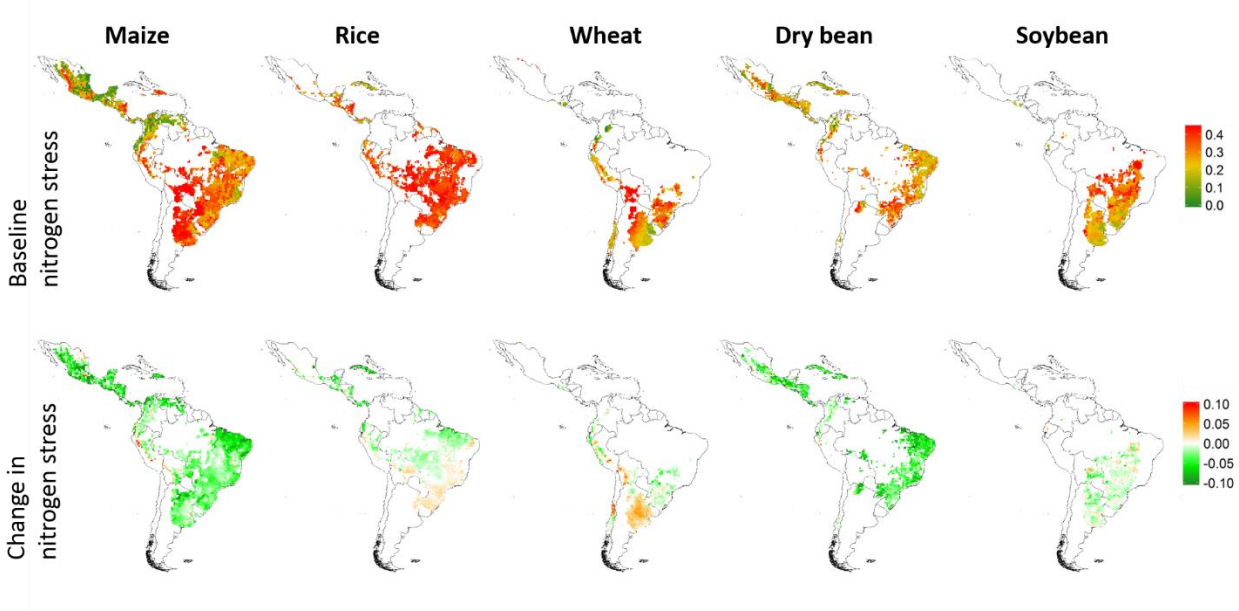

Figure 10. Nitrogen stress indices for rain-fed simulations. Actual indices in the historical period top row), and mean absolute changes between historical and future periods (bottom row).

The simulated changes in duration and nitrogen and water stress shown here can help to explain the yield changes shown in Figure 6. Increases in water and nitrogen stress are generally associated with yield reductions, although final yield changes reflect the influence of many competing factors, some of which were not analyzed here (Ramirez-Villegas 2014; Asseng et al. 2014; Rosenzweig et al. 2014; Lesk et al. 2016; Webber et al. 2015). For most crops and crop varieties, shorter durations are associated with lower yields due to longer periods of time for grain-filling. In this study, DSSAT simulations show this relationship between duration and yields for all crops except rice, for which reductions in duration are associated with yield increases (Figure A16 in the appendix). It may be that rice grains cannot grow larger than some limit, and yields are therefore more directly associated with grain number set at flowering time, rather than grain size for this crop. It could also be possible that rice productivity is more nitrogen limited than water or radiation limited, and thus the yield increases are more related with the projected reductions in nitrogen stress shown in Figure 10.

The spatial patterns of yield reductions for rain-fed maize are correlated with increases in water stress, particularly for Mexico, northern South America, north-east Brazil and Argentina (Elliott et al. 2014). The shortened durations across cultivation areas are also likely contributing to more generalized yield reductions (Asseng et al. 2013a; Bassu et al. 2014; Li et al. 2015). Yield decreases for wheat in Argentina and southern Brazil are primarily associated with increases in water stress, although shortened durations and increased nitrogen stress in Argentina also contribute (also see Asseng et al. 2013b). The strongest

decreases in crop duration for dry bean are seen in the mountainous regions of the Andes and Central America, which can help to explain yield decreases in Colombia and Central America (also see Jones and Thornton 2003). However, in Ecuador, Venezuela and northeast Brazil, yield changes are most influenced by changes in water stress.

In contrast to the other crops, rain-fed rice shows yield increases in the vast majority of cultivation areas. Research on climate change impacts on rice productivity for rice is scarce; however, positive climate change impacts on rice in tropical areas at low levels of warming have been reported elsewhere (Porter et al. 2014; Rosenzweig et al. 2014). These increases can be explained by the following factors: cultivar-specific temperature optima that are higher than baseline temperatures in many areas, reduced durations which have a minimal or even positive effect on yields, and increases in radiation which improves yields in radiation-limited tropical systems. In addition, the fact that this study analyses near-term climate change means that heat stress does not constitute a constraint to future rice productivity (Peng et al. 2004; van Oort et al. 2015). Yield decreases are seen in a few areas (Cuba, southern Mexico and isolated areas in eastern Brazil) for rain-fed rice, which are likely associated with increases in water stress out-weighing the impact of other factors in these areas.

3.3.3 Identification of hotspots at FPU scale

In examining the observed changes throughout Latin America and Caribbean, it is clear that certain cropping systems and areas are more vulnerable to the effects of climate change than others. From a food security standpoint, increases in inter-annual variability (IAV) may be as equally concerning as declines in long-term mean yields (Wheeler and von Braun 2013). Therefore, in order to identify "hotspots" where both mean yields are declining and IAV is increasing, we aggregated results to the FPU scale and plotted changes in yield vs. changes in IAV. We defined and labeled as hotspots, those FPUs showing declines in mean yield greater than -25% and increases in IAV of more than 10%. These cutoffs were chosen as they usually represent the upper bounds of yield or variability changes in impact studies (see Asseng et al. 2013a; Porter et al. 2014; Challinor et al. 2014).

The analysis of hotspots identified a different number of FPUs per crop system and, for some systems (i.e. rain-fed wheat, rain-fed and irrigated soybean), it suggested that no FPUs are climate change hotspots. The results of the analysis are shown in Figure 11 and Table 7. We note that the number of FPUs is largely a result of the geography of the crop and, more specifically, the location and coverage of the crop across the region.

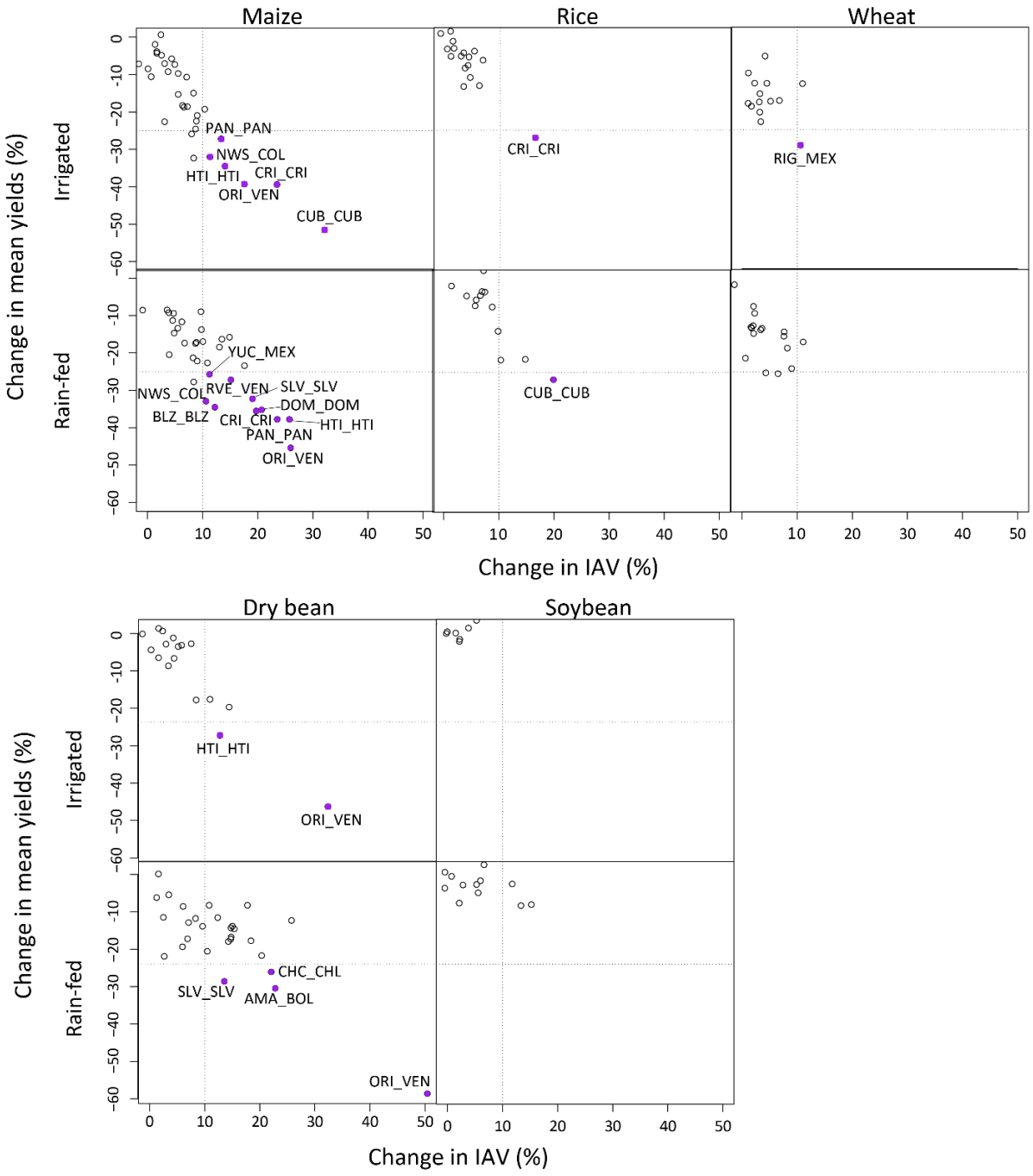

Figure 11. Increases in inter-annual variability (IAV) vs. decreases in mean yields for yields aggregated to the FPU scale. Decreases in IAV and increases in mean yields are not shown. The highlighted FPUs are identified as "hotspots", in which IAV increases 10% or more and mean yields decrease by 25% or more.

Maize, both for irrigated and rain-fed systems, has the largest number of FPUs defined as hotspots throughout Latin America and the Caribbean (Figure 11). For maize, the 6 irrigated FPUs and 10 rain-fed FPUs identified as hotspots are all located in the drying areas of the Caribbean, Central America and northern South America, principally in Mexico, Belize, El Salvador, Costa Rica, Panama, Haiti, the Dominican Republic, Cuba, Colombia and Venezuela. Together these represent 14% of the harvested area for rain-fed maize in Latin America and the Caribbean, but only 4% of irrigated area. The few areas in this

general vicinity not identified as hotspots are in Guatemala, Honduras and Nicaragua, which contain a mix of humid and drier areas. Strong yield reductions in parts of Mexico for rain-fed maize are not accompanied by strong increases in IAV, and are therefore not technically considered as hotspots here. However, there are important vulnerabilities in sub-FPU areas these regions (see Figure 7).

The cropping system with the second largest number of FPUs identified as hotspots is rain-fed dry bean. Hotspots for bean are located in two major producer countries: Venezuela for irrigated and rain-fed systems and El Salvador for rain-fed. Beans have been identified in previous studies as a highly climate change sensitive crop (Beebe et al. 2011; Ramirez-Cabral et al. 2016). Additional hotspots are in Bolivia and Chile for rain-fed systems, and Haiti for irrigated, although harvested area is low in these countries. Although not many studies use the FPU as a unit of reporting, it is noted that the results presented are broadly consistent with the results of Nelson et al. (2010), as reviewed by Wheeler and von Braun (2013).

The only other hotspots identified by this analysis are irrigated rice in Costa Rica, rain-fed rice in Cuba and irrigated wheat in the Rio Grande region of Mexico. While economically important crops for these countries, their total production in Latin America and the Caribbean is relatively small (1% for irrigated rice in Costa Rica, 2% for rain-fed rice in Cuba and 4% for irrigated wheat in the Rio Grande region of Mexico).

Table 7. Continental changes in simulated inter-annual yield variability, expressed as the coefficient of variation (standard deviation/mean yield over a 30-year period), for rainfed and irrigated maize, rice, and soybean. We determined yields and their CVs at the pixel scale, and then aggregated to Latin America, weighted by cultivated areas per pixel. We then calculated the mean, range, and confidence intervals of changes in CV relative to the historical period across GCMs. Significant increases in CV are shown in bold.

	Maize: irrigated	**Maize: rainfed**	**Rice: irrigated**	**Rice: rainfed**	**Soybean: irrigated**	**Soybean: rainfed**
Historical baseline (t/ha): 1971–2000	3.3	4.8	2.1	5.1	2.9	5.6
Multi-model mean (t/ha): 2020–2049	4.3	6.6	2.8	10.5	4.1	8.3
% change (future - baseline)	**1.0**	**1.8**	**0.6**	**5.4**	**1.2**	**2.7**
95% confidence intervals (of % change)	0.4 to 1.6	0.8 to 2.8	0.3 to 1.0	3.6 to 7.1	0.5 to 2.0	1.6 to 3.8

3.3.4 Projected changes at the regional scale

Across the various regions in LAC, the changes in yields at a regional scale are fairly dramatic in percentage terms, e.g. projected declines in irrigated and rain-fed maize in Central America and the Caribbean (CEN)

of around -25% (Figure 12). While some cropping systems, e.g. rice in Brazil and the southern Cone, will likely benefit, in the case of critical staples such as wheat, maize and dry bean, projected declines in yield are nearly universal and independent of whether the systems are irrigated or not.

Declines in rain-fed yields are generally more severe than declines for irrigated systems due to the influence of increasing water stress in many areas. For maize and dry bean, the strongest declines are projected in Central America and the Caribbean (CEN), the Andean region (AND) and in Brazil (BRA), and especially for rain-fed systems. Rain-fed rice also shows significant declines in CEN. Soybean changes are relatively mild, but still significantly negative in the Andean (AND) and Southern cone (SUR) regions, whereas yield declines of about -15% are predicted for all wheat cropping systems.

At the aggregated Latin American and Caribbean scale, only rice yields are projected to benefit, with all other crops seeing significant yield declines. The differences between crops and regions is because of the interplay between the changes in temperature and precipitation and their interactions with the crop characteristics such as crop duration and crop cardinal temperatures. We refer the reader to Sections 3.3.1 and 3.3.2 for more detailed descriptions and explanations of these projected yield changes.

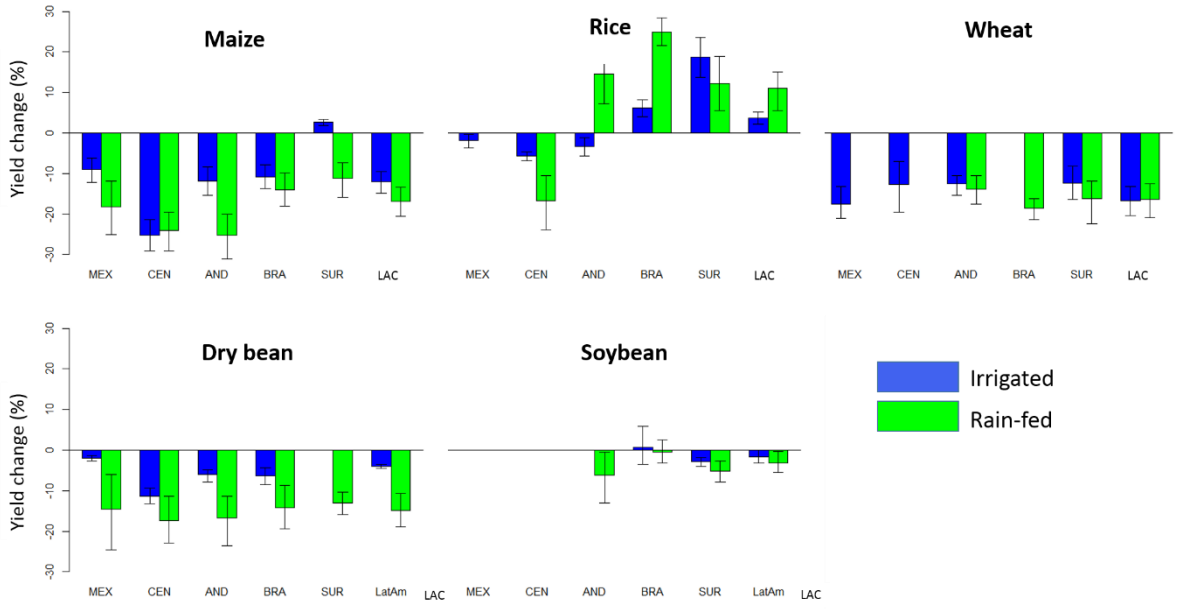

Figure 12. Changes in mean yields, aggregated to the regional scale shown in Figure 3, for irrigated and rain-fed production.

Baseline levels of inter-annual variability differ among cropping systems, with as expected, rain-fed systems having higher levels of IAV than irrigated (Figure 12). The most variable systems are rain-fed rice and soybean in AND, rice and wheat in SUR, and dry bean in MEX, which start out with baseline IAV of between 20 and 30%. (It should be noted however that inter-annual variability at the aggregated spatial scale will tend to average out across regions that contain cultivation areas with varying climate zones.)

Nearly all regions and crops will see significant increases in inter-annual variability for both rain-fed and irrigated systems (Figure 13). Although the increases tend to be more dramatic in rain-fed systems, even small increases in IAV in irrigated systems imply that the overall volatility associated with the production of these commodities in Latin America and the Caribbean is expected to increase.

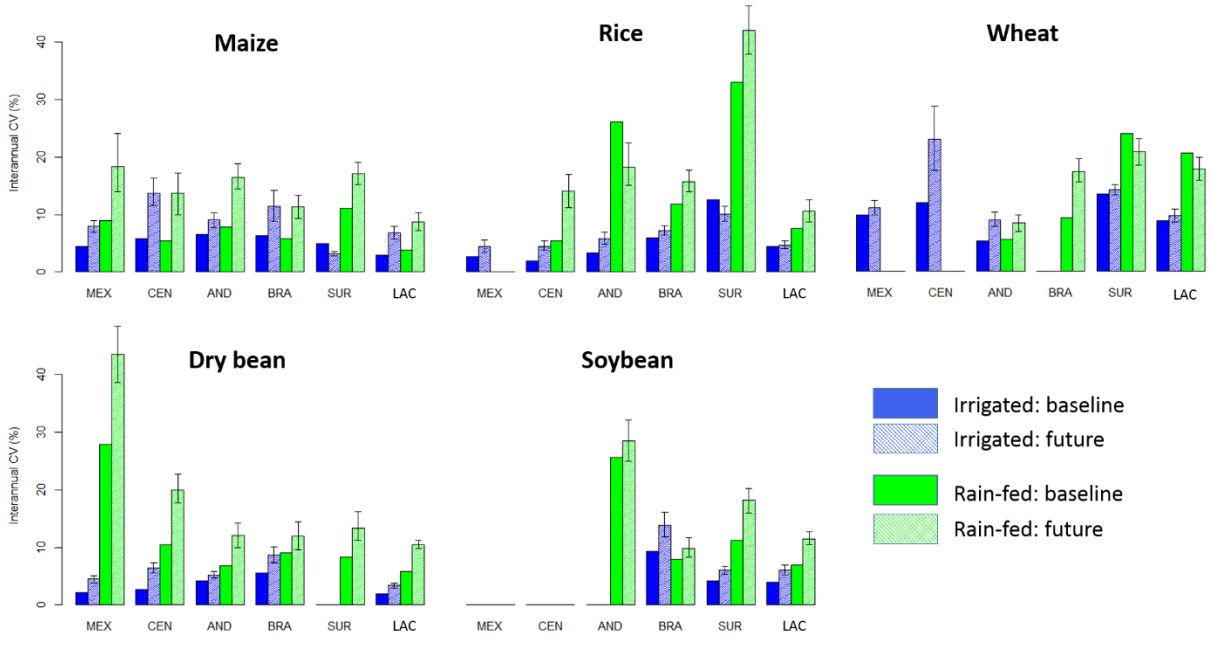

Figure 13. Inter-annual variability values at the aggregated regional scale for rain-fed and irrigated production in both the historical and future periods.

3.4 Results of EcoCrop crop model simulations

3.4.1 Model performance in predicting suitability

When using an empirical model parameterized based on statistical evidence such as EcoCrop, it is useful to compare the model output with a benchmark dataset. Here, EcoCrop predictions of suitable area are compared with the SPAM database of crop physical area (see Figure A6 in the Appendix), using the metric of the area under the ROC curve (AUC), a measure of the accuracy to discriminate presences and absences, as previously described in Section 2.4. The results of the AUC analysis are shown in Table 6.

The AUC values indicate reasonable accuracy (AUC ≥ 0.7) for five of the seven crops: banana, cassava, *Coffea robusta*, sugarcane and potato. The other two crops show AUC higher than 0.6, implying that the agreement between EcoCrop and the SPAM database for all crops is higher than random guessing (Rippke, 2014). The highest values of this metric are seen for cassava and potato, followed by banana, *Coffea robusta* and sugarcane, and with the lowest values for yam and *Coffea arabica*. Differences in AUC can be due to a number of reasons, including the length of the cycle of the crop, the quality of the SPAM data, the extent to which the observed crop distribution follows the potential niche of the crop (Challinor et al. 2015). For instance, relatively low values for arabica coffee may be attributed to the fact that it is a perennial crop whose range is sometimes restricted by national regulations (Ramirez-Villegas et al. 2013; Bunn et al. 2014). In agreement with previous studies, EcoCrop compared well with observed crop distribution databases (Ramirez-Villegas et al. 2013; Challinor et al. 2015).

Table 8. Value of area under the ROC curve (AUC), characterizing correspondence between SPAM physical area and suitable areas estimated by EcoCrop.

Crop	AUC
Banana	0.76
Yam	0.63
Coffea arabica	0.61
Cassava	0.82
Coffea robusta	0.78
Sugarcane	0.74
Potato	0.83

The high correspondence for cassava can potentially be explained by the broad distribution of this crop throughout Latin America and the Caribbean, along with correspondingly widespread suitability predicted by EcoCrop. Potato has a difference of just 5 degrees in the optimum temperature range (from 12.4 ˚C to 17.8 ˚C), which reduces the suitable area to very specific regions which are either mountainous or with low temperatures in temperate climates (Schafleitner et al. 2011; Hijmans 2001). In this case, the predicted areas from EcoCrop for potato are relatively consistent with actual cultivation areas in SPAM.

For banana and sugarcane, the suitability maps broadly coincide with the harvested area distribution, although with some lack of correspondence in the north of Argentina, where SPAM shows some harvested areas which are not climatically suitable according to EcoCrop (Figure 13, 14, and A6 in the appendix). Further analysis showed that the principal restriction for these crops is the lack of temperature suitability

in this region, which points to an area of improvement for EcoCrop with regards to perennial crops (also see discussion in Ramirez-Villegas et al. 2013). The model evaluates temperature suitability by comparing the month with the minimum temperature to a set of specified temperature ranges. However, many perennial crops can survive a month or two of low or high temperatures outside their ranges and still remain productive (Yamori et al. 2014; Eccel et al. 2009; Diamond et al. 2012). For this reason, EcoCrop may underestimate their overall climatic suitability, as seen here to some extent for banana and sugarcane.

The suitability map for *Coffea robusta* (Figure 16) has an overall good correspondence with the physical area map from SPAM (AUC=0.78), except in the eastern part of Brazil where the rainfall is lower than the absolute minimum (Rmin) precipitation values defined for the model. In those regions, according with WFD, the annual rainfall is between 900 mm and 1300 mm however the minimum optimum rainfall defined for *Coffea robusta* was 1700 mm. In this area, more drought-tolerant varieties are likely planted. However, since only one set of representative parameters was used across Latin America and the Caribbean for each crop, EcoCrop is limited in its ability to simulate regional variation in cultivars (see discussion in Ramirez-Villegas et al. 2013).

In the case of *Coffea arabica* (Figure 15) and yam (Figure 19), the low values of AUC (0.61 and 0.63 respectively) appear to correspond to the low predicted suitability for both crops in Brazil in comparison with the registered data in the SPAM dataset. For *Coffea arabica*, the principal restriction is the temperature suitability due to the relatively narrow range between the minimum and maximum optimum temperature, and also biased temperatures in mountainous areas for the EcoCrop runs due to the averaging effect for the 50 km grid-cell size. The narrow range for the cardinal temperatures in *Coffea arabica* creates a difference with *Coffea robusta*; then while *Coffea robusta* has 8 ˚C between the minimum and maximum optimum temperature, *Coffea arabica* just has 5 ˚C (Bunn et al. 2014, 2015). There is a similar situation with the difference between the minimum and maximum temperature for those crops with 9 and 21 ˚C for *Coffea arabica* and *Coffea robusta*, respectively.

Yam appears to have its principal restriction due to rainfall, which in many cases is less than the minimum optimum rainfall parameter value (RopMin). In the case of Brazil, it is likely that drought-tolerant cultivars allow yam to be planted in dry areas according to SPAM.

3.4.2 Projected changes in suitable area by crop

The previous section illustrates the agreement between EcoCrop and SPAM for each of the seven crops included in the analysis. This section shows the high degree of heterogeneity in suitability, both geographically and by crop under the current climate, and explains the suitability changes that can be expected under future climate conditions. The section first presents suitability results aggregated for each crop to the regions shown in Figure 3 and to the aggregated Latin American and Caribbean scale. Maps of current and future suitability, and pixel-level changes (both quantitative and categorical) are then shown for assessing spatial patterns. These maps reflect the combined temperature and precipitation suitability, although the independent effects of temperature and precipitation in EcoCrop are shown for each crop in Figures A16-22 in the appendix. Detailed descriptions and explanations of driving biophysical factors are all provided when presenting the crop-specific results.

At the regional scale, banana, *Coffea robusta* and *C. arabica* show significant decreases in all tropical regions (CEN, AND and BRA) across GCM future climate scenarios, while potato shows significant

decreases in the more temperate latitudes (MEX and SUR; Figure 14, Table 9). Suitability changes for potato in the Andean region (AND) are not significant, given that there are areas that are both gaining and losing suitability. In line with previous studies (see Ceballos et al. 2011), cassava has significant increases in suitable area in Brazil (BRA) and the southern cone (SUR).

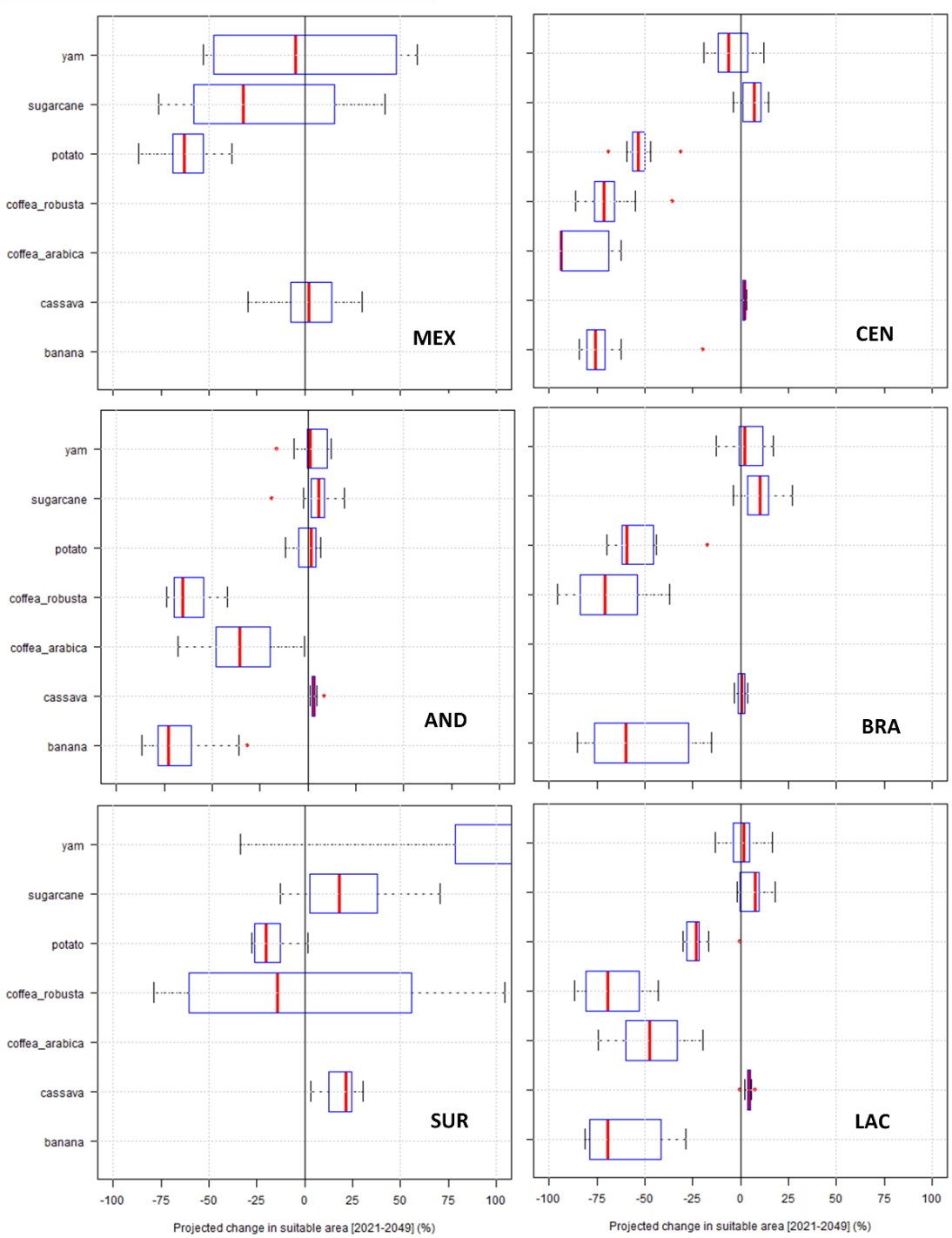

Figure 14. Projected changes from EcoCrop in total suitable area between the historical and future periods for all crops aggregated to the regions shown in Figure 3. Only crop/region combinations with at least 6,200 km^2 of suitable area are shown here. Boxplots show the spread in results across the various GCMs.

Table 9. Current and future period suitable areas by crop and region, along with the mean suitability change between historical and future periods. Suitable areas are averaged across years and GCM's (for the future period) and aggregated to the regions shown in Figure 3. Also shown are the bootstrapped confidence intervals across the 10 GCMs for the mean suitability change.

Crop	Region	Current area (km^2)	Future area (km^2)	Mean suitability change (%)	95% confidence intervals on suitability change	
					Lower	Upper
banana	AND	1,125,217	391,755	-65.2	-75.8	-52.5
	BRA	3,596,320	1,652,318	-54.1	-68.4	-40.8
	CEN	812,731	245,405	-69.8	-78.6	-57.2
	LAC	**6,002,842**	**2,371,832**	**-60.5**	**-69.4**	**-49.4**
cassava	AND	2,117,887	2,187,412	3.3	2.3	4.8
	BRA	5,678,332	5,715,860	0.7	-0.5	2.1
	CEN	1,279,167	1,301,648	1.8	1.2	2.2
	MEX	345,085	353,906	2.6	-8.0	10.1
	SUR	970,514	1,152,064	18.7	12.7	23.1
	LAC	**11,291,364**	**11,750,781**	**4.1**	**2.6**	**5.0**
C. arabica	AND	172,149	112,301	-34.8	-44.3	-24.7
	CEN	47,635	8,290	-82.6	-90.6	-74.8
	LAC	**229,037**	**121,276**	**-47.0**	**-57.8**	**-36.0**
C. robusta	AND	1,124,430	442,310	-60.7	-67.3	-53.9
	BRA	3,586,148	1,135,947	-68.3	-80.2	-58.0
	CEN	654,090	210,443	-67.8	-75.1	-58.5
	SUR	78,988	78,205	-1.0	-40.2	40.6
	LAC	**5,708,976**	**1,907,053**	**-66.6**	**-74.8**	**-58.4**
potato	AND	591,539	587,123	-0.7	-4.0	2.3
	BRA	348,149	162,656	-53.3	-60.8	-43.9
	CEN	94,583	44,878	-52.6	-59.2	-46.7
	MEX	231,106	91,499	-60.4	-69.1	-51.0
	SUR	1,444,062	1,183,761	-18.0	-23.5	-10.8
	LAC	**3,125,658**	**2,448,483**	**-21.7**	**-26.3**	**-15.8**
sugarcane	AND	1,009,777	1,044,955	3.5	-3.5	9.5
	BRA	3,183,999	3,521,770	10.6	4.7	16.8
	CEN	702,346	743,539	5.9	2.1	9.2
	MEX	110,557	84,751	-23.3	-47.5	4.0
	SUR	112,151	135,907	21.2	7.0	34.0
	LAC	**5,610,761**	**5,994,211**	**6.8**	**1.8**	**10.7**
yam	AND	1,473,330	1,495,158	1.5	-4.5	6.7
	BRA	4,135,570	4,294,851	3.9	-1.5	9.1
	CEN	976,862	933,846	-4.4	-9.9	1.7
	MEX	54,780	54,269	-0.9	-31.1	28.3
	SUR	42,966	119,492	178.1	82.6	279.4
	LAC	**7,260,107**	**7,396,969**	**1.9**	**-3.5**	**7.3**

All changes for yam and sugarcane are shown to be insignificant across climate modeling scenarios at the regional scale, although some gains in area are seen for both crops in the southern cone (SUR). At the aggregated scale for Latin America and the Caribbean (Figure 4, Table 9), banana, *C. robusta* and *C. arabica*, and potato are all shown to have significant and substantial decreases in suitable area, with area reductions of -61, -67, -47 and -22% respectively. Cassava and sugarcane show modest increases in area (of 4 and 7% respectively), whereas overall changes in yam suitable area are not significant across the climate scenarios. For all crops, changes of similar direction have been projected in previous global (Bunn et al. 2014, 2015; Lobell et al. 2008; Beebe et al. 2011; Ceballos et al. 2011; Schafleitner et al. 2011, amongst others).

The region with more crops decreasing their suitable area is Central America and the Caribbean (CEN) followed by Brazil and northern South America (BRA) and the Andean region (AND) (Figure 14). In contrast, the Southern Cone (SUR) shows an increase in suitable areas to grow crops as yam, cassava and sugarcane; however, this increase of suitability is accompanied by a high variability between GCMs and could be not significant due to the few areas currently suitable for those crops in that region.

Sugarcane shows both increases and decreases in suitability throughout Latin America and the Caribbean (Figure 15). Increases in suitable area are evident in parts of Brazil, the Andean region and a few areas in Central America and the Caribbean. Losses in climatic suitability for this crop are found in areas that are drying, namely, the Yucatán peninsula of Mexico, the Caribbean, northern South America and northeast Brazil. While some parts of eastern Brazil show losses, there are more areas in Brazil that preserve or increase climatic suitability for this crop because of local variation in future precipitation and due to an increase of temperature suitability in the Southeast of Brazil in contrast to a decrease in rainfall suitability in the Northeast (Figure A18 in the appendix). For Brazil, Marin et al. (2013) and Lobell et al. (2008) also report positive climate change impacts on sugarcane, and a similar result is presented by Ramirez-Villegas et al. (2012) for Colombia. Some areas in the Andean region (Ecuador and Bolivia) and south of Brazil show increases in suitability due to increasing maximum temperatures and greater temperature and precipitation suitability (Figure A18). Among all the crops analyzed here, sugarcane presents the highest dispersion in climatic suitability values, especially in Mexico, where many parts lose suitability while others maintain or even increase suitability. The same behavior is seen in Bolivia and Brazil, where nearby zones have losses and increases in suitability for the same reasons as above. In the case of Mexico, it is a result of increases of temperature suitability but decrease of precipitation suitability in some regions. Additionally, in some zones there is an increase of temperature suitability without a change in the precipitation suitability, which has as effect an overall suitability increase (Figure A18).

Results for banana show the potential for larger losses in suitable areas across the region (Figure 16). Areas with particularly large losses in suitability are in the Caribbean, Central America, central and north of Brazil, and northern parts of Colombia and Venezuela, while some increases in suitability are shown in southern Brazil, and parts of Colombia and Honduras. For Colombia, Ramirez-Villegas et al. (2012) showed banana as a vulnerable crop to climate change. The decline of suitability for banana is principally related to the fact that the optimal temperature range is only 3 ˚C wide (Table 4), and that most of the regions with current suitability of banana will have between 2 and 4 ˚C of temperature increase (also see Ramirez et al. 2011; Van den Bergh et al. 2012; Turner 1998). It is possible that the cultivars tend to be regionally specific for banana, which is not possible to capture with one set of parameters. The increases of suitability are also related with greater values for temperature suitability (see Figure A-19) as result of the increase of temperature for those regions (Figure 4).

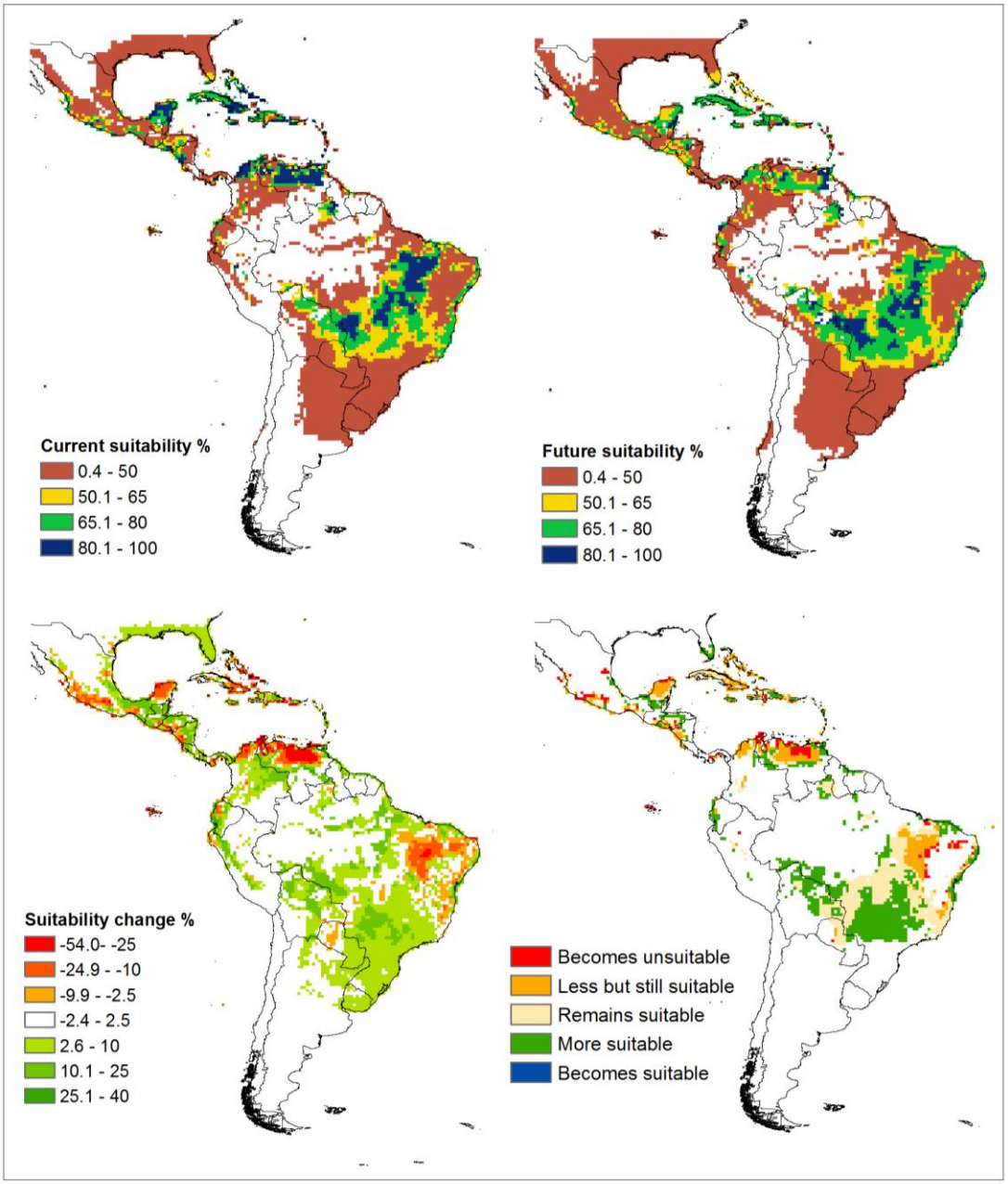

Figure 15. Results of EcoCrop runs for sugarcane. Subplots show current suitability, future suitability, difference in suitability (future – current), and categorical changes in suitability relative to a threshold of 50% (see Methods). Suitable areas were defined as having suitability values greater than that threshold.

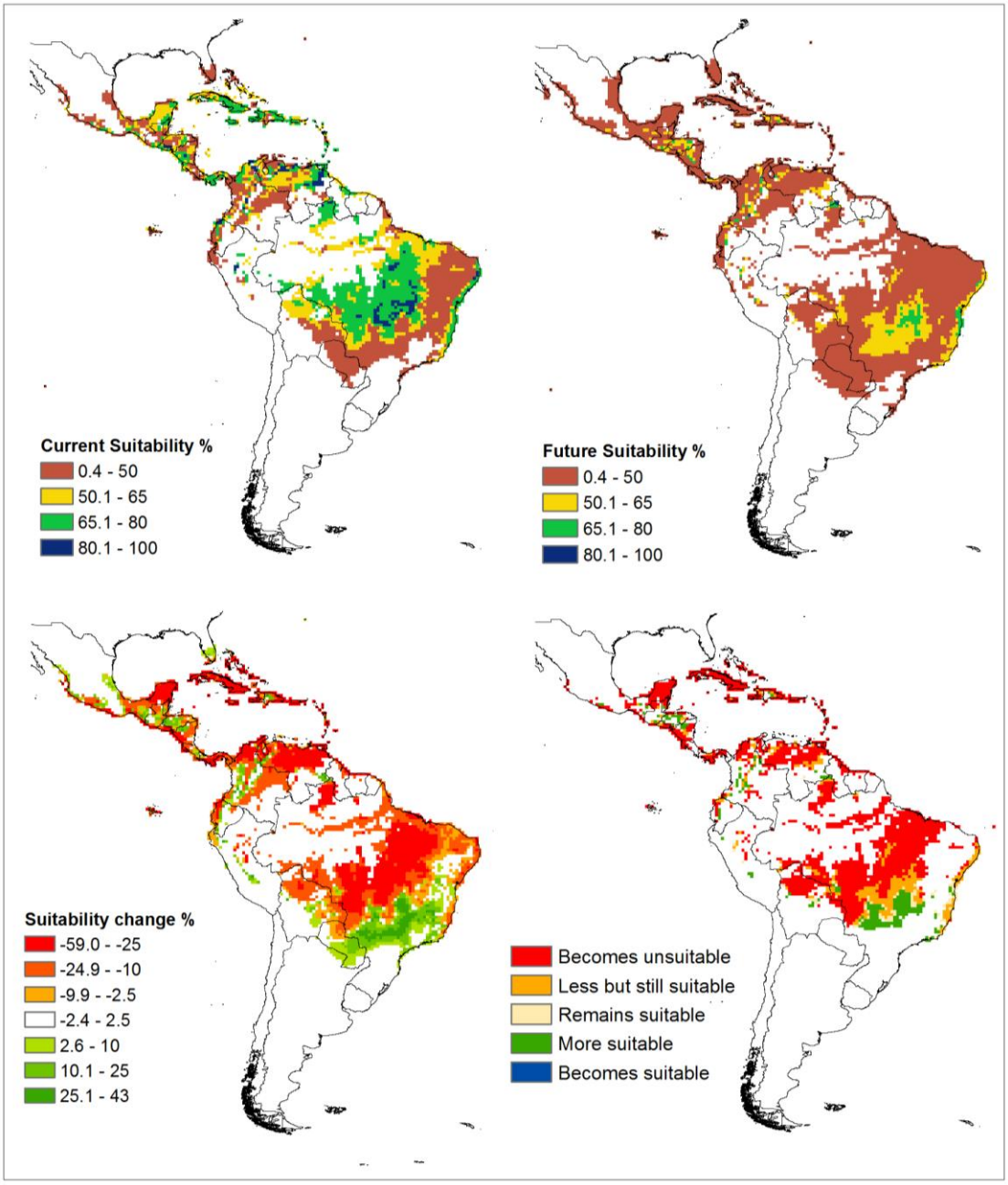

Figure 16. Results of EcoCrop runs for banana. Subplots show current suitability, future suitability, difference in suitability (future – current), and categorical changes in suitability relative to a threshold of 50%.

Coffea arabica shows significant losses in suitability in countries such as Colombia, Peru, Ecuador, and Mexico, for which *Coffea arabica* is an economically important product (Figure 17). The losses in suitability in current cultivation areas are due to the increase of temperature in these regions between 2 and 3 ˚C (see Figure A15). *Coffea arabica* is similar to banana in the sense that the narrow range of the optimum temperatures implies that projected temperature increases have a high effect on the suitability of the crop. The loss in suitability shown here is consistent with the most recent findings regarding the effects of climate change on global coffee production (Ovalle-Rivera et al., 2015; Bunn et al. 2014, 2015).

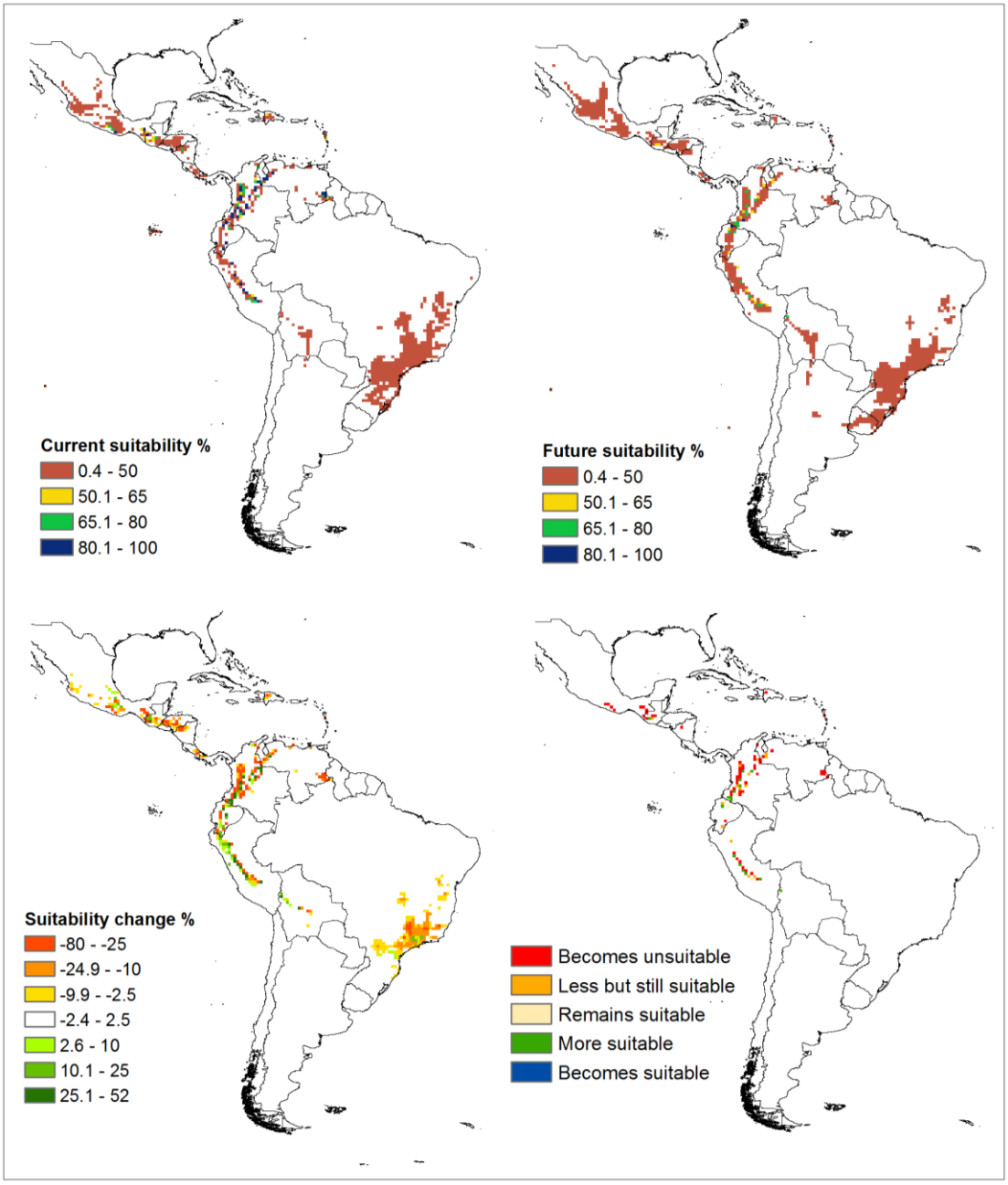

Figure 17. Results of EcoCrop runs for *Coffea arabica*. Subplots show current suitability, future suitability, difference in suitability (future – current), and categorical changes in suitability relative to a threshold of 50%.

Coffea robusta shows much broader climatic suitability across the region than *Coffea arabica* in the historical period (Figure 18), although drastic reductions in suitability in the future period are shown here across Brazil, Bolivia, Colombia, Venezuela and throughout Central America and the Caribbean. These reductions in suitable are related with losses in temperature suitability, as for *Coffea arabica* (Figure A16 in the appendix) (also see Bunn et al. 2014, 2015).

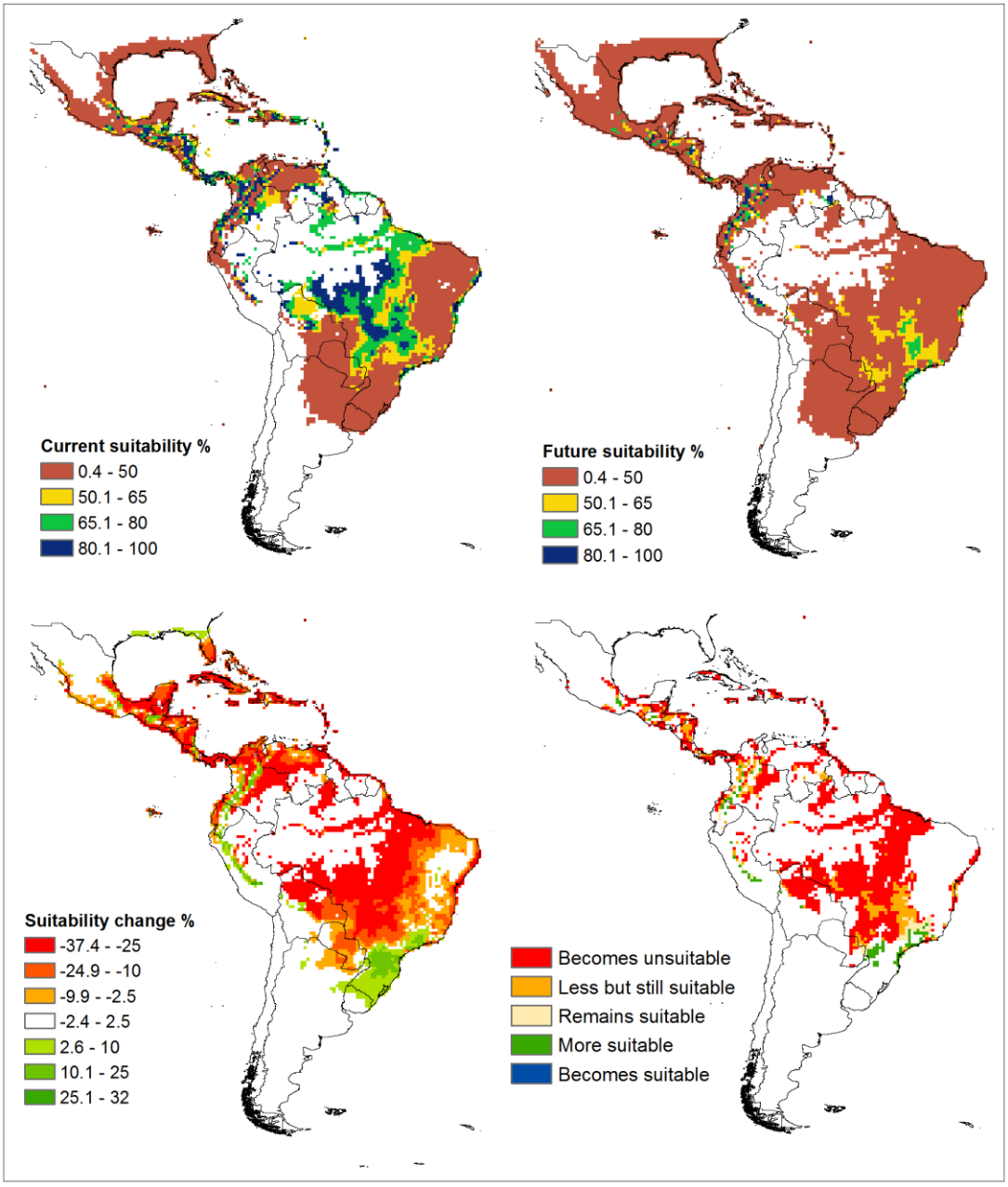

Figure 18. Results of EcoCrop runs for *Coffea robusta*. Subplots show current suitability, future suitability, difference in suitability (future – current), and categorical changes in suitability relative to a threshold of 50%.

Potato has an increase of suitability in some areas of Bolivia, Peru, northern Argentina and southern Chile due to increasing temperatures in areas previously too cold to grow potato (Figure 19, Figure A22 in the appendix) (Schafleitner et al. 2011; Hijmans 2001, 2003). However, increasing temperatures also lead to reductions in suitability in the south of Brazil, Paraguay, northern Argentina and the highlands of Colombia and Mexico (Schafleitner et al. 2011).

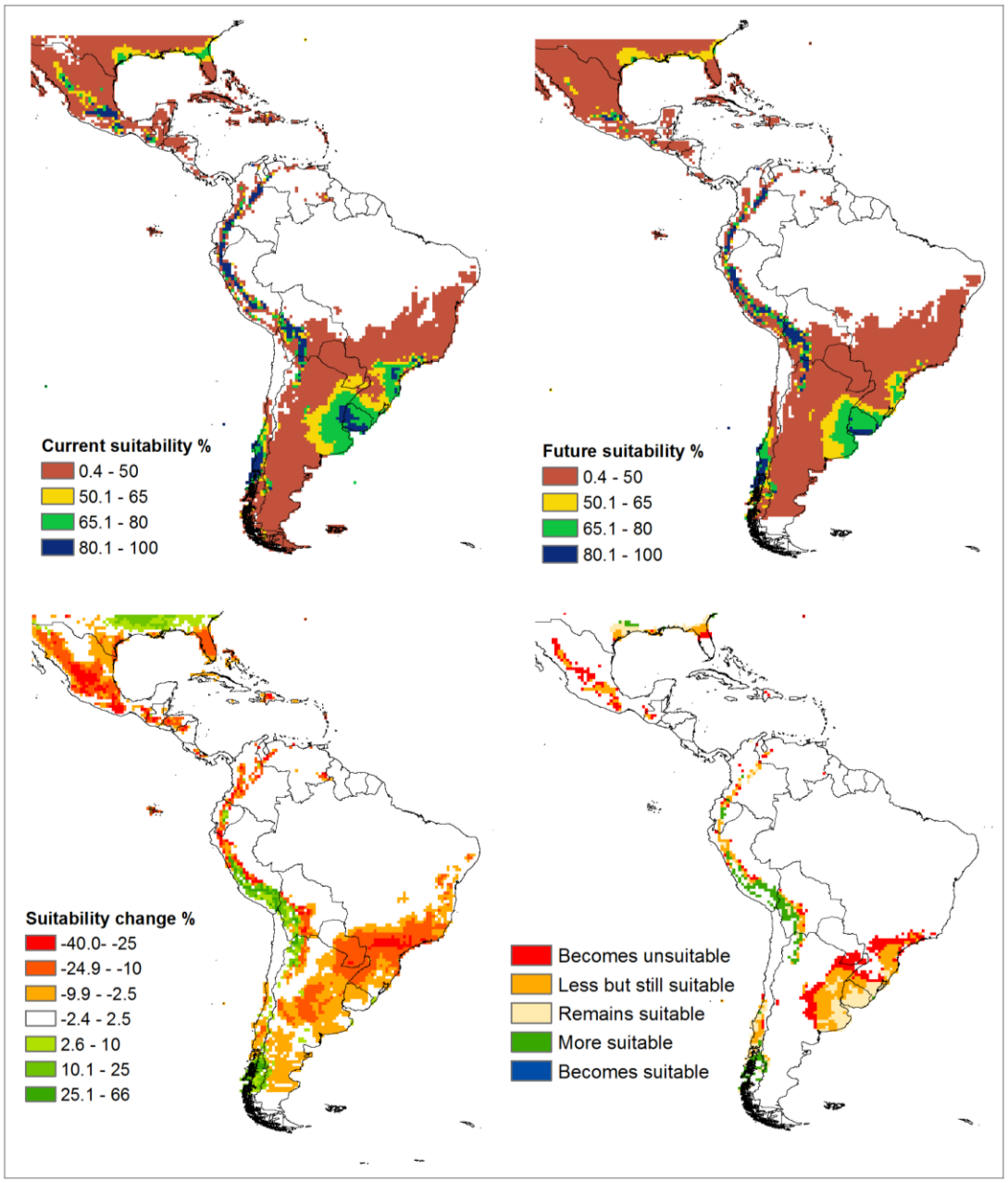

Figure 19. Results of EcoCrop runs for potato. Subplots show current suitability, future suitability, difference in suitability (future – current), and categorical changes in suitability relative to a threshold of 50%.

In general, the staple crops that are widely cultivated in the region, but with less commercial importance (i.e. cassava and yams; Figure 20 and 21) show less significant decreases in climatic suitability. Research on yam is scarce, but the study of Ceballos et al. (2011) for cassava shows similar results to those reported here. Both crops have broad ranges of temperature suitability, with a span of 10 and 9 ˚C respectively within the optimal temperature ranges. This flexibility helps to illustrate why these crops are important for ensuring food security in many areas. Crop physiology studies of cassava's climate sensitivity support the fact that cassava would outperform most crops under climate change (Rosenthal et al. 2012; Bellotti et al. 2012; El-Sharkawy 2014). Cassava cultivation, especially, has the fewest losses in climatic suitability throughout Latin America and the Caribbean under future climate conditions, and the results for this crop

also show the least variability across GCMs (Figure 20 and Table 7). Cassava and yams both increase in suitability in southern Brazil, northern Argentina and parts of the Andes and Central America due to the increase of temperature in these regions (figures A23 and A24 in the appendix). In contrast to cassava, yam shows losses in current cultivation areas in the Caribbean, Central America, northern South America, and parts of Brazil due to this drying in these areas (Figure 21).

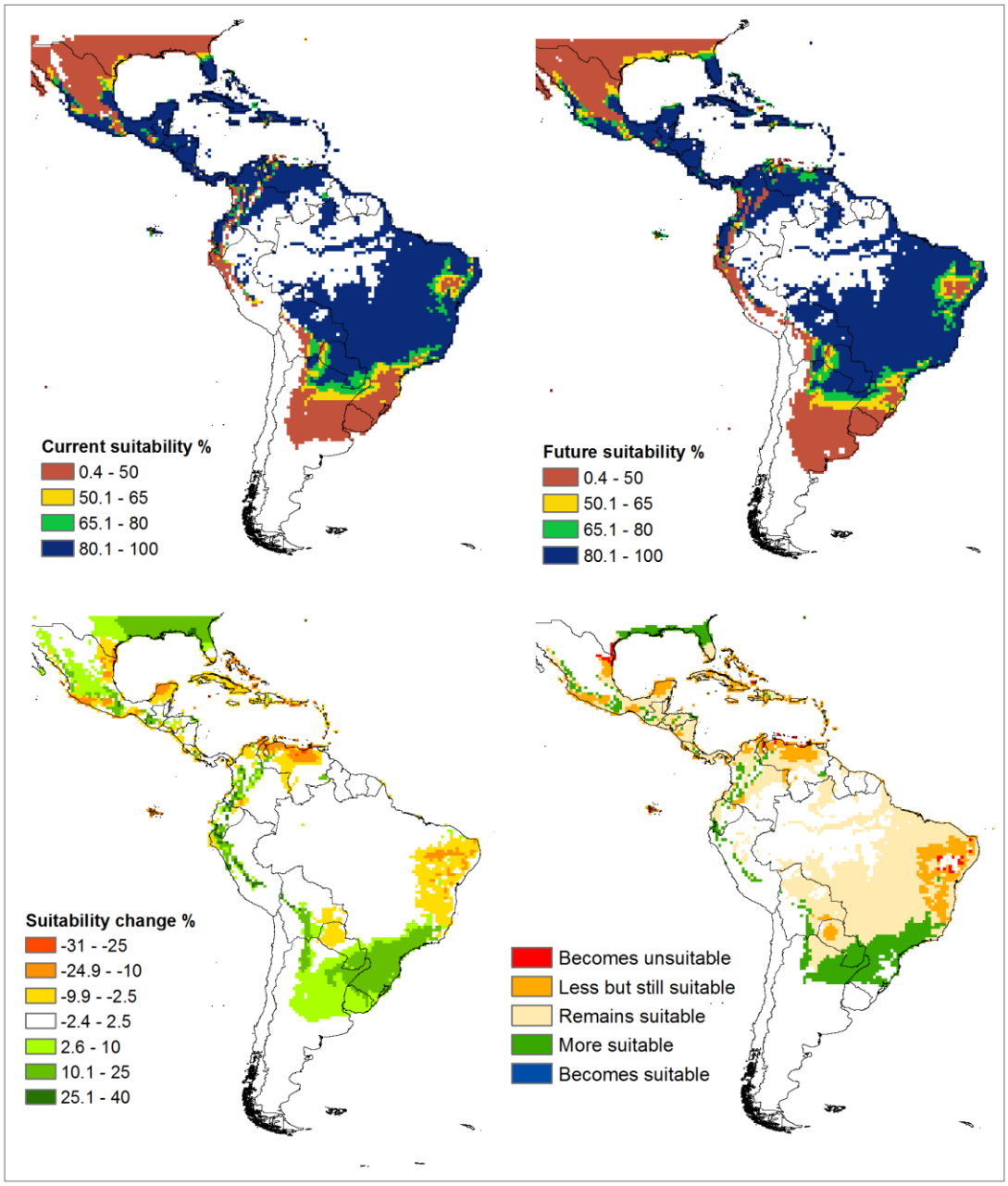

Figure 20. Results of EcoCrop runs for cassava. Subplots show current suitability, future suitability, difference in suitability (future – current), and categorical changes in suitability relative to a threshold of 50%.

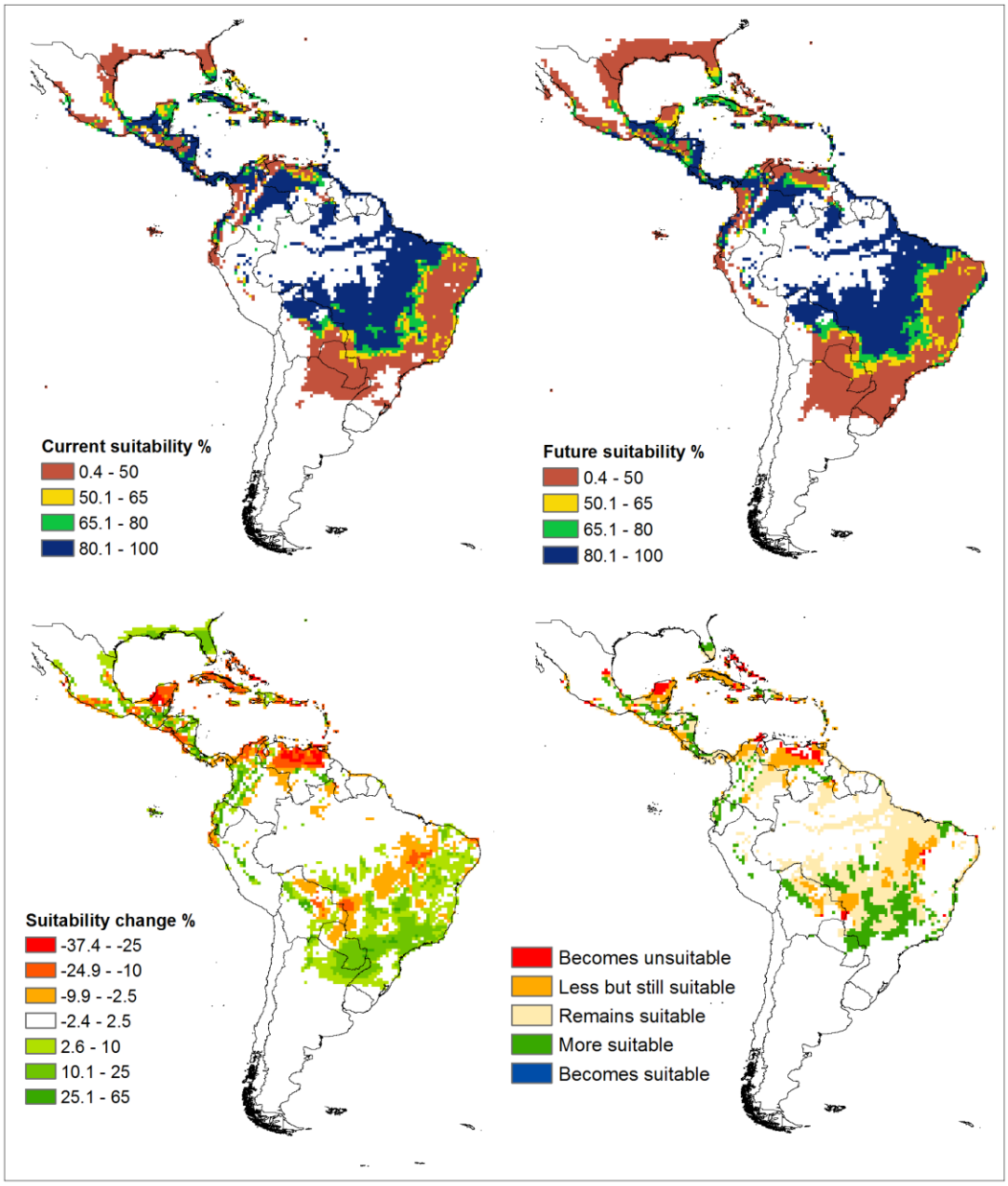

Figure 21. Results of EcoCrop runs for yam. Subplots show current suitability, future suitability, difference in suitability (future – current), and categorical changes in suitability relative to a threshold of 50%.

4 Summary and conclusions

The results of the DSSAT and EcoCrop modeling simulations shown here help to identify cropping systems and regions that will be most affected by long-term progressive climate change. While the magnitude of the yield and suitability changes for some systems shown here may seem drastic, these simulations assume no ongoing adaptation, which is a pessimistic assumption in the real world. However, the results of the analysis can suggest regions and adaptation measures that should be prioritized for investment in the region in order to minimize risks.

The DSSAT simulations show that all cropping systems, with the exception of rice, are likely to experience yield declines at the Latin American scale. Maize, wheat and dry bean are most affected, with less severe yield declines for soybean. Rice may actually benefit across many growing areas due to increases in radiation, warming temperatures and shortened durations that reduce terminal drought stress, which affect this crop differently than the others.

Reduced precipitation along with warming temperatures in northern South America, Mexico, Central America and the Caribbean and northeast Brazil could have severe impacts on rain-fed production of maize and dry bean through increases in seasonal water stress. The most severe hotspots across all cropping systems are identified for both rain-fed and irrigated maize in these areas, as well as for rain-fed dry bean in Venezuela. Rain-fed rice in Cuba could also be severely affected due to drying. Not surprisingly, the Central American and Caribbean region (CEN) had the most severe yield declines across cropping systems compared to the other four regions in Latin America and the Caribbean. These changes are a product of intensifying drought stress during the rainy season. Strong yield declines are also seen for irrigated wheat in Mexico and Argentina, and for rain-fed wheat in Argentina (about 15-20%).

Simulated decreases in yields, especially for rain-fed systems, are generally accompanied by increases in inter-annual variability (IAV). This is partly due to the same absolute variability around a lower mean, but also reflects an increasing variability in weather conditions. Increases in IAV are of concern for the economic stability of farms and could also potentially increase the volatility of regional markets. A better understanding of how to address the projected reductions yield stability in LAC is a topic that warrants more research.

The analysis of DSSAT results also included a discussion of changes in ancillary non-yield variables. We find that, in many cases, changes in yield are, at least in part, a result of shorter growing cycles. With higher temperatures, crop durations are expected to decrease for almost all crops and cultivation areas. This is because development of most crops at any given latitude, which controls photoperiod, is largely dependent on thermal time. That is the hotter it is, the quicker crops mature. Also, for most crops with the exception of rice, shorter life-cycles are associated with lower yields due to a shorter grain-filling period. However, this is a trait that can potentially be addressed through genotypic adaptation by increasing the GDD requirements in the grain-filling stage, or by farmers simply switching to existing longer-duration cultivars.

The complex nature of the soil-plant-atmosphere interaction means that yield changes are both in our modeling and in reality, a product of the interaction between multiple stresses. DSSAT results show that water stress is likely to increase for all crops across the continent, necessitating potential investment in irrigation infrastructure or switching to more drought-tolerant cultivars or crops. Although not considered here, irrigated yields will likely be affected due to reductions in water availability in dry years. An analysis of water availability for irrigated production would necessitate the use of a hydrological model, which is

beyond the scope of this study. DSSAT modeling results also suggests that nitrogen stress for most cropping systems and regions is likely to reduce under future climate conditions, due to shorter durations and reduced leaching. These decreases in nitrogen stress may be counteracting the yield declines due to other factors.

The analyses using the EcoCrop model shows the largest overall losses in suitability for *Coffea Arabica, Coffea Robusta*, banana and potato with -47, -66, -61 and -22% losses in suitable areas, respectively. In contrast, sugarcane, yam and cassava have small gains in suitable areas (7, 2 and 4%). It is important to mention that the crops with the strongest decreases in suitability are perennial crops. The EcoCrop model likely under-estimates suitability for these crops in both the historical and future periods due to their narrow temperature ranges relative to the ability of these crops to withstand short periods outside of their optimal ranges (i.e. plasticity). However, for changes in long-term average conditions (i.e. climate change), it may be that these temperature ranges are still well-defined, and that genotypic adaptation is required to help these crops adapt to more consistent changes in average temperatures.

For most of the crops, the decrease in suitability shown in the EcoCrop results is related to the projected temperature increases. However, for sugarcane, precipitation is the principal factor reducing the suitability, which may be less relevant in areas where sugarcane is irrigated. In the case of cassava and yam, increasing temperatures are helping to expand the limits of high suitability for these crops in southern Brazil and Argentina.

While the results presented here are useable and indicative of future trends, all models have the potential to be improved. In the case of the DSSAT model, work is constantly ongoing, with updates coming from improvement in the representation of processes, better input datasets, and improved availability of trial data to evaluate the model and calibrate varieties. Similarly, future adjustments to include soil data are ongoing for the EcoCrop model. Improvements in the climate models and the bias-correction procedures used to adjust them may also occur in the next years. Therefore, modeling results should be interpreted as being performed with the best available models, methodologies and input data at the current moment, and additional analysis may be warranted in the future as relevant model improvements and access to improved datasets are made available.

It is also worth noting that, as in any model-based analysis, the present work operates in a context of uncertainty. Although a multi-GCM framework is used together with state-of-the-art datasets on management and climate, and in many cases results show robust changes in yields and suitable areas, this analysis is subject to various uncertainties and assumptions. First, the yield analyses are based on a single process-based crop model (DSSAT, Jones et al. 2003), and hence assume that the responses of the crops analyzed are well represented by such a model. Nonetheless, recent work has shown that crop responses to temperature, [CO_2], and precipitation changes can vary substantially across models (e.g., Bassu et al. 2014 for maize, Li et al. 2015 for rice, and Asseng et al. 2013a for wheat). Another key source of uncertainty is the CO_2 fertilization effect, which was not included in the DSSAT simulations here, and may help to mitigate increases in water stress for all rain-fed systems, and increase photosynthesis, biomass and yields due to the CO_2 fertilization effect for all crops (except for maize which has the C4 pathway for photosynthesis). The parameterization of this effect merits both testing and improvement in existing models, including DSSAT (see, e.g., Challinor and Wheeler, 2008; Long et al. 2005, 2006). Further experimental work is also required in order to improve the simulation of crop responses to enhanced atmospheric CO_2 concentrations. Yield levels and projected changes were also seen to be sensitive to cultivar choice in DSSAT. To get a better sense of the magnitude of projected changes, it would be ideal to run 2 or 3 high-yielding representative cultivars in different regions per crop, and then average the

results. The individual cultivar runs could also be used to examine varietal-specific sensitivity to projected climate changes, and to investigate the underlying mechanisms for these differences. Future studies may also conduct sensitivity analyses through targeted simulations with certain stresses `switched off` so as to determine the individual role of different processes on the yield outcomes.

Limitations of niche modeling are also apparent. Foremost, the EcoCrop model uses only monthly means of a prescribed growing season to compute precipitation and temperature suitability. Further research is needed to identify sub-monthly limitations and/or other climatic (e.g. VPD) as well as non-climatic factors (e.g. soil, pest/diseases) that reduce crop suitability (e.g. Zabel et al. 2014). Improvements in EcoCrop's consideration of water stress could also improve its predictions. Despite that, the niche model EcoCrop robustly simulated crop presence across LAC for the 7 crops analyzed.

Despite the simplifications and imperfections inherent in any modeling study, the results of the DSSAT and EcoCrop model simulations shown here highlight regions and crops that are most vulnerable to climate change, and hence can serve to help guide and provided insight into necessary climate change adaptation measures in the agricultural sector throughout Latin America and the Caribbean.

References

Adiku S, Braddock R, Rose C (1996) Modelling the effect of varying soil water on root growth dynamics of annual crops. Plant Soil 185:125–135. doi: 10.1007/bf02257569.

Ahmed KF, Wang G, Yu M, et al. 2015. Potential impact of climate change on cereal crop yield in West Africa. Clim Change 133:321–334. doi: 10.1007/s10584-015-1462-7

Alexandratos, N. and J. Bruinsma. 2012. World agriculture towards 2030/2050: the 2012 revision. ESA Working paper No. 12-03. Rome, FAO.

Allen RJ, Norris JR, Wild M (2013) Evaluation of multidecadal variability in CMIP5 surface solar radiation and inferred underestimation of aerosol direct effects over Europe, China, Japan, and India. J Geophys Res Atmos 118:6311–6336. doi: 10.1002/jgrd.50426.

Ainsworth EA, Leakey ADB, Ort DR, Long SP. 2008. FACE-ing the facts: inconsistencies and interdependence among field, chamber and modeling studies of elevated [CO2] impacts on crop yield and food supply. New Phytol 179:5–9. doi: 10.1111/j.1469-8137.2008.02500.x

Andrews T, Gregory JM, Webb MJ, Taylor KE (2012) Forcing, feedbacks and climate sensitivity in CMIP5 coupled atmosphere-ocean climate models. Geophys Res Lett 39:L09712. doi: 10.1029/2012gl051607.

Asseng S; Ewert F; Rosenzweig C; et al. 2013a. Uncertainty in simulating wheat yields under climate change. Nat. Clim. Change 3:827–832. doi: 10.1038/nclimate1916.

Asseng S, Travasso M, Ludwig F, Magrin G. 2013b. Has climate change opened new opportunities for wheat cropping in Argentina? Clim Change 117:181–196. doi: 10.1007/s10584-012-0553-y

Asseng S, Ewert F, Martre P, et al. 2014. Rising temperatures reduce global wheat production. Nat Clim Chang 5:143–147. doi: 10.1038/nclimate2470

AVA (Agricultura, vulnerabilidad y adaptación). 2013. Análisis interinstitucional y multisectorial de vulnerabilidad y adaptación al cambio climático para el sector agrícola de la cuenca alta del río Cauca, Impactando políticas de adaptación. Reporte técnico: Metodología de análisis de vulnerabilidad para la cuenca alta del río Cauca. 85 p.

Bassu S; Brisson N; Durand J-L; et al. 2014. How do various maize crop models vary in their responses to climate change factors? Glob. Change Biol. 20:2301–2320. doi: 10.1111/gcb.12520.

Bellotti A, Herrera Campo B, Hyman G. 2012. Cassava Production and Pest Management: Present and Potential Threats in a Changing Environment. Trop Plant Biol 5:39–72. doi: 10.1007/s12042-011-9091-4.

Boote K. J., Jones JW; Hoogenboom 1989. Simutating growth and yield response of soybean to temperature and photoperiod. Proc World Soybean Reseach Conf. IV mar 5-9 Buenos Aires, Argentina pp 273 – 278.

Bunn, C., Läderach, P., Ovalle-Rivera, O., & Kirschke, D. 2014. A bitter cup: climate changes profile of global production of Arabica and Robusta coffee. Climatic Change, 1-13.

Bunn C, Läderach P, Pérez Jimenez JG, et al. 2015. Multiclass Classification of Agro-Ecological Zones for Arabica Coffee: An Improved Understanding of the Impacts of Climate Change. PLoS One 10:e0140490. doi: 10.1371/journal.pone.0140490.

Cairns JE, Hellin J, Sonder K, et al. (2013) Adapting maize production to climate change in sub-Saharan Africa. Food Secur 5:345–360. doi: 10.1007/s12571-013-0256-x.

Cassman KG (1999) Ecological intensification of cereal production systems: Yield potential, soil quality, and precision agriculture. Proc Natl Acad Sci 96:5952–5959. doi: 10.1073/pnas.96.11.5952.

Ceballos H; Ramirez J; Bellotti A; Jarvis A; Alvarez E. 2011. Adaptation of cassava to changing climates. In: Yadav et al. (Eds.): Crop Adaptation to Climate Change. Oxford, pp. 411–425.

CGIAR (2015) Developing beans that can beat the heat. Cali, Colombia

Challinor AJ; Wheeler TR. 2008. Use of a crop model ensemble to quantify CO_2 stimulation of water-stressed and well-watered crops. Agric. For. Meteorol. 148:1062–1077. doi: 10.1016/j.agrformet.2008.02.006.

Challinor AJ, Watson J, Lobell DB, et al. 2014. A meta-analysis of crop yield under climate change and adaptation. Nat Clim Chang 4:287–291. doi: 10.1038/nclimate2153.

Challinor AJ, Parkes B, Ramirez-Villegas J. 2015. Crop yield response to climate change varies with cropping intensity. Glob Chang Biol 21:1679–1688. doi: 10.1111/gcb.12808.

Chavez E, Conway G, Ghil M, Sadler M. 2015. An end-to-end assessment of extreme weather impacts on food security. Nat Clim Chang. doi: 10.1038/nclimate2747

CMIP5. 2014. Coupled Model Inter-comparison Project Phase 5. [online] Available from http://pcmdi9.llnl.gov/esgf-web-fe/http://faostat.fao.org/ [Accessed in April 2015]

Connor, D.J., Loomis, R.S. and Cassman, K.G. (2011). Crop Ecology: Productivity and Management in Agricultural Systems. Cambridge: University Press. 562 pp.

Cook BI, Ault TR, Smerdon JE. 2015. Unprecedented 21st century drought risk in the American Southwest and Central Plains. Sci Adv 1:e1400082–e1400082. doi: 10.1126/sciadv.1400082.

Dai A. 2013. Increasing drought under global warming in observations and models. Nat Clim Chang 3:52–58. doi: 10.1038/nclimate1633.

Diamond SE, Sorger DM, Hulcr J, et al. 2012. Who likes it hot? A global analysis of the climatic, ecological, and evolutionary determinants of warming tolerance in ants. Glob Chang Biol 18:448–456. doi: 10.1111/j.1365-2486.2011.02542.x.

Do Rio A, Sentelhas PC, Farias JRB, et al. 2015. Alternative sowing dates as a mitigation measure to reduce climate change impacts on soybean yields in southern Brazil. Int J Climatol n/a–n/a. doi: 10.1002/joc.4583.

Eccel E, Rea R, Caffarra A, Crisci A. 2009. Risk of spring frost to apple production under future climate scenarios: the role of phenological acclimation. Int J Biometeorol 53:273–286. doi: 10.1007/s00484-009-0213-8

El-Sharkawy MA. 2014. Global warming: causes and impacts on agroecosystems productivity and food security with emphasis on cassava comparative advantage in the tropics/subtropics. Photosynthetica 52:161–178. doi: 10.1007/s11099-014-0028-7.

Elliott J, Deryng D, Müller C, et al. 2014a. Constraints and potentials of future irrigation water availability on agricultural production under climate change. Proc Natl Acad Sci 111:3239–3244. doi: 10.1073/pnas.1222474110

Elliott J; Müller C; Deryng D; Chryssanthacopoulos J; Boote KJ; Büchner M; Foster I; Glotter M; Heinke J; Iizumi T; Izaurralde RC; Mueller ND; Ray DK; Rosenzweig C; Ruane AC; Sheffield J. 2014b. The Global Gridded Crop Model inter-comparison: data and modeling protocols for Phase 1 (v1.0). Geosci. Model Dev. Discuss. 7:4383−4427.

Estes LD, Beukes H, Bradley BA, et al. 2013. Projected climate impacts to South African maize and wheat production in 2055: A comparison of empirical and mechanistic modeling approaches. Glob Chang Biol. doi: 10.1111/gcb.12325

Evans, L.T. 1996. Crop Evolution, Adaptation and Yield. Cambridge: University Press.

Ewert F, Rodriguez D, Jamieson P, et al. 2002. Effects of elevated CO2 and drought on wheat: testing crop simulation models for different experimental and climatic conditions. Agric Ecosyst Environ 93:249–266. doi: 10.1016/s0167-8809(01)00352-8

Eyshi Rezaei, E., H. Webber, T. Gaiser, J. Naab, & F. Ewert. 2014., Heat stress in cereals: mechanisms and modeling. Eur. J. Agron., http://dx.doi.org/10.1016/eja.2014.10.003.

FAO. 2007. EcoCrop. Available online at http://ecocrop.fao.org/ecocrop/srv/en/home, checked on 25 November 2014.

FAO/IIASA/ISRIC/ISS-CAS/JRC, 2012. *Harmonized World Soil Database (version 1.2)*. FAO, Rome, Italy and IIASA, Laxenburg, Austria.

FAOSTAT. 2015. Food and Agriculture Organization of the United Nations [online] Available from http://faostat.fao.org/ [Accessed in April 2015]

Freeman EA, Moisen GG. 2008. A comparison of the performance of threshold criteria for binary classification in terms of predicted prevalence and kappa. Ecol Modell 217:48–58. doi: DOI: 10.1016/j.ecolmodel.2008.05.015.

Fuhrer J. 2003. Agroecosystem responses to combinations of elevated CO2, ozone, and global climate change. Agric Ecosyst Environ 97:1–20. doi: Doi: 10.1016/s0167-8809(03)00125-7.

Godwin DC & Singh U. 1998. Nitrogen balance and crop response to nitrogen in upland and lowland cropping systems. In: Tsuji GY; Hoogenboom G; Thornton PK (eds.). Understanding Options for Agricultural Production. Dorordrecht: Kluwer Academic Publishers. p. 55-77.

Gourdji SM, Mathews KL, Reynolds M, et al. 2013. An assessment of wheat yield sensitivity and breeding gains in hot environments. Proc R Soc B Biol Sci. doi: 10.1098/rspb.2012.2190.

Hawkins E, Sutton R (2009) The Potential to Narrow Uncertainty in Regional Climate Predictions. Bull Am Meteorol Soc 90:1095–1107. doi: 10.1175/2009bams2607.1.

Hawkins E, Sutton R (2011) The potential to narrow uncertainty in projections of regional precipitation change. Clim Dyn 37:407–418. doi: 10.1007/s00382-010-0810-6.

Hawkins E, Fricker TE, Challinor AJ, et al. (2013) Increasing influence of heat stress on French maize yields from the 1960s to the 2030s. Glob Chang Biol 19:937–947. doi: 10.1111/gcb.12069.

Heinemann AB, Barrios-Perez C, Ramirez-Villegas J, et al. 2015. Variation and impact of drought-stress patterns across upland rice target population of environments in Brazil. J Exp Bot 66:3625–3638. doi: 10.1093/jxb/erv126.

Heinemann AB, Ramirez-Villegas J, Souza T, et al. 2016. Drought impact on rainfed common bean production areas in Brazil. Agric. For. Meteorol. in revision.

Hijmans R; Guarino L; Cruz M; Rojas E. 2001. Computer tools for spatial analysis of plant genetic resources data: 1. DIVA-GIS. In: Plant Genet. Res. Newsl. 127:15–19.

Hijmans R. 2001. Global distribution of the potato crop. Am J Potato Res 78:403–412. doi: 10.1007/bf02896371.

Hijmans R. 2003. The effect of climate change on global potato production. Am J Potato Res 80:271–279. doi: 10.1007/bf02855363

Horie T. 1993. Predicting the effect of climate variation and elevated CO2 on rice yield in Japan. J. Agr. Met. 48:567-574

Hoogenboom G; Jones JW; Porter CH: Wilkens PW; Boote KJ; Hunt LA; Tsuji GY (Editors). 2010. Decision Support System for Agrotechnology Transfer Version 4.5. Volume 1: Overview. University of Hawaii, Honolulu, HI.

Hoogenboom, G., Romero, C.C., Gijsman, A.J., Koo, J., Wood, S., (2009). Strengthening soil quality databases for application to agricultural production and resource management policy. Project Report, The University of Georgia, Griffin, Georgia 30223, USA.

Iglesias, A., Schlickenrieder J., Pereira D. 2011. From the farmer to global food production: use of crop models for climate change impact assessment. pp. 49-72. In: Dinar, A. & R. Mendelsohn. 2011. Handbook on climate change and agriculture. 515 p.

Iizumi T, Luo J-J, Challinor AJ, et al. 2014. Impacts of El Niño Southern Oscillation on the global yields of major crops. Nat Commun. doi: 10.1038/ncomms4712.

van Ittersum MK, Cassman KG, Grassini P, et al. 2013. Yield gap analysis with local to global relevance—A review. F Crop Res 143:4–17. doi: 10.1016/j.fcr.2012.09.009

Jarvis A; Ramirez J; Bonilla-Findji O; Zapata E. 2011. Impacts of climate change on crop production in Latin America. In: Crop Adaptation to Climate Change (eds. S.S. Yadav, R.J. Redden, J.L. Hatfield, H. Lotze-Campen, and A.E. Hall), Wiley-Blackwell, Oxford, UK.

Jones JW; Hoogenboom G; Porter CH; Boote KJ; Batchelor WD; Hunt LA; Wilkens PW; Singh U; Gijsman AJ; Ritchie JT. 2003. The DSSAT cropping system model. Eur. J. Agron. 18(3−4):235−265.

Kharin V V., Zwiers FW, Zhang X, Wehner M (2013) Changes in temperature and precipitation extremes in the CMIP5 ensemble. Clim Change 119:345–357. doi: 10.1007/s10584-013-0705-8.

Kim HY; Horie T; Nakagawa H & Wada K. 1996. Effect of elevated CO2 concentration and high temperature on growth and yield of rice I. The effect on yield and its components of Akihikari rice. Jpn. J. Crop Sci. 65(4):644-651.

Knutti R, Sedláček J. 2012. Robustness and uncertainties in the new CMIP5 climate model projections. Nat Clim Chang 3:369–373. doi: 10.1038/nclimate1716

Koo J; Dimes J. 2013, HC27 Generic Soil Profile database, Version V1. Washington, DC: International Food Policy Research Institute. http://hdl.handle.net/1902.1/20299.

Leakey ADB, Ainsworth EA, Bernacchi CJ, et al. 2009. Elevated CO2 effects on plant carbon, nitrogen, and water relations: six important lessons from FACE. J Exp Bot 60:2859–2876. doi: 10.1093/jxb/erp096

Lesk C, Rowhani P, Ramankutty N. 2016. Influence of extreme weather disasters on global crop production. Nature 529:84–87. doi: 10.1038/nature16467.

Li T, Hasegawa T, Yin X, et al. 2015. Uncertainties in predicting rice yield by current crop models under a wide range of climatic conditions. Glob Chang Biol 21:1328–1341. doi: 10.1111/gcb.12758.

Liu C, Berry PM, Dawson TP, Pearson RG. 2005. Selecting thresholds of occurrence in the prediction of species distributions. Ecography (Cop) 28:385–393. doi: 10.1111/j.0906-7590.2005.03957.x

Liu C, White M, Newell G. 2013a. Selecting thresholds for the prediction of species occurrence with presence-only data. J Biogeogr 40:778–789. doi: 10.1111/jbi.12058

Liu J, Folberth C, Yang H, et al. 2013b. A Global and Spatially Explicit Assessment of Climate Change Impacts on Crop Production and Consumptive Water Use. PLoS One 8:e57750. doi: 10.1371/journal.pone.0057750.

Lizaso, J.I., K.J. Boote, J.W. Jones, C.H. Porter, L. Echarte, M.E. Westgate, G. Sonohat. 2011. CSM-IXIM: A New Maize Simulation Model for DSSAT version 4.5. *Agron J* 103:766-779.

Lobell DB; et al. 2008. Prioritizing climate change adaptation needs for food security in 2030. Science 319(5863):607–610.

Lobell DB, Cassman KG, Field CB (2009) Crop Yield Gaps: Their Importance, Magnitudes, and Causes. Annu Rev Environ Resour 34:179–204. doi: 10.1146/annurev.environ.041008.093740

Lobell DB; Gourdji SM. 2012. The influence of climate change on global crop productivity. Plant Physiol. 160:1686−1697.

Lobell, D.B., Hammer, G.L., McLean, G., Messina, C., Roberts, M.J., Schlenker, W., 2013.The critical role of extreme heat for maize production in the United States. Nat.Clim. Change 3, 497–501.

Lobell DB, Hammer GL, McLean G, et al. (2013) The critical role of extreme heat for maize production in the United States. Nat Clim Chang 3:497–501. doi: 10.1038/nclimate1832.

Lobell DB. 2014. Climate change adaptation in crop production: Beware of illusions. Glob Food Sec. doi: 10.1016/j.gfs.2014.05.002.

Lobell DB, Hammer GL, Chenu K, et al. (2015) The shifting influence of drought and heat stress for crops in northeast Australia. Glob Chang Biol 21:4115–4127. doi: 10.1111/gcb.13022.

Long SP, Ainsworth EA, Leakey ADB, et al. 2006. Food for thought: lower-than-expected crop yield stimulation with rising CO_2 concentrations. Science (80-)312:1918–1921. doi: 10.1126/science.1114722.

Long SP; Ainsworth EA; Leakey ADB; Morgan PB. 2005. Global food insecurity: treatment of major food crops with elevated carbon dioxide or ozone under large-scale fully open-air conditions suggests

recent models may have overestimated future yields. Philos. Trans. R Soc. Lond. B Biol. Sci. 360:2011–2020. doi: 10.1098/rstb.2005.1749.

Magrin G, Travasso M, Rodríguez G. 2005. Changes in Climate and Crop Production During the 20th Century in Argentina. Clim Change 72:229–249. doi: 10.1007/s10584-005-5374-9.

Magrin GO; Marengo JA; Boulanger J-P; Buckeridge MS; Castellanos E; Poveda G; Scarano FR; Vicuña S. 2014. Central and South America. In: Climate Change 2014: Impacts, Adaptation, and Vulnerability. Part B: Regional Aspects. Contribution of Working Group II to the Fifth Assessment Report of the Intergovernmental Panel on Climate Change [Barros VR; Field CB; Dokken DJ; Mastrandrea MD; Mach KJ; Bilir TE; Chatterjee M; Ebi KL; Estrada YO; Genova RC; Girma B; Kissel ES; Levy AN; MacCracken S; Mastrandrea PR; White LL (eds.)]. Cambridge University Press, Cambridge, United Kingdom, and New York, NY, USA. p. 1499−1566.

Marin F, Jones J, Singels A, et al. 2013. Climate change impacts on sugarcane attainable yield in southern Brazil. Clim Change 117:227–239. doi: 10.1007/s10584-012-0561-y.

Markelz RJC, Strellner RS, Leakey ADB (2011) Impairment of C4 photosynthesis by drought is exacerbated by limiting nitrogen and ameliorated by elevated [CO2] in maize. J Exp Bot 62: 3235–3246

Marteau R, Sultan B, Moron V, et al. 2011. The onset of the rainy season and farmers' sowing strategy for pearl millet cultivation in Southwest Niger. Agric For Meteorol 151:1356–1369. doi: 10.1016/j.agrformet.2011.05.018

Matsui T; Namuco OS; Ziska L & Horie T. 1997. Effects of high temperature and CO_2 concentration on spikelet sterility in indica rice. Field Crops Res. 51:213-219.

Monfreda C, Ramankutty N, Foley JA (2008) Farming the planet: 2. Geographic distribution of crop areas, yields, physiological types, and net primary production in the year 2000. Glob Biogeochem Cycles 22:GB1022. doi: 10.1029/2007gb002947.

Nelson GC, Rosegrant M, Palazzo A, et al. 2010. Food Security, Farming and Climate Change to 2050: Scenarios, Results and Policy Options. International Food Policy Research Institute, Washinton D.C., USA.

Olmstead AL, Rhode PW. 2011. Adapting North American wheat production to climatic challenges, 1839–2009. Proc Natl Acad Sci 108:480–485. doi: 10.1073/pnas.1008279108.

Osborne T, Rose G, Wheeler T. 2013. Variation in the global-scale impacts of climate change on crop productivity due to climate model uncertainty and adaptation. Agric For Meteorol 170:183–194. doi: 10.1016/j.agrformet.2012.07.006

Ovalle-Rivera, O., P. Läderach, C. Bunn, M. Obersteiner & G. Schroth (2015), Projected shifts in *Coffea arabica* suitability among major global producing regions due to climate change. *PloS ONE* 10(4):e0124155. doi:10.1371/journal.pone.012455.

Pearson R. 2010. Species' distribution modeling for conservation educators and practitioners. In: Lessons in conservation. Am. Museum Nat. Hist. 3:54–89.

Peel MC, Finlayson BL, McMahon TA. 2007. Updated world map of the Köppen-Geiger climate classification. Hydrol Earth Syst Sci 11:1633–1644. doi: 10.5194/hess-11-1633-2007.

Peng S, Huang J, Sheehy JE, et al. (2004) Rice yields decline with higher night temperature from global warming. Proc Natl Acad Sci U S A 101:9971–9975. doi: 10.1073/pnas.0403720101

Peterson AT, Papes M, Soberón J. 2008. Rethinking receiver operating characteristic analysis applications in ecological niche modeling. Ecol Modell 213:63–72. doi: DOI: 10.1016/j.ecolmodel.2007.11.008.

Porter JR, Semenov MA. 2005. Crop responses to climatic variation. Philos Trans R Soc B Biol Sci 360:2021–2035. doi: 10.1098/rstb.2005.1752

Porter JR, Xie L, Challinor AJ, et al. 2014. Chapter 7. Food Security and Food Production Systems. Climate Change 2014: Impacts, Adaptation and Vulnerability. Working Group II Contribution to the IPCC 5th Assessment Report. Geneva, Switzerland.

Portmann FT; Siebert S; Döll P. 2010. MIRCA2000 – Global monthly irrigated and rainfed crop areas around the year 2000: A new high-resolution data set for agricultural and hydrological modeling. *Global Biogeochemical Cycles* 24, GB 1011. doi: 10.1029/2008GB003435.

Quintero-Durán R. 1995. Fertilización y nutrición. In: CENICAÑA. El cultivo de la caña en la zona azucarera de Colombia. p. 153−177.

Ramirez J; Jarvis A; Van Den Bergh I; Staver C; Turner D. 2011. Changing climates: effects on growing conditions for banana and plantain (*Musa* spp.) and possible responses. In: Yadav et al. (eds.): Crop Adaptation to Climate Change. Oxford. p. 426–438.

Ramirez-Cabral NYZ, Kumar L, Taylor S. 2016. Crop niche modeling projects major shifts in common bean growing areas. Agric For Meteorol 218-219:102–113. doi: 10.1016/j.agrformet.2015.12.002.

Ramirez-Villegas J, Salazar M, Jarvis A, Navarro-Racines C. 2012. A way forward on adaptation to climate change in Colombian agriculture: perspectives towards 2050. Clim Change 115:611–628. doi: 10.1007/s10584-012-0500-y.

Ramirez-Villegas J; Jarvis A; Läderach P. 2013. Empirical approaches for assessing impacts of climate change on agriculture: The EcoCrop model and a case study with grain sorghum. Agricultural and Forest Meteorology 170: 67−78.

Ramirez-Villegas J. 2014. Genotypic adaptation of Indian groundnut to climate change: an ensemble approach. PhD thesis. University of Leeds.

Ramirez-Villegas J, Thornton PK. 2015. Climate change impacts on African crop production. Working paper No. 119. Copenhagen, Denmark

Rippke U. 2014. Thresholds of crop suitability: When does sub-Saharan Africa need transformational climate change adaptation? MSc thesis in Geography. Geographisches Institut – Rheinische Friedrich-Wilhelms-Universität, Bonn. 122 p.

Ritchie JT. 1998. Soil water balance and plant water stress. In: Tsuji GY; Hoogenboom G; Thornton PK (eds.). Understanding Options for Agricultural Production. Dordrecht: Kluwer Academic Publishers. p. 41−54.

Rosegrant MW; Koo J; Cenacchi N; Ringler C; Robertson RD; Fisher M; Cox CM; Garrett K; Perez ND; Sabbagh P. 2014. Food security in a world of natural resource scarcity: the role of agricultural technologies. Washington, D.C.: International Food Policy Research Institute (IFPRI).

Rosenthal DM, Slattery RA, Miller RE, et al. 2012. Cassava about-FACE: Greater than expected yield stimulation of cassava (Manihot esculenta) by future CO2 levels. Glob Chang Biol 18:2661–2675. doi: 10.1111/j.1365-2486.2012.02726.x.

Rosenzweig C, Jones JW, Hatfield JL, et al. 2013. The Agricultural Model Intercomparison and Improvement Project (AgMIP): Protocols and pilot studies. Agric For Meteorol 170:166–182. doi: 10.1016/j.agrformet.2012.09.011

Rosenzweig C, et al. 2014. Assessing agricultural risks of climate change in the 21st century in a global gridded crop model intercomparison. *Proc Natl Acad Sci USA* 111:3268–3273.

Rötter RP; Tao F; Hohn JG; Palosuo T. 2015. Use of crop simulation modeling to aid ideotype design of future cereal cultivars. J. Exp. Bot. doi: 10.1093/jxb/erv098.

Rötter RP; Carter TR; Olesen JE; Porter JR. 2011. Crop-climate models need an overhaul. Nat. Clim. Change 1:175−177.

Ruane AC, McDermid S, Rosenzweig C, et al. 2014. Carbon-Temperature-Water change analysis for peanut production under climate change: a prototype for the AgMIP Coordinated Climate-Crop Modeling Project (C3MP). Glob Chang Biol 20:394–407. doi: 10.1111/gcb.12412.

Ruane AC, Goldberg R, Chryssanthacopoulos J (2015) Climate forcing datasets for agricultural modeling: Merged products for gap-filling and historical climate series estimation. Agric For Meteorol 200:233–248. doi: 10.1016/j.agrformet.2014.09.016.

Sacks WJ, Deryng D, Foley JA, Ramankutty N. 2010. Crop planting dates: an analysis of global patterns. Glob Ecol Biogeogr 19:607–620. doi: 10.1111/j.1466-8238.2010.00551.x

Sánchez B, Rasmussen A, Porter JR (2014) Temperatures and the growth and development of maize and rice: a review. Glob Chang Biol 20:408–17. doi: 10.1111/gcb.12389.

Satake T; Yoshida S. 1978. High temperature -induced sterility in indica rices at flowering. Japan Jour. Crop Sci. 6-11.

Schafleitner R, Ramirez-Villegas J, Jarvis A, et al. 2011. Chapter 11: Adaptation of the Potato Crop to Changing Climates. Wiley & Sons.

Sheffield J, Goteti G, Wood EF. 2006. Development of a 50-Year High-Resolution Global Dataset of Meteorological Forcings for Land Surface Modeling. J Clim 19:3088–3111. doi: 10.1175/jcli3790.1

Sheffield J, Wood EF. 2008. Global trends and variability in soil moisture and drought characteristics, 1950-2000, from observation-driven simulations of the terrestrial hydrologic cycle. J Clim 21: 432–458.

Sheffield J, Wood EF, Roderick ML. 2012. Little change in global drought over the past 60 years. Nature 491:435–438. doi: 10.1038/nature11575.

Sillmann J, Kharin V V, Zwiers FW, et al. 2013. Climate extremes indices in the CMIP5 multimodel ensemble: Part 2. Future climate projections. J Geophys Res Atmos 118:2473–2493. doi: 10.1002/jgrd.50188

Soberón J, Nakamura M. 2009. Niches and distributional areas: Concepts, methods, and assumptions. Proc Natl Acad Sci 106:19644–19650. doi: 10.1073/pnas.0901637106

Stack, D; Kafatos, M. 2013. ApsimRegions: A Gridded Modeling Framework for the APSIM Crop Model. *Conference Paper Pycon.*

Suleiman AA, Ritchie JT (2001) Estimating saturated hydraulic conductivity from soil porosity. Trans ASAE 44:235–239.

Taylor KE, Stouffer RJ, Meehl GA. 2012. An Overview of CMIP5 and the Experiment Design. Bull Am Meteorol Soc 93:485–498. doi: 10.1175/BAMS-D-11-00094.1

Teixeira EI, Fischer G, van Velthuizen H, Walter C, Ewert F. 2013. Global hot-spots of heat stress on agricultural crops due to climate change. Agricultural Forest Meteorology 70: 206-215

Thibeault JM, Seth A, Garcia M. 2010. Changing climate in the Bolivian Altiplano: CMIP3 projections for temperature and precipitation extremes. J Geophys Res 115:D08103. doi: 10.1029/2009jd012718.

Trnka M, Rötter RP, Ruiz-Ramos M, et al. 2014. Adverse weather conditions for European wheat production will become more frequent with climate change. Nat Clim Chang 4:637–643. doi: 10.1038/nclimate2242.

Turner DW. 1998. Ecophysiology of bananas: the generation and functioning of the leaf canopy. Acta Hortic 490:211–222.

Ureta C, Martínez-Meyer E, Perales HR, Álvarez-Buylla ER. 2012. Projecting the effects of climate change on the distribution of maize races and their wild relatives in Mexico. Glob Chang Biol 18:1073–1082. doi: 10.1111/j.1365-2486.2011.02607.x.

van Bussel LGJ, Stehfest E, Siebert S, et al. 2015. Simulation of the phenological development of wheat and maize at the global scale. Glob Ecol Biogeogr 24:1018–1029. doi: 10.1111/geb.12351.

Van den Bergh I, Ramirez-Villegas J, Staver C, et al. (2012) Climate Change in the Subtropics: The Impacts of Projected Averages and Variability on Banana Productivity. Acta Hortic 928:89–99.

van Oort PAJ, de Vries ME, Yoshida H, Saito K. 2015. Improved Climate Risk Simulations for Rice in Arid Environments. PLoS One 10:e0118114. doi: 10.1371/journal.pone.0118114.

Vergara W; Rios A; Trapido P; Malarín H. 2014. Agriculture and Future Climate in Latin America and the Caribbean: Systemic Impacts and Potential Responses. Washington, D.C.: Inter-American Development Bank.

Vitousek PM, Menge DNL, Reed SC, Cleveland CC. 2013. Biological nitrogen fixation: rates, patterns and ecological controls in terrestrial ecosystems. Philos Trans R Soc B Biol Sci 368:20130119–20130119. doi: 10.1098/rstb.2013.0119.

Waha K, van Bussel LGJ, Müller C, Bondeau A. 2012. Climate-driven simulation of global crop sowing dates. Glob Ecol Biogeogr 21:247–259. doi: 10.1111/j.1466-8238.2011.00678.x

Watterson IG; Bathols J; Heady C. 2014. What influences the skill of climate models over the continents? Bull. Am. Meteorol. Soc. 95:689–700.

Webber H, Zhao G, Wolf J, et al. (2015) Climate change impacts on European crop yields: Do we need to consider nitrogen limitation? Eur J Agron 71:123–134. doi: 10.1016/j.eja.2015.09.002.

Weedon GP; Gomes S; Viterbo P; Shuttleworth WJ; Blyth E; Österle H; Adam JC; Bellouin N; Boucher O; Best M. 2011. Creation of the WATCH Forcing Data and its use to assess global and regional reference crop evaporation over land during the twentieth century. Journal of Hydrometeorology 12(5): 823–848. doi: 10.1175/2011JHM1369.1.

Wiens JA, Stralberg D, Jongsomjit D, et al. 2009. Niches, models, and climate change: Assessing the assumptions and uncertainties. Proc Natl Acad Sci 106:19729–19736. doi: 10.1073/pnas.0901639106

Wheeler T, von Braun J. 2013. Climate change impacts on global food security. Science (80-) 341:508–513. doi: 10.1126/science.1239402.

White JW; Hoogenboom G; Kimball BA; Wall GW. 2011. Methodologies for simulating impacts of climate change on crop production. Field Crops Res. 124:357–368.

Wilkerson, G. G., Jones, J. W., Boote, K. J., Ingram, K. T. & Mishoe, J. W. (1983). Modeling soybean growth for crop management. Trans. ASAE, 26: 63−73.

World Bank 2014, World Bank Open Data, available at http://data.worldbank.org/, last accessed July 30, 2015.

Worster A; Fan J; Upadhye S. 2006. Understanding receiver operating characteristic (ROC) curves. CJEM 8(1):19−20.

Yamori W, Hikosaka K, Way DA. 2014. Temperature response of photosynthesis in C3, C4, and CAM plants: temperature acclimation and temperature adaptation. Photosynth Res 119:101–17. doi: 10.1007/s11120-013-9874-6.

You L; Wood-Sichra U; Fritz S; Guo Z; See L; Koo J. 2014. Spatial Production Allocation Model (SPAM) 2005 v2.0. 5 April 2015. Available from http://mapspam.info.

Zabel F, Putzenlechner B, Mauser W. 2014. Global Agricultural Land Resources – A High Resolution Suitability Evaluation and Its Perspectives until 2100 under Climate Change Conditions. PLoS One 9:e107522. doi: 10.1371/journal.pone.0107522

Appendix

Tables

Table A- 1. Crop cultivars simulated in DSSAT for each of the regions shown in Figure 3.

Crop	Altitude	Latitude				
		0-10	10-20	20-30	30-40	>40
Maize	400	IB0056 (FM 6)	IB0056 (FM 6)	IB0056 (FM 6)	IB0056 (FM 6)	IB0056 (FM 6)
	900	IB0056 (FM 6)	IB0056 (FM 6)	IB0056 (FM 6)	IB0056 (FM 6)	IB0056 (FM 6)
	1400	IB0056 (FM 6)	IB0056 (FM 6)	IB0056 (FM 6)	IB0056 (FM 6)	IB0081 (PIO3790)
	1900	IB0056 (FM 6)	IB0056 (FM 6)	IB0056 (FM 6)	IB0007 (EDO)	NA
	2400	IB0006 (INRA)	IB0068 (PIO3475)	IB0011 (DEKALBXL45)	NA	NA
	2900	NA	NA	NA	NA	NA
	>2900	NA	NA	NA	NA	NA
Rice dryland	400	IB0001 (IR8)	IB0001 (IR8)	IB0001 (IR8)	IB0001 (IR8)	NA
	900	IB0001 (IR8)	IB0001 (IR8)	IB0001 (IR8)	IB0001 (IR8)	NA
	1400	IB0001 (IR8)	IB0001 (IR8)	IB0001 (IR8)	IB0001 (IR8)	NA
	1900	IB0023 (LOWTTOL)	*IB0023 (LOWTTOL)*	*IB0023 (LOWTTOL)*	*IB0023 (LOWTTOL)*	NA
	2400	NA	NA	NA	NA	NA
	2900	NA	NA	NA	NA	NA
	>2900	NA	NA	NA	NA	NA
Rice Flooded	400	IB0001 (IR8)	IB0001 (IR8)	IB0001 (IR8)	IB0001 (IR8)	NA
	900	IB0001 (IR8)	IB0001 (IR8)	IB0001 (IR8)	IB0001 (IR8)	NA
	1400	IB0001 (IR8)	IB0001 (IR8)	IB0001 (IR8)	IB0001 (IR8)	NA
	1900	IB0023 (LOWTTOL)	*IB0023 (LOWTTOL)*	*IB0023 (LOWTTOL)*	*IB0023 (LOWTTOL)*	NA
	2400	*IB0023 (LOWTTOL)*	*IB0023 (LOWTTOL)*	*IB0023 (LOWTTOL)*	*IB0023 (LOWTTOL)*	NA
	2900	NA	NA	NA	NA	NA
	>2900	NA	NA	NA	NA	NA
Wheat	500	*IB0020*	*IB0020*	*IB0020*	IB0020	IB0024
	750	*IB0020*	*IB0020*	IB0024	IB0024	IB0024
	1250	*IB0020*	IB0024	IB0024	IB0024	IB0024
	1750	IB0024	IB0024	IB0024	IB0024	*IB0024*
	2250	IB0024	IB0024	IB0024	*IB0024*	*IB0024*
	2750	IB0024	IB0024	IB0024	*IB0024*	*IB0024*
	>2750	IB0024	IB0024	*IB0024*	*IB0024*	*IB0024*
Drybean	400	IB0033 (A193)	IB0033 (A193)	IB0033 (A193)	IB0033 (A193)	NA
	900	IB0033 (A193)	IB0033 (A193)	IB0033 (A193)	IB0033 (A193)	NA

	1400	IB0033 (A193)	IB0033 (A193)	IB0033 (A193)	IB0033 (A193)	NA
	1900	IB0033 (A193)	IB0033 (A193)	IB0033 (A193)	IB0033 (A193)	NA
	2400	IB0012 (Manitou+)	IB0012 (Manitou+)	IB0032 (A486)	NA	NA
	2900	IB0032 (A486)	IB0034 (A195)	NA	NA	NA
	>2900	NA	NA	NA	NA	NA
Soybean	400	IB0045 (DON MARIO4)	IB0045 (DON MARIO4)	MS0079 (MS_MAT_ GROUP_ 2)	MS0078 (PIO9202)	NA
	900	IB0045 (DON MARIO4)	IB0045 (DON MARIO4)	MS0079 (MS_MAT_ GROUP_ 2)	MS0078 (PIO9202)	NA
	1400	IB0055 (Hutcheson)	IB0045 (DON MARIO4)	MS0079 (MS_MAT_ GROUP_ 2)	UC0003 (MCCALL_00)	NA
	1900	IB0055 (Hutcheson)	IB0045 (DON MARIO4)	UC0003 (MCCALL_00)	MS0078 (PIO9202)	NA
	2400	NA	NA	NA	NA	NA
	2900	NA	NA	NA	NA	NA
	>2900	NA	NA	NA	NA	NA

Table A- 3. Current and future period suitable areas by crop and country for the EcoCrop simulations, along with the mean suitability change between historical and future periods. Suitable areas are averaged across years and GCM's (for the future period) and aggregated to countries. Also shown are the bootstrapped confidence intervals across the 9 GCM's for the mean suitability change.

Crop	Country	Current area (km^2)	Future area (km^2)	Mean suitability change (%)	SD (%)	95% confidence intervals	
						Lower (%)	Upper (%)
banana	ARG	-	-	NA	NA	NA	NA
	BLZ	14,768	4,934	NA	NA	-85.9	-47.9
	BOL	324,130	109,182	-66.3	38.2	-85.4	-40.1
	BRA	3,494,690	1,629,392	-53.4	25.7	-69.3	-38.1
	CHL	-	-	NA	NA	NA	NA
	COL	273,476	122,886	-55.1	14.2	-63.0	-46.6
	CRB	58,623	7,923	-86.5	18.7	-95.6	-76.1
	CRI	24,393	3,727	-84.7	24.8	-96.2	-70.2
	CUB	132,387	15,035	-88.6	30.1	-99.8	-72.3
	DOM	35,140	15,296	-56.5	19.0	-65.8	-45.8
	ECU	46,460	29,248	-37.0	30.4	-55.0	-16.6
	GSA	83,216	13,030	-84.3	15.0	-92.5	-76.1
	GTM	41,583	19,571	-52.9	25.8	-67.1	-39.6
	HND	59,871	55,232	-7.7	26.1	-22.7	7.6
	HTI	41,025	16,264	-60.4	27.9	-74.1	-46.7
	JAM	14,719	4,251	NA	NA	-87.6	-48.4
	MEX	228,968	37,057	-83.8	12.2	-89.7	-76.1
	NIC	84,654	47,645	-43.7	32.6	-59.6	-25.4
	PAN	61,268	13,612	-77.8	26.7	-90.0	-59.2
	PER	61,487	36,401	-40.8	16.7	-48.8	-31.5
	PRY	-	319	NA	NA	NA	NA
	SLV	24,086	9,358	-61.1	30.9	-76.3	-42.5
	URY	-	-	NA	NA	NA	NA
	VEN	438,077	103,934	-76.3	13.2	-84.0	-70.4
	LAM	**6,002,842**	**2,371,832**	**-60.5**	**20.9**	**-69.4**	**-49.4**
cassava	ARG	512,680	598,344	16.7	10.5	10.8	22.2
	BLZ	20,709	20,709	0.0	0.0	0.0	0.0
	BOL	614,956	636,815	3.6	2.1	2.4	4.6
	BRA	5,632,680	5,764,071	2.3	2.5	0.7	3.7
	CHL	-	-	NA	NA	NA	NA
	COL	662,073	681,295	2.9	3.0	1.4	4.7
	CRB	81,349	80,051	-1.6	4.8	-4.3	0.0
	CRI	51,870	54,923	5.9	0.0	5.9	5.9
	CUB	138,150	138,150	0.0	0.0	0.0	0.0
	DOM	46,866	49,473	5.6	2.1	4.4	6.3
	ECU	130,051	140,014	7.7	5.8	4.8	11.2
	GSA	92,475	92,475	0.0	0.0	0.0	0.0
	GTM	98,347	101,671	3.4	2.8	1.8	4.9
	HND	113,768	113,768	0.0	0.0	0.0	0.0
	HTI	43,967	43,313	-1.5	3.0	-3.3	0.0
	JAM	14,719	14,719	NA	NA	0.0	0.0
	MEX	765,643	789,913	3.2	8.8	-2.0	8.2

	NIC	135,928	135,928	0.0	0.0	0.0	0.0
	PAN	88,849	88,849	0.0	0.0	0.0	0.0
	PER	125,586	156,571	24.7	15.2	17.0	34.6
	PRY	389,515	388,574	-0.2	4.3	-3.1	1.9
	SLV	24,086	24,086	0.0	0.0	0.0	0.0
	URY	-	2,964	NA	NA	NA	NA
	VEN	606,718	594,213	-2.1	2.7	-3.6	-0.6
	LAM	**11,291,364**	**11,750,781**	**4.1**	**2.1**	**2.6**	**5.0**
coffea arabica	ARG	-	-	NA	NA	NA	NA
	BLZ	-	-	NA	NA	NA	NA
	BOL	-	2,663	NA	NA	NA	NA
	BRA	3,087	-	NA	NA	NA	NA
	CHL	-	-	NA	NA	NA	NA
	COL	95,639	54,555	-43.0	16.1	-50.6	-34.2
	CRB	2,989	-	NA	NA	NA	NA
	CRI	-	-	NA	NA	NA	NA
	CUB	-	-	NA	NA	NA	NA
	DOM	2,925	-	NA	NA	NA	NA
	ECU	15,480	15,134	NA	NA	-28.0	22.0
	GSA	3,082	342	NA	NA	NA	NA
	GTM	14,951	5,987	NA	NA	-74.0	-44.0
	HND	-	-	NA	NA	NA	NA
	HTI	-	-	NA	NA	NA	NA
	JAM	-	-	NA	NA	NA	NA
	MEX	23,754	2,303	-90.3	16.2	-100.0	-81.3
	NIC	3,016	-	NA	NA	NA	NA
	PAN	-	-	NA	NA	NA	NA
	PER	36,492	32,119	-12.0	30.0	-28.7	5.0
	PRY	-	-	NA	NA	NA	NA
	SLV	-	-	NA	NA	NA	NA
	URY	-	-	NA	NA	NA	NA
	VEN	27,622	8,172	-70.4	27.7	-84.7	-54.5
	LAM	**229,037**	**121,276**	**-47.0**	**17.0**	**-57.8**	**-36.0**
Coffea robusta	ARG	2,742	8,913	NA	NA	NA	NA
	BLZ	17,767	3,626	-79.6	11.1	-83.3	-73.3
	BOL	327,069	51,950	-84.1	14.1	-91.0	-75.2
	BRA	3,487,588	1,145,715	-67.1	19.5	-77.9	-55.7
	CHL	-	-	NA	NA	NA	NA
	COL	447,156	210,915	-52.8	8.2	-58.3	-47.8
	CRB	32,882	4,293	-86.9	16.3	-94.5	-76.6
	CRI	39,649	10,513	-73.5	26.1	-88.5	-56.9
	CUB	28,681	-	-100.0	0.0	-100.0	-100.0
	DOM	23,425	3,583	-84.7	15.0	-92.5	-75.0
	ECU	61,943	48,174	-22.2	18.4	-32.0	-12.5
	GSA	83,207	8,215	-90.1	13.5	-95.9	-81.9
	GTM	71,504	26,570	-62.8	10.7	-68.3	-55.3
	HND	68,784	31,585	-54.1	29.5	-74.5	-35.8
	HTI	20,499	4,551	-77.8	30.4	-92.9	-58.6
	JAM	11,769	1,308	NA	NA	-100.0	-75.0

	MEX	153,359	59,775	-61.0	14.2	-69.6	-53.3
	NIC	102,629	45,925	-55.3	21.3	-68.0	-42.7
	PAN	79,655	17,011	-78.6	22.4	-89.7	-63.4
	PER	101,024	78,301	-22.5	15.8	-30.8	-13.2
	PRY	76,247	48,226	-36.8	45.9	-63.8	-8.2
	SLV	15,046	2,673	NA	NA	-100.0	-65.3
	URY	-	-	NA	NA	NA	NA
	VEN	202,591	56,052	-72.3	13.7	-79.2	-65.2
	LAM	**5,708,976**	**1,907,053**	**-66.6**	**15.9**	**-74.8**	**-58.4**
potato	ARG	787,253	604,814	-23.2	14.3	-30.5	-15.2
	BLZ	-	-	NA	NA	NA	NA
	BOL	196,795	191,816	-2.5	5.5	-5.4	0.0
	BRA	557,418	311,283	-44.2	16.9	-52.4	-34.4
	CHL	196,596	238,243	21.2	10.6	14.3	26.5
	COL	98,754	78,169	-20.8	8.7	-26.0	-16.6
	CRB	-	-	NA	NA	NA	NA
	CRI	-	-	NA	NA	NA	NA
	CUB	-	-	NA	NA	NA	NA
	DOM	5,858	1,955	NA	NA	NA	NA
	ECU	61,911	56,407	-8.9	11.4	-15.7	-3.0
	GSA	-	-	NA	NA	NA	NA
	GTM	20,929	9,306	-55.5	11.2	-61.4	-48.5
	HND	-	-	NA	NA	NA	NA
	HTI	-	-	NA	NA	NA	NA
	JAM	-	-	NA	NA	NA	NA
	MEX	298,902	125,117	-58.1	13.4	-64.8	-50.3
	NIC	-	-	NA	NA	NA	NA
	PAN	-	-	NA	NA	NA	NA
	PER	212,631	254,945	19.9	10.0	13.7	25.0
	PRY	61,028	2,162	-96.5	10.6	-100.0	-90.4
	SLV	-	-	NA	NA	NA	NA
	URY	189,915	189,915	0.0	0.0	0.0	0.0
	VEN	21,447	5,785	-73.0	13.3	-80.0	-64.8
	LAM	**3,125,658**	**2,448,483**	**-21.7**	**9.1**	**-26.3**	**-15.8**
sugarcane	ARG	-	10,003	NA	NA	NA	NA
	BLZ	8,843	11,145	NA	NA	13.4	40.2
	BOL	357,388	404,930	13.3	10.6	7.6	19.0
	BRA	3,143,947	3,463,930	10.2	10.7	4.4	16.4
	CHL	-	-	NA	NA	NA	NA
	COL	174,508	175,159	0.4	26.1	-12.7	17.1
	CRB	55,067	56,891	3.3	31.7	-12.6	20.2
	CRI	9,141	7,111	NA	NA	-57.7	21.0
	CUB	138,150	132,371	-4.2	6.5	-7.5	-1.5
	DOM	32,224	38,396	19.2	9.6	14.8	23.6
	ECU	37,155	56,066	50.9	36.9	28.3	68.6
	GSA	24,700	40,447	63.8	70.1	21.4	105.9
	GTM	32,699	41,296	26.3	22.1	12.7	37.1
	HND	62,979	69,247	10.0	15.5	0.6	16.6
	HTI	41,025	39,067	-4.8	8.0	-9.1	-0.7

	JAM	11,777	13,411	NA	NA	2.5	22.5
	MEX	339,330	335,630	-1.1	16.8	-13.8	8.5
	NIC	48,384	53,102	9.8	33.4	-10.0	27.8
	PAN	9,198	10,553	NA	NA	-49.1	86.5
	PER	30,647	47,308	54.4	44.0	28.8	78.1
	PRY	112,151	125,904	12.3	22.7	0.3	24.4
	SLV	24,086	20,070	-16.7	25.8	-32.5	-3.7
	URY	-	-	NA	NA	NA	NA
	VEN	425,430	378,885	-10.9	10.5	-16.3	-5.4
	LAM	**5,610,761**	**5,994,211**	**6.8**	**7.4**	**1.8**	**10.7**
yam	ARG	-	18,171	NA	NA	NA	NA
	BLZ	20,709	19,729	-4.7	7.1	-8.5	-1.4
	BOL	418,754	440,039	5.1	14.9	-3.5	12.1
	BRA	4,027,763	4,193,867	4.1	9.4	-2.2	10.1
	CHL	-	-	NA	NA	NA	NA
	COL	498,736	529,554	6.2	6.7	3.2	9.9
	CRB	70,048	47,880	-31.6	26.4	-48.7	-17.5
	CRI	42,710	50,172	17.5	5.2	15.0	20.4
	CUB	123,685	103,473	-16.3	19.7	-27.5	-4.5
	DOM	29,309	25,712	-12.3	14.8	-20.1	-4.0
	ECU	61,944	81,896	32.2	12.3	26.0	38.0
	GSA	89,393	89,734	0.4	2.1	-0.7	1.4
	GTM	59,500	74,411	25.1	5.0	23.0	28.1
	HND	62,791	74,455	18.6	15.4	10.1	29.7
	HTI	29,300	28,954	-1.2	24.8	-16.2	16.1
	JAM	14,719	13,080	NA	NA	-16.5	-5.6
	MEX	363,274	319,159	-12.1	22.2	-26.2	-2.4
	NIC	108,785	119,823	10.1	7.4	4.4	13.8
	PAN	82,725	88,849	7.4	0.0	7.4	7.4
	PER	67,592	79,815	18.1	8.4	13.4	22.9
	PRY	42,966	101,321	135.8	124.5	65.9	218.8
	SLV	24,086	22,417	-6.9	9.1	-12.5	-2.5
	URY	-	-	NA	NA	NA	NA
	VEN	444,717	375,104	-15.7	16.4	-25.0	-6.1
	LAM	**7,260,107**	**7,396,969**	**1.9**	**8.7**	**-3.5**	**7.3**

Table A- 4. Average yields and % changes for irrigated dry-bean, maize, rice, wheat and soybean, aggregated to regions for all cultivation areas.

Crop	Yield for Irrigated	MEX	CEN	AND	BRA	SUR
Bean	Historical baseline (t/ha): 1971−2000	1.7	1.6	1.4	1.3	1.8
	Future multi -model mean (t/ha): 2020−2049	1.6	1.4	1.3	1.2	1.7
	% change (in multi-model mean relative to baseline)	-2.1	-11.4	-5.9	-6.3	-3.6
Maize	Historical baseline (t/ha): 1971−2000	9.8	7.7	6.1	8.4	10.1
	Future multi-model mean (t/ha): 2020−2049	8.9	5.7	5.3	7.4	10.3
	% change (in multi-model mean relative to baseline)	-8.9	-25.2	-11.8	-10.9	2.6
Rice	Historical baseline (t/ha): 1971−2000	9.3	7.5	6.6	3.2	4.2
	Future multi-model mean (t/ha): 2020−2049	9.1	7.0	6.4	3.4	5.0
	% change (in multi-model mean relative to baseline)	-1.8	-5.7	-3.4	6.1	18.7
Soy-Bean	Historical baseline (t/ha): 1971−2000	NA	NA	NA	0.8	1.2
	Future multi-model mean (t/ha): 2020−2049	NA	NA	NA	0.8	1.2
	% change (in multi-model mean relative to baseline)	NA	NA	NA	0.7	-2.9
Wheat	Historical baseline (t/ha): 1971−2000	4.3	5.7	1.7	2.1	3.2
	Future multi-model mean (t/ha): 2020−2049	3.6	5.0	1.5	1.7	2.8
	% change (in multi-model mean relative to baseline)	-17.5	-12.7	-12.6	-17.5	-12.4

Table A- 5. Average yields and % changes for rain-fed dry-bean, maize, rice, wheat and soybean, aggregated to regions for all cultivation areas.

Crop	Yield for rainfed	MEX	CEN	AND	BRA	SUR
Bean	Historical baseline (t/ha): 1971−2000	0.5	0.7	0.7	0.6	0.7
	Future multi-model mean (t/ha): 2020−2049	0.4	0.6	0.6	0.5	0.6
	% change (in multi-model mean relative to baseline)	-14.6	-17.3	-16.7	-14.2	-13.1
Maize	Historical baseline (t/ha): 1971−2000	6.8	6.3	4.1	4.6	4.0
	Future multi -model mean (t/ha): 2020−2049	5.6	4.8	3.1	3.9	3.6
	% change (in multi-model mean relative to baseline)	-18.2	-24.0	-25.3	-14.0	-11.1
Rice	Historical baseline (t/ha): 1971−2000	5.8	5.9	2.5	1.1	1.1
	Future multi -model mean (t/ha): 2020−2049	5.3	4.9	2.8	1.4	1.3
	% change (in multi-model mean relative to baseline)	-8.1	-16.7	14.5	24.9	12.2
Soy-Bean	Historical baseline (t/ha): 1971−2000	NA	1.3	0.4	0.6	0.7
	Future multi -model mean (t/ha): 2020−2049	NA	1.3	0.4	0.6	0.6
	% change (in multi-model mean relative to baseline)	NA	-4.5	-6.2	-0.5	-5.2
Wheat	Historical baseline (t/ha): 1971−2000	2.3	4.3	3.0	3.0	4.0
	Future multi -model mean (t/ha): 2020−2049	1.6	3.6	2.6	2.4	3.3
	% change (in multi-model mean relative to baseline)	-31.5	-17.0	-13.8	-18.5	-16.1

Table A- 6. Mean crop durations for irrigated simulations and % changes for rain-fed dry-bean, maize, rice, wheat and soybean, aggregated to regions for all cultivation areas.

Crop	Crop Duration for Irrigated	AND	BRA	CEN	MEX	SUR
Bean	Historical baseline: 1971–2000	124	114	115	118	133
	Multi-model mean: 2020–2049	110	106	103	105	123
	% change (in multi-model mean relative to baseline)	-10	-7	-10	-11	-7
Maize	Historical baseline: 1971–2000	124	114	115	118	133
	Multi-model mean: 2020–2049	110	106	103	105	123
	% change (in multi-model mean relative to baseline)	-10	-7	-10	-11	-7
Rice	Historical baseline: 1971–2000	118	111	113	115	124
	Multi-model mean: 2020–2049	106	102	102	103	115
	% change (in multi-model mean relative to baseline)	-9	-8	-10	-9	-7
Soy-Bean	Historical baseline: 1971–2000	82	89	NA	NA	90
	Multi-model mean: 2020–2049	84	88	NA	NA	88
	% change (in multi-model mean relative to baseline)	2	-1	NA	NA	-2
Wheat	Historical baseline: 1971–2000	113	69	86	79	86
	Multi-model mean: 2020–2049	102	67	77	75	82
	% change (in multi-model mean relative to baseline)	-9	-4	-9	-6	-4

Table A- 7 Mean crop durations for rain-fed simulations and % changes for rain-fed dry-bean, maize, rice, wheat and soybean, aggregated to regions for all cultivation areas.

Crop	Crop Duration for Rainfed	AND	BRA	CEN	MEX	SUR
Bean	Historical baseline: 1971–2000	111	97	101	112	105
	Multi-model mean: 2020–2049	104	97	98	110	103
	% change (in multi-model mean relative to baseline)	-5	0	-3	-2	-2
Maize	Historical baseline: 1971–2000	119	108	112	118	123
	Multi-model mean: 2020–2049	107	101	101	105	114
	% change (in multi-model mean relative to baseline)	-9	-7	-10	-11	-7
Rice	Historical baseline: 1971–2000	115	111	109	124	142
	Multi-model mean: 2020–2049	106	104	106	121	135
	% change (in multi-model mean relative to baseline)	-7	-6	-2	-1	-5
Soy-Bean	Historical baseline: 1971–2000	98	102	119	NA	98
	Multi-model mean: 2020–2049	99	103	114	NA	96
	% change (in multi-model mean relative to baseline)	1	1	-4	NA	-1
Wheat	Historical baseline: 1971–2000	114	93	87	155	137
	Multi-model mean: 2020–2049	102	88	79	142	131
	% change (in multi-model mean relative to baseline)	-10	-5	-8	-9	-4

Table A- 8. Nitrogen stress indices for irrigated simulations, and mean absolute changes between historical and future periods stress indices aggregated to regions.

Crop	N stress for Irrigated	AND	BRA	CEN	MEX	SUR
Bean	Historical baseline: 1971–2000	0.319	0.274	0.235	0.299	0.326
	Multi-model mean: 2020–2049	0.283	0.239	0.187	0.277	0.325
	Change in absolute values of index (in multi-model mean relative to baseline)	-0.036	-0.036	-0.048	-0.022	-0.001
Maize	Historical baseline: 1971–2000	0.211	0.193	0.112	0.122	0.330
	Multi-model mean: 2020–2049	0.195	0.159	0.075	0.092	0.312
	Change in absolute values of index (in multi-model mean relative to baseline)	-0.016	-0.034	-0.037	-0.030	-0.018
Rice	Historical baseline: 1971–2000	0.123	0.289	0.111	0.097	0.268
	Multi-model mean: 2020–2049	0.109	0.260	0.091	0.063	0.253
	Change in absolute values of index (in multi-model mean relative to baseline)	-0.014	-0.029	-0.019	-0.034	-0.015
Soy-Bean	Historical baseline: 1971–2000	0.216	0.339	NA	NA	0.260
	Multi-model mean: 2020–2049	0.229	0.337	NA	NA	0.261
	Change in absolute values of index (in multi-model mean relative to baseline)	0.013	-0.002	NA	NA	0.001
Wheat	Historical baseline: 1971–2000	0.396	0.253	0.051	0.074	0.078
	Multi-model mean: 2020–2049	0.392	0.235	0.043	0.071	0.076
	Change in absolute values of index (in multi-model mean relative to baseline)	-0.005	-0.018	-0.008	-0.003	-0.002

Table A- 9 Nitrogen stress indices for rainfed simulations, and mean absolute changes between historical and future periods stress indices aggregated to regions.

Crop	N stress for Irrigated for Rainfed	AND	BRA	CEN	MEX	SUR
Bean	Historical baseline: 1971−2000	0.21	0.28	0.22	0.23	0.31
	Multi-model mean: 2020−2049	0.19	0.23	0.17	0.20	0.26
	Change in absolute values of index (in multi-model mean relative to baseline)	-0.03	-0.05	-0.05	-0.03	-0.04
Maize	Historical baseline: 1971−2000	0.26	0.31	0.18	0.17	0.38
	Multi-model mean: 2020−2049	0.24	0.28	0.13	0.13	NA
	Change in absolute values of index (in multi-model mean relative to baseline)	-0.02	-0.03	-0.05	-0.04	NA
Rice	Historical baseline: 1971−2000	0.36	0.36	0.20	0.23	0.38
	Multi-model mean: 2020−2049	0.35	0.34	0.17	0.19	0.38
	Change in absolute values of index (in multi-model mean relative to baseline)	-0.02	-0.02	-0.02	-0.03	0.00
Soy-Bean	Historical baseline: 1971−2000	0.34	0.34	0.18	0.24	NA
	Multi-model mean: 2020−2049	0.33	0.33	0.17	NA	0.24
	Change in absolute values of index (in multi-model mean relative to baseline)	-0.01	-0.01	-0.01	NA	-0.01
Wheat	Historical baseline: 1971−2000	0.30	0.32	0.13	0.40	0.28
	Multi-model mean: 2020−2049	0.30	0.31	0.11	0.41	NA
	Change in absolute values of index (in multi-model mean relative to baseline)	0.00	-0.01	-0.01	0.02	NA

Table A- 10. Water stress indices for rain-fed simulations, and mean changes in absolute values of index between historical and future periods.

Crop	Water Stress for Rainfed	AND	BRA	CEN	MEX	SUR
Bean	Historical baseline: 1971−2000	0.10	0.07	0.13	0.23	0.09
	Multi-model mean: 2020−2049	0.12	0.09	0.15	0.25	0.11
	% change (in multi-model mean relative to baseline)	0.02	0.02	0.02	0.02	0.03
Maize	Historical baseline: 1971−2000	0.05	0.05	0.03	0.18	0.10
	Multi-model mean: 2020−2049	0.08	0.07	0.09	0.24	NA
	% change (in multi-model mean relative to baseline)	0.03	0.02	0.06	0.06	NA
Rice	Historical baseline: 1971−2000	0.01	0.01	0.02	0.06	0.08
	Multi-model mean: 2020−2049	0.03	0.02	0.07	0.12	0.09
	% change (in multi-model mean relative to baseline)	0.02	0.01	0.05	0.06	0.02
Soy-Bean	Historical baseline: 1971−2000	0.04	0.01	0.00	NA	0.05
	Multi-model mean: 2020−2049	0.06	0.01	0.02	NA	0.06
	% change (in multi-model mean relative to baseline)	0.02	0.01	0.02	NA	0.02
Wheat	Historical baseline: 1971−2000	0.17	0.06	0.03	0.33	0.13
	Multi-model mean: 2020−2049	0.18	0.08	0.04	0.33	NA
	% change (in multi-model mean relative to baseline)	0.02	0.02	0.01	0.00	NA

Figures

```
*EXP.DETAILS: BID17101RZ MAIZE LAC

*GENERAL
@PEOPLE
DObando JMesa
@ADDRESS
CIAT
@SITE
CALI
*TREATMENTS                        -------------FACTOR LEVELS------------
@N R O C TNAME.................... CU FL SA IC MP MI MF MR MC MT ME MH SM
 1 1 1 0 BID001                    1  1  0  1  1  0  1  0  0  0  0  0  1

*CULTIVARS
@C CR INGENO CNAME
 1 MZ IB0056 MZNA

*FIELDS
@L ID_FIELD WSTA....  FLSA  FLOB  FLDT  FLDD  FLDS  FLST SLTX  SLDP  ID_SOIL    FLNAME
 1 BID1     JBID       -99   -99 DR000   -99   -99   -99 -99    -99  BID0000001 FIELD01
@L .........XCRD ...........YCRD .....ELEV .............AREA .SLEN .FLWR .SLAS FLHST FHDUR
 1         -99.000         -99.000       -99               -99   -99   -99   -99   -99   -99

*INITIAL CONDITIONS
@C   PCR ICDAT  ICRT  ICND  ICRN  ICRE  ICWD ICRES ICREN ICREP ICRIP ICRID ICNAME
 1    MZ 72151     1   -99     1     1   -99   -99   -99   -99   -99   -99 -99
@C  ICBL  SH2O  SNH4  SNO3
 1    15  0.15 12.10 12.10
 1    25  0.15  5.46  5.46
 1    45  0.04  1.49  1.49
 1    55  0.04  0.96  0.96
 1    65  0.04  0.76  0.76
 1   100  0.04  0.49  0.49

*PLANTING DETAILS
@P PDATE EDATE  PPOP  PPOE  PLME  PLDS  PLRS  PLRD  PLDP  PLWT  PAGE  PENV  PLPH  SPRL
 1   -99   -99     7     5     S     R   -99     0     5   -99   -99   -99   -99   -99

*FERTILIZERS (INORGANIC)
@F FDATE  FMCD  FACD  FDEP  FAMN  FAMP  FAMK  FAMC  FAMO  FOCD FERNAME
 1     0 FE005 AP002     4  92.0     0   -99   -99   -99   -99 -99

*SIMULATION CONTROLS
@N GENERAL     NYERS NREPS START SDATE RSEED SNAME.................... SMODEL
 1 GE             25     1     S 72151  2150 simctr1                   MZCER045
@N OPTIONS     WATER NITRO SYMBI PHOSP POTAS DISES  CHEM  TILL   CO2
 1 OP              Y     Y     N     N     N     N     N     N     D
@N METHODS     WTHER INCON LIGHT EVAPO INFIL PHOTO HYDRO NSWIT MESOM MESEV MESOL
 1 ME              M     M     E     R     S     C     R     1     G     S     2
@N MANAGEMENT  PLANT IRRIG FERTI RESID HARVS
 1 MA              A     N     D     R     M
@N OUTPUTS     FNAME OVVEW SUMRY FROPT GROUT CAOUT WAOUT NIOUT MIOUT DIOUT VBOSE CHOUT OPOUT
 1 OU              N     Y     Y     1     Y     Y     Y     Y     Y     Y     Y     Y     Y

@  AUTOMATIC MANAGEMENT
@N PLANTING    PFRST PLAST PH2OL PH2OU PH2OD PSTMX PSTMN
 1 PL            166 72226    50   100    30    40    10
@N IRRIGATION  IMDEP ITHRL ITHRU IROFF IMETH IRAMT IREFF
 1 IR             30    50   100 GS000 IR001    10     1
@N NITROGEN    NMDEP NMTHR NAMNT NCODE NAOFF
 1 NI             30    50    25 FE001 GS000
@N RESIDUES    RIPCN RTIME RIDEP
 1 RE            100     1    20
@N HARVEST     HFRST HLAST HPCNP HPCNR
 1 HA              0     1   100     0
```

Figure A- 1. Example of x-file for rain-fed maize in DSSAT Shell.

```
*EXP.DETAILS: BID17101RZ MAIZE LAC

*GENERAL
@PEOPLE
Diego Obando Jeison Mesa
@ADDRESS
CIAT
@SITE
CALI
*TREATMENTS                        -------------FACTOR LEVELS------------
@N R O C TNAME..................... CU FL SA IC MP MI MF MR MC MT ME MH SM
 1 1 1 0 BID001                     1  1  0  1  1  0  1  0  0  0  0  0  1

*CULTIVARS
@C CR INGENO CNAME
 1 MZ IB0056 MZNA

*FIELDS
@L ID_FIELD WSTA....  FLSA  FLOB  FLDT  FLDD  FLDS  FLST SLTX  SLDP  ID_SOIL    FLNAME
 1 BID1     JBID       -99   -99 DR000   -99   -99   -99 -99    -99  BID0000001 FIELD01
@L ..........XCRD ...........YCRD .....ELEV .............AREA .SLEN .FLWR .SLAS FLHST FHDUR
 1         -99.000         -99.000       -99               -99   -99   -99   -99   -99   -99

*INITIAL CONDITIONS
@C   PCR ICDAT  ICRT  ICND  ICRN  ICRE  ICWD ICRES ICREN ICREP ICRIP ICRID ICNAME
 1    MZ 72166     1   -99     1     1   -99   -99   -99   -99   -99   -99 -99
@C  ICBL  SH2O  SNH4  SNO3
 1    15   -99 12.10 12.10
 1    25   -99  5.46  5.46
 1    45   -99  1.49  1.49
 1    55   -99  0.96  0.96
 1    65   -99  0.76  0.76
 1   100   -99  0.49  0.49

*PLANTING DETAILS
@P PDATE EDATE  PPOP  PPOE  PLME  PLDS  PLRS  PLRD  PLDP  PLWT  PAGE  PENV  PLPH  SPRL                          PLNAME
 1 72166   -99     7     5     S     R   -99     0     5   -99   -99   -99   -99   -99

*FERTILIZERS (INORGANIC)
@F FDATE  FMCD  FACD  FDEP  FAMN  FAMP  FAMK  FAMC  FAMO  FOCD FERNAME
 1     0 FE005 AP002     4  92.0     0   -99   -99   -99   -99 -99
 1    40 FE005 AP002     0  92.0     0   -99   -99   -99   -99 -99

*SIMULATION CONTROLS
@N GENERAL     NYERS NREPS START SDATE RSEED SNAME.................... SMODEL
 1 GE             25     1     S 72166  2150 simctr1                  MZCER045
@N OPTIONS     WATER NITRO SYMBI PHOSP POTAS DISES  CHEM  TILL   CO2
 1 OP             Y     Y     N     N     N     N     N     N     D
@N METHODS     WTHER INCON LIGHT EVAPO INFIL PHOTO HYDRO NSWIT MESOM MESEV MESOL
 1 ME             M     M     E     R     S     C     R     1     G     S     2
@N MANAGEMENT  PLANT IRRIG FERTI RESID HARVS
 1 MA             R     A     D     R     M
@N OUTPUTS     FNAME OVVEW SUMRY FROPT GROUT CAOUT WAOUT NIOUT MIOUT DIOUT VBOSE CHOUT OPOUT
 1 OU             N     Y     Y     1     Y     Y     Y     Y     Y     Y     Y     Y     Y

@  AUTOMATIC MANAGEMENT
@N PLANTING    PFRST PLAST PH2OL PH2OU PH2OD PSTMX PSTMN
 1 PL            -99   -99    50   100    30    40    10
@N IRRIGATION  IMDEP ITHRL ITHRU IROFF IMETH IRAMT IREFF
 1 IR             30    50   100 GS000 IR001    10     1
@N NITROGEN    NMDEP NMTHR NAMNT NCODE NAOFF
 1 NI             30    50    25 FE001 GS000
@N RESIDUES    RIPCN RTIME RIDEP
 1 RE            100     1    20
@N HARVEST     HFRST HLAST HPCNP HPCNR
 1 HA              0     1   100     0
```

Figure A- 2. Example of x-file for irrigated rice in DSSAT Shell.

```
*EXP.DETAILS: BID17101RZ WHEAT LAC

*GENERAL
@PEOPLE
Diego Obando Jeison Mesa
@ADDRESS
CIAT
@SITE
CALI
*TREATMENTS                        -------------FACTOR LEVELS------------
@N R O C TNAME.................. CU FL SA IC MP MI MF MR MC MT ME MH SM
 1 1 1 0 BID001                  1  1  0  1  1  0  1  0  0  0  0  0  1

*CULTIVARS
@C CR INGENO CNAME
 1 WH IB0020 WHNA

*FIELDS
@L ID_FIELD WSTA....  FLSA  FLOB  FLDT  FLDD  FLDS  FLST SLTX  SLDP  ID_SOIL    FLNAME
 1 BID1     JBID       -99   -99 DR000   -99   -99   -99 -99    -99  BID0000001 FIELD01
@L ..........XCRD ...........YCRD .....ELEV .............AREA .SLEN .FLWR .SLAS FLHST FHDUR
 1         -99.000         -99.000       -99               -99   -99   -99   -99   -99   -99

*INITIAL CONDITIONS
@C   PCR ICDAT  ICRT  ICND  ICRN  ICRE  ICWD ICRES ICREN ICREP ICRIP ICRID ICNAME
 1    MZ 72015     1   -99     1     1   -99   -99   -99   -99   -99   -99 -99
@C  ICBL  SH2O  SNH4  SNO3
 1     6   -99  3.62  3.62
 1    12   -99  2.82  2.82
 1    25   -99  0.78  0.78
 1    40   -99  0.65  0.65
 1    60   -99  0.08  0.08

*PLANTING DETAILS
@P PDATE EDATE  PPOP  PPOE  PLME  PLDS  PLRS  PLRD  PLDP  PLWT  PAGE  PENV  PLPH  SPRL                          PLNAME
 1 72015   -99   250   250     S     R   -99     0     4   -99   -99   -99   -99   -99

*FERTILIZERS (INORGANIC)
@F FDATE  FMCD  FACD  FDEP  FAMN  FAMP  FAMK  FAMC  FAMO  FOCD FERNAME
 1     0 FE005 AP002     4 108.0     0   -99   -99   -99   -99 -99
 1    30 FE005 AP002     0 108.0     0   -99   -99   -99   -99 -99

*SIMULATION CONTROLS
@N GENERAL     NYERS NREPS START SDATE RSEED SNAME.................... SMODEL
 1 GE             25     1     S 72015  2150 simctr1                  WHCER045
@N OPTIONS     WATER NITRO SYMBI PHOSP POTAS DISES  CHEM  TILL   CO2
 1 OP              Y     Y     N     N     N     N     N     N     D
@N METHODS     WTHER INCON LIGHT EVAPO INFIL PHOTO HYDRO NSWIT MESOM MESEV MESOL
 1 ME              M     M     E     R     S     C     R     1     G     S     2
@N MANAGEMENT  PLANT IRRIG FERTI RESID HARVS
 1 MA              R     A     D     R     M
@N OUTPUTS     FNAME OVVEW SUMRY FROPT GROUT CAOUT WAOUT NIOUT MIOUT DIOUT VBOSE CHOUT OPOUT
 1 OU              N     Y     Y     1     Y     Y     Y     Y     Y     Y     Y     Y     Y

@  AUTOMATIC MANAGEMENT
@N PLANTING    PFRST PLAST PH2OL PH2OU PH2OD PSTMX PSTMN
 1 PL            -99   -99    50   100    30    40    10
@N IRRIGATION  IMDEP ITHRL ITHRU IROFF IMETH IRAMT IREFF
 1 IR             30    50   100 GS000 IR001    10     1
@N NITROGEN    NMDEP NMTHR NAMNT NCODE NAOFF
 1 NI             30    50    25 FE001 GS000
@N RESIDUES    RIPCN RTIME RIDEP
 1 RE            100     1    20
@N HARVEST     HFRST HLAST HPCNP HPCNR
 1 HA              0     1   100     0
```

Figure A- 3. Example of x-file for irrigated wheat in DSSAT Shell.

```
*EXP.DETAILS: BID17101RZ BEAN LAC

*GENERAL
@PEOPLE
Diego Obando Jeison Mesa
@ADDRESS
CIAT
@SITE
CALI
*TREATMENTS                        -------------FACTOR LEVELS------------
@N R O C TNAME..................... CU FL SA IC MP MI MF MR MC MT ME MH SM
 1 1 1 0 BID001                     1  1  0  1  1  0  1  0  0  0  0  0  1

*CULTIVARS
@C CR INGENO CNAME
 1 BN IB0033 BZNA

*FIELDS
@L ID_FIELD WSTA....  FLSA  FLOB  FLDT  FLDD  FLDS  FLST SLTX  SLDP  ID_SOIL    FLNAME
 1 BID1     JBID       -99   -99 DR000   -99   -99   -99 -99    -99  BID0000001 FIELD01
@L ..........XCRD ...........YCRD .....ELEV .............AREA .SLEN .FLWR .SLAS FLHST FHDUR
 1         -99.000         -99.000       -99               -99   -99   -99   -99   -99   -99

*INITIAL CONDITIONS
@C   PCR ICDAT  ICRT  ICND  ICRN  ICRE  ICWD ICRES ICREN ICREP ICRIP ICRID ICNAME
 1    MZ 72243     1   -99     1     1   -99   -99   -99   -99   -99   -99 -99
@C  ICBL  SH2O  SNH4  SNO3
 1    15  0.08  0.50  0.50
 1    35  0.17  0.30  0.30
 1    60  0.21  0.20  0.20
 1    80  0.21  0.20  0.20
 1   100  0.21  0.20  0.20
 1   160  0.19  0.10  0.10

*PLANTING DETAILS
@P PDATE EDATE  PPOP  PPOE  PLME  PLDS  PLRS  PLRD  PLDP  PLWT  PAGE  PENV  PLPH  SPRL                      PLNAME
 1   -99   -99    20    20     S     R   -99     0     2   -99   -99   -99   -99   -99

*FERTILIZERS (INORGANIC)
@F FDATE  FMCD  FACD  FDEP  FAMN  FAMP  FAMK  FAMC  FAMO  FOCD FERNAME
 1     0 FE005 AP002     4  30.0     0   -99   -99   -99   -99 -99
 1     2 FE005 AP002     0   0.0     0   -99   -99   -99   -99 -99

*SIMULATION CONTROLS
@N GENERAL     NYERS NREPS START SDATE RSEED SNAME.................... SMODEL
 1 GE             25     1     S 72243  2150 simctr1                  BNGRO045
@N OPTIONS     WATER NITRO SYMBI PHOSP POTAS DISES  CHEM  TILL   CO2
 1 OP               Y     Y     N     N     N     N     N     N     D
@N METHODS     WTHER INCON LIGHT EVAPO INFIL PHOTO HYDRO NSWIT MESOM MESEV MESOL
 1 ME               M     M     E     R     S     C     R     1     G     S     2
@N MANAGEMENT  PLANT IRRIG FERTI RESID HARVS
 1 MA               A     N     D     R     M
@N OUTPUTS     FNAME OVVEW SUMRY FROPT GROUT CAOUT WAOUT NIOUT MIOUT DIOUT VBOSE CHOUT OPOUT
 1 OU               N     Y     Y     1     Y     Y     Y     Y     Y     Y     Y     Y     Y

@  AUTOMATIC MANAGEMENT
@N PLANTING    PFRST PLAST PH2OL PH2OU PH2OD PSTMX PSTMN
 1 PL            258 72318    50   100    30    40    10
@N IRRIGATION  IMDEP ITHRL ITHRU IROFF IMETH IRAMT IREFF
 1 IR             30    50   100 GS000 IR001    10     1
@N NITROGEN    NMDEP NMTHR NAMNT NCODE NAOFF
 1 NI             30    50    25 FE001 GS000
@N RESIDUES    RIPCN RTIME RIDEP
 1 RE            100     1    20
@N HARVEST     HFRST HLAST HPCNP HPCNR
 1 HA               0     1   100     0
```

Figure A- 4. Example of x-file for rain-fed drybean in DSSAT Shell.

```
*EXP.DETAILS: BID17101RZ SOY LAC

*GENERAL
@PEOPLE
Diego Obando Jeison Mesa
@ADDRESS
CIAT
@SITE
CALI
*TREATMENTS                        -------------FACTOR LEVELS------------
@N R O C TNAME..................... CU FL SA IC MP MI MF MR MC MT ME MH SM
 1 1 1 0 BID001                     1  1  0  1  1  0  1  0  0  0  0  0  1

*CULTIVARS
@C CR INGENO CNAME
 1 SB IB0045 SZNA

*FIELDS
@L ID_FIELD WSTA....  FLSA  FLOB  FLDT  FLDD  FLDS  FLST SLTX  SLDP  ID_SOIL    FLNAME
 1 BID1     JBID       -99   -99 DR000   -99   -99   -99 -99    -99  BID0000001 FIELD01
@L ..........XCRD ...........YCRD .....ELEV .............AREA .SLEN .FLWR .SLAS FLHST FHDUR
 1         -99.000         -99.000       -99               -99   -99   -99   -99   -99   -99

*INITIAL CONDITIONS
@C   PCR ICDAT  ICRT  ICND  ICRN  ICRE  ICWD ICRES ICREN ICREP ICRIP ICRID ICNAME
 1    MZ 72015     1   -99     1     1   -99   -99   -99   -99   -99   -99 -99
@C  ICBL  SH2O  SNH4  SNO3
 1    15   -99  1.68  1.68
 1    45   -99  0.89  0.89
 1    70   -99  0.55  0.55
 1    92   -99 -99.00 -99.00
 1   126   -99 -99.00 -99.00
 1   140   -99 -99.00 -99.00

*PLANTING DETAILS
@P PDATE EDATE  PPOP  PPOE  PLME  PLDS  PLRS  PLRD  PLDP  PLWT  PAGE  PENV  PLPH  SPRL                          PLNAME
 1 72015   -99    20    20     S     R   -99     0     3   -99   -99   -99   -99   -99

*FERTILIZERS (INORGANIC)
@F FDATE  FMCD  FACD  FDEP  FAMN  FAMP  FAMK  FAMC  FAMO  FOCD FERNAME
 1     0 FE005 AP002     4  27.0     0   -99   -99   -99   -99 -99
 1    21 FE005 AP002     0   0.0     0   -99   -99   -99   -99 -99

*SIMULATION CONTROLS
@N GENERAL     NYERS NREPS START SDATE RSEED SNAME.................... SMODEL
 1 GE             25     1     S 72015  2150 simctr1                   SBGRO045
@N OPTIONS     WATER NITRO SYMBI PHOSP POTAS DISES  CHEM  TILL   CO2
 1 OP               Y     Y     N     N     N     N     N     N     D
@N METHODS     WTHER INCON LIGHT EVAPO INFIL PHOTO HYDRO NSWIT MESOM MESEV MESOL
 1 ME               M     M     E     R     S     C     R     1     G     S     2
@N MANAGEMENT  PLANT IRRIG FERTI RESID HARVS
 1 MA               R     A     D     R     M
@N OUTPUTS     FNAME OVVEW SUMRY FROPT GROUT CAOUT WAOUT NIOUT MIOUT DIOUT VBOSE CHOUT OPOUT
 1 OU               N     Y     Y     1     Y     Y     Y     Y     Y     Y     Y     Y     Y

@  AUTOMATIC MANAGEMENT
@N PLANTING    PFRST PLAST PH2OL PH2OU PH2OD PSTMX PSTMN
 1 PL            -99   -99    50   100    30    40    10
@N IRRIGATION  IMDEP ITHRL ITHRU IROFF IMETH IRAMT IREFF
 1 IR             30    50   100 GS000 IR001    10     1
@N NITROGEN    NMDEP NMTHR NAMNT NCODE NAOFF
 1 NI             30    50    25 FE001 GS000
@N RESIDUES    RIPCN RTIME RIDEP
 1 RE            100     1    20
@N HARVEST     HFRST HLAST HPCNP HPCNR
 1 HA               0     1   100     0
```

Figure A- 5. Example of x-file for irrigated soybean in DSSAT Shell.

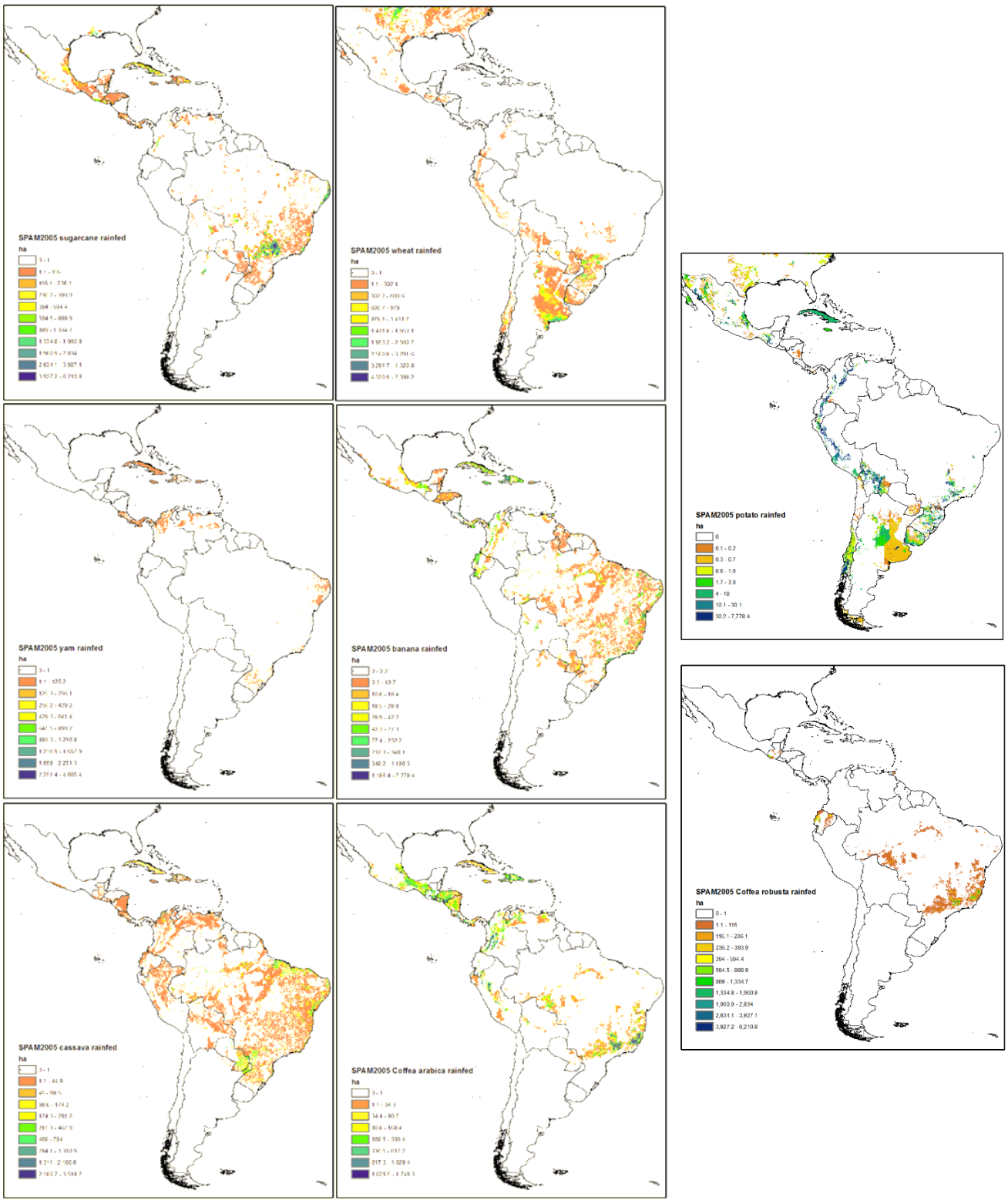

Figure A- 6. Rainfed physical cultivation areas according to SPAM for the year 2005 for the crops included in the EcoCrop analysis.

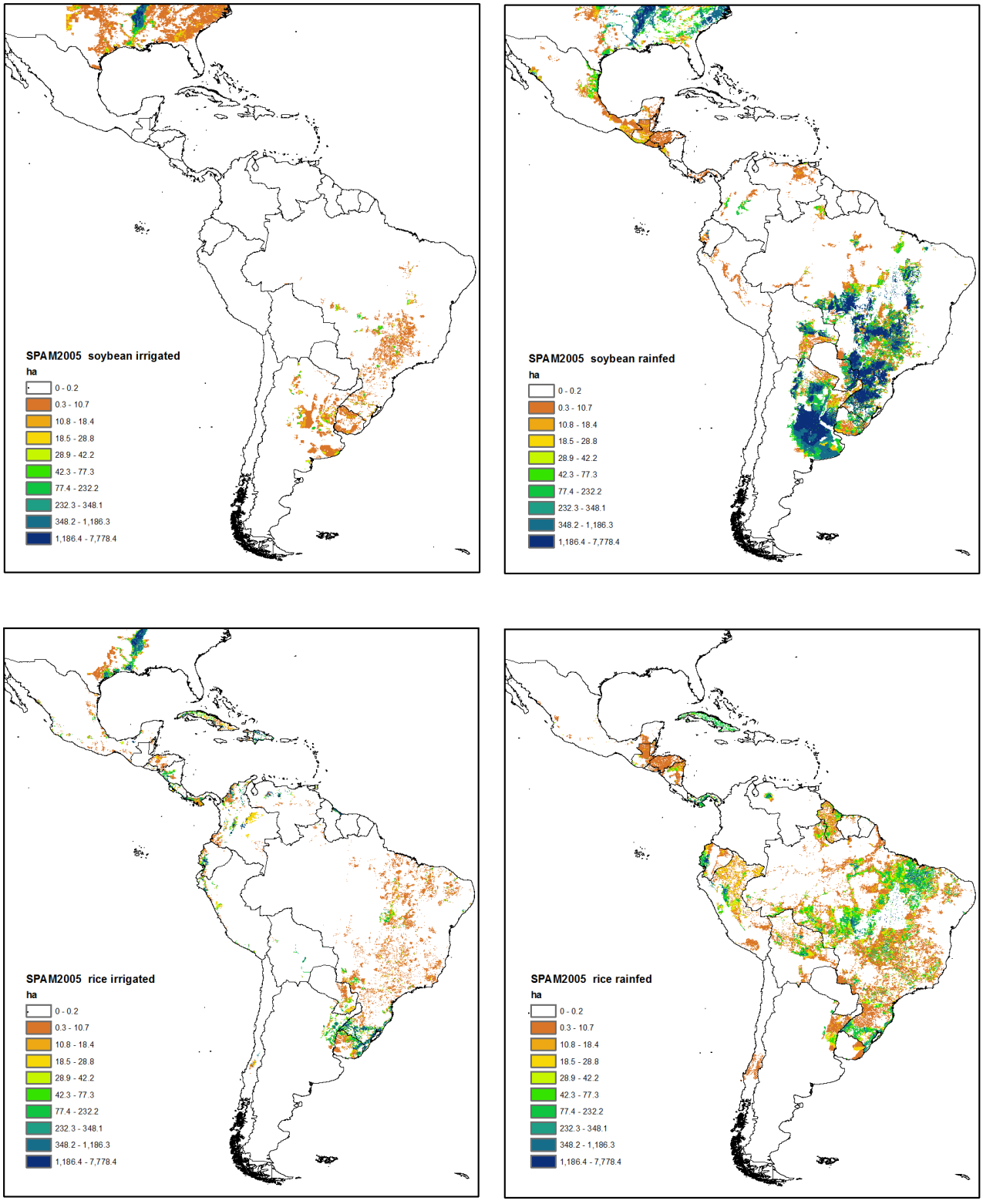

Figure A- 7. Physical cultivation areas according to SPAM for the year 2005 for soybean and rice.

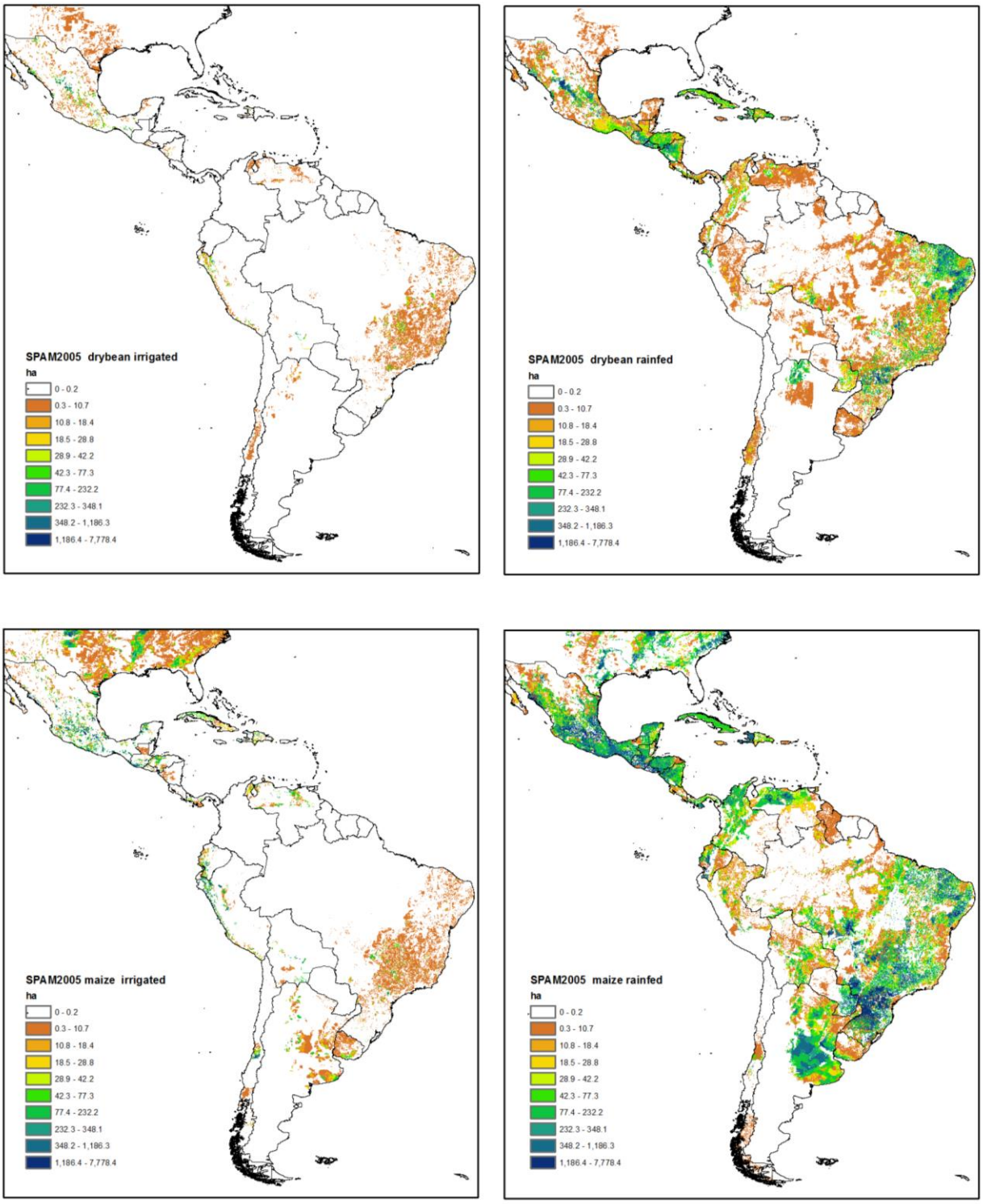

Figure A- 8. Physical cultivation areas according to SPAM for the year 2005 for drybean and maize.

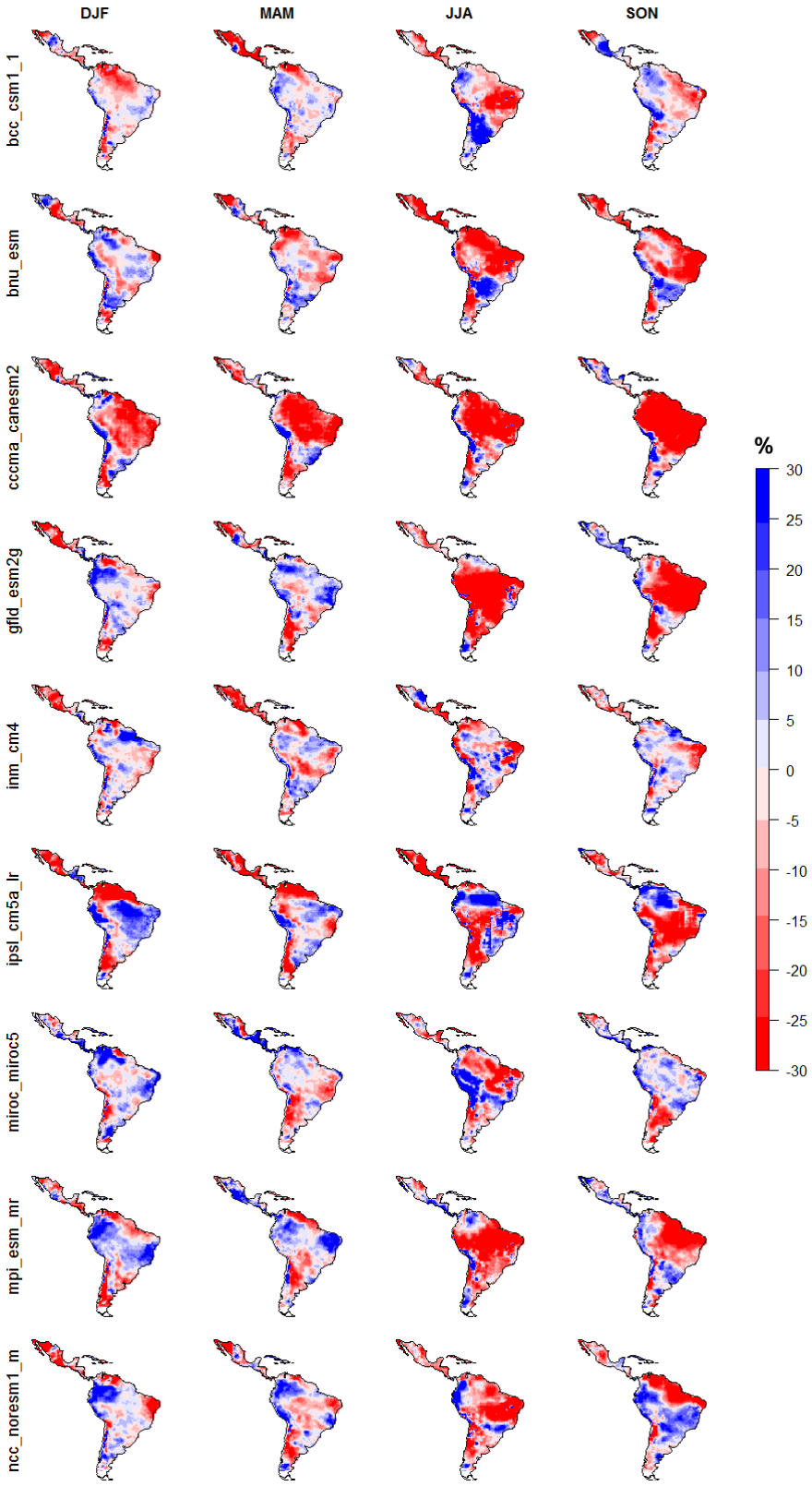

Figure A- 9. Changes in average of accumulated rainfall (one GCM by line from top to bottom) aggregated by seasons: December-January-February (DJF), March-April-May (MAM), June-July-August (JJA) and September-October-November (SON).

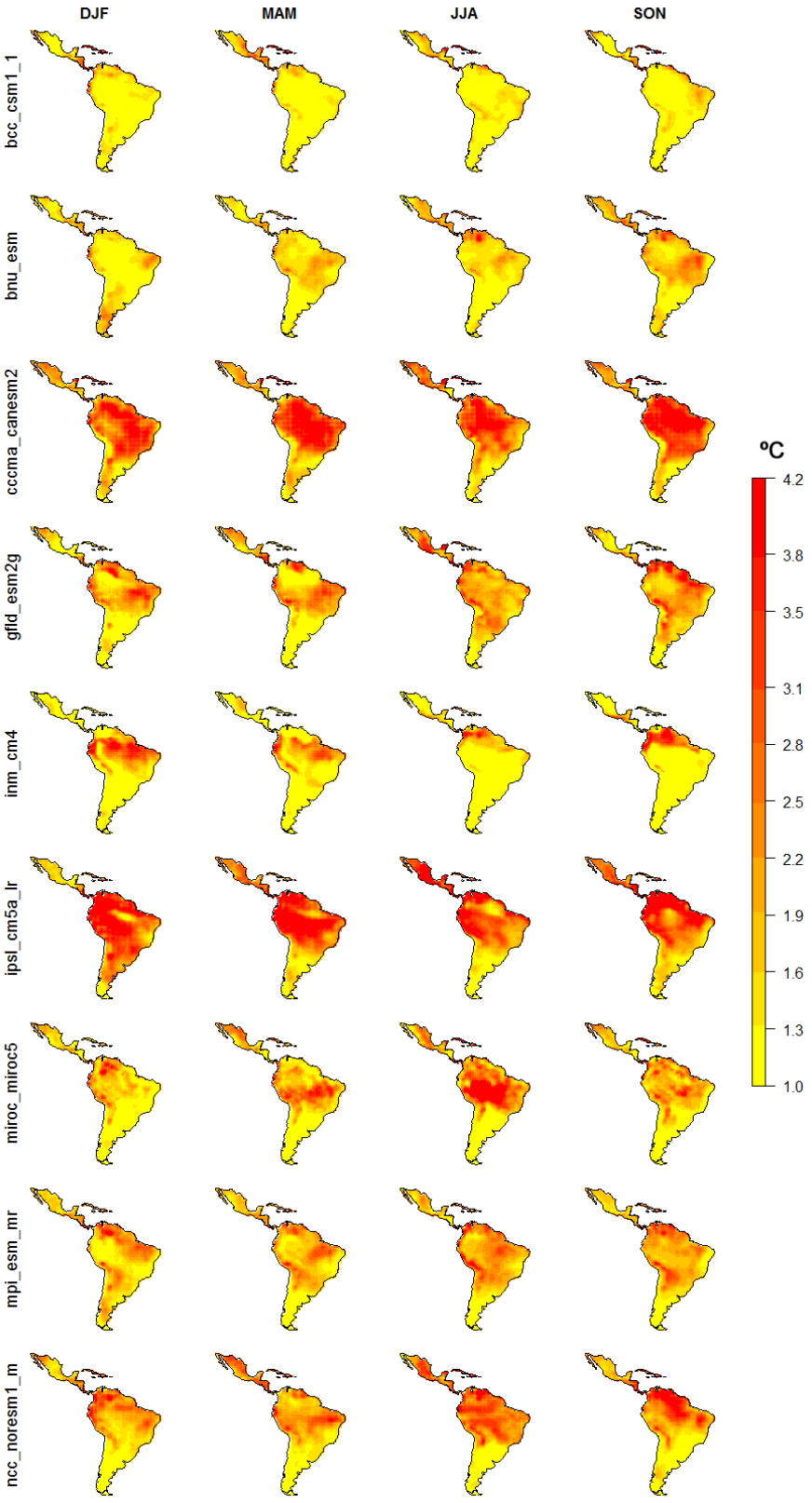

Figure A- 10. Changes in average of daily maximum temperature (one GCM by line from top to bottom) aggregated by seasons: December-January-February (DJF), March-April-May (MAM), June-July-August (JJA) and September-October-November (SON).

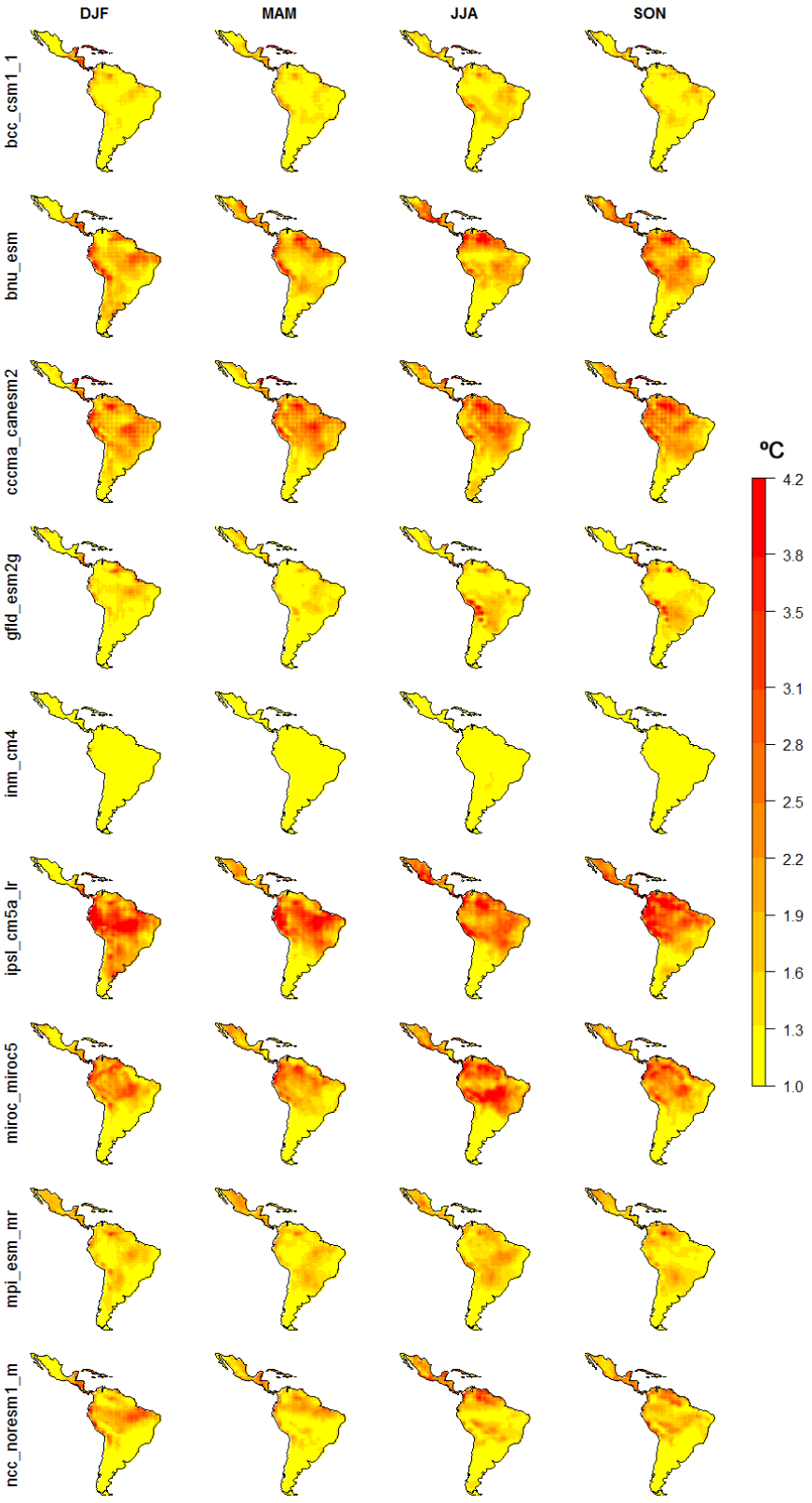

Figure A- 11. Changes in average of daily minimum temperature (one GCM by line from top to bottom) aggregated by seasons: December-January-February (DJF), March-April-May (MAM), June-July-August (JJA) and September-October-November (SON).

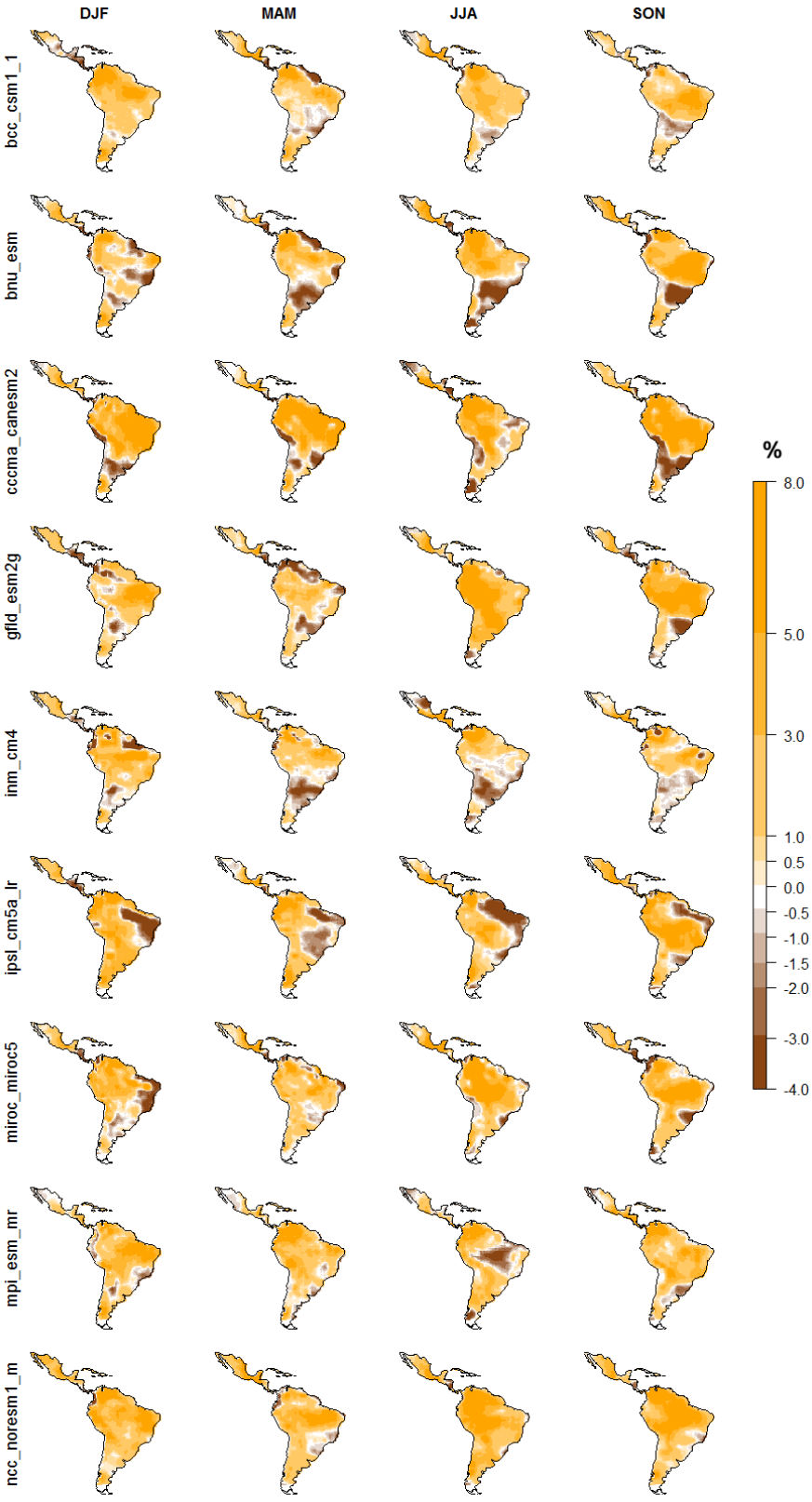

Figure A- 12. Changes in average of solar radiation aggregated (one GCM by line from top to bottom) aggregated by seasons: December-January-February (DJF), March-April-May (MAM), June-July-August (JJA) and September-October-November (SON).

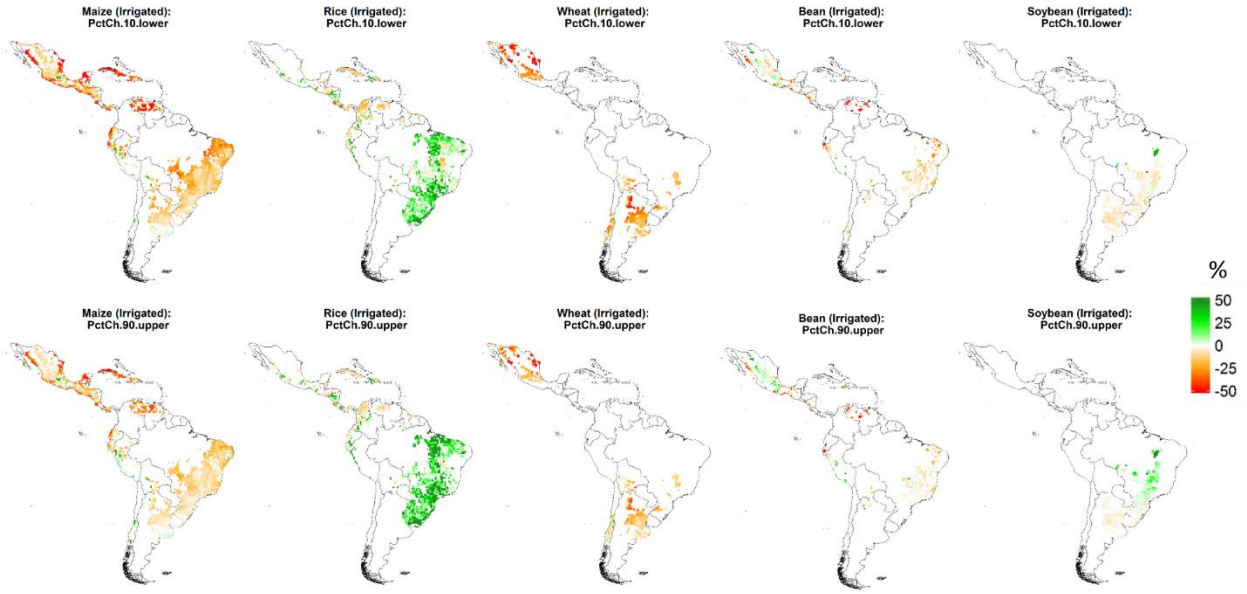

Figure A- 13. 10th and 90th percentiles of projected yield changes across GCM's (with percentiles calculated from bootstrapping procedure) for irrigated production.

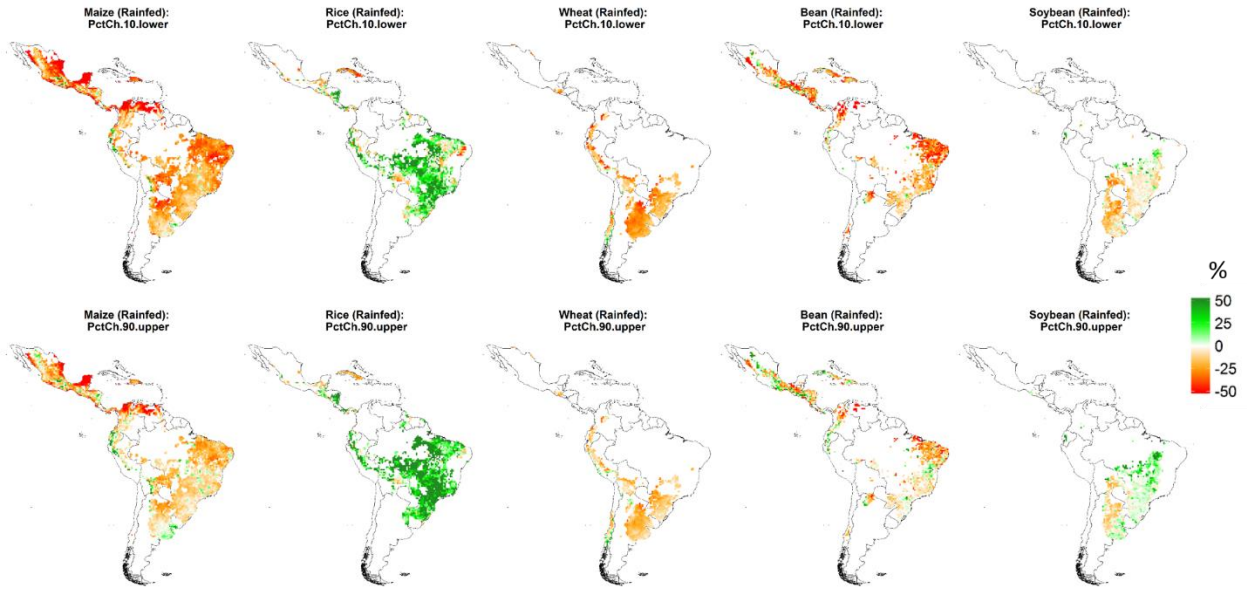

Figure A- 14. 10th and 90th percentiles of projected yield changes across GCM's (with percentiles calculated from bootstrapping procedure) for rain-fed production.

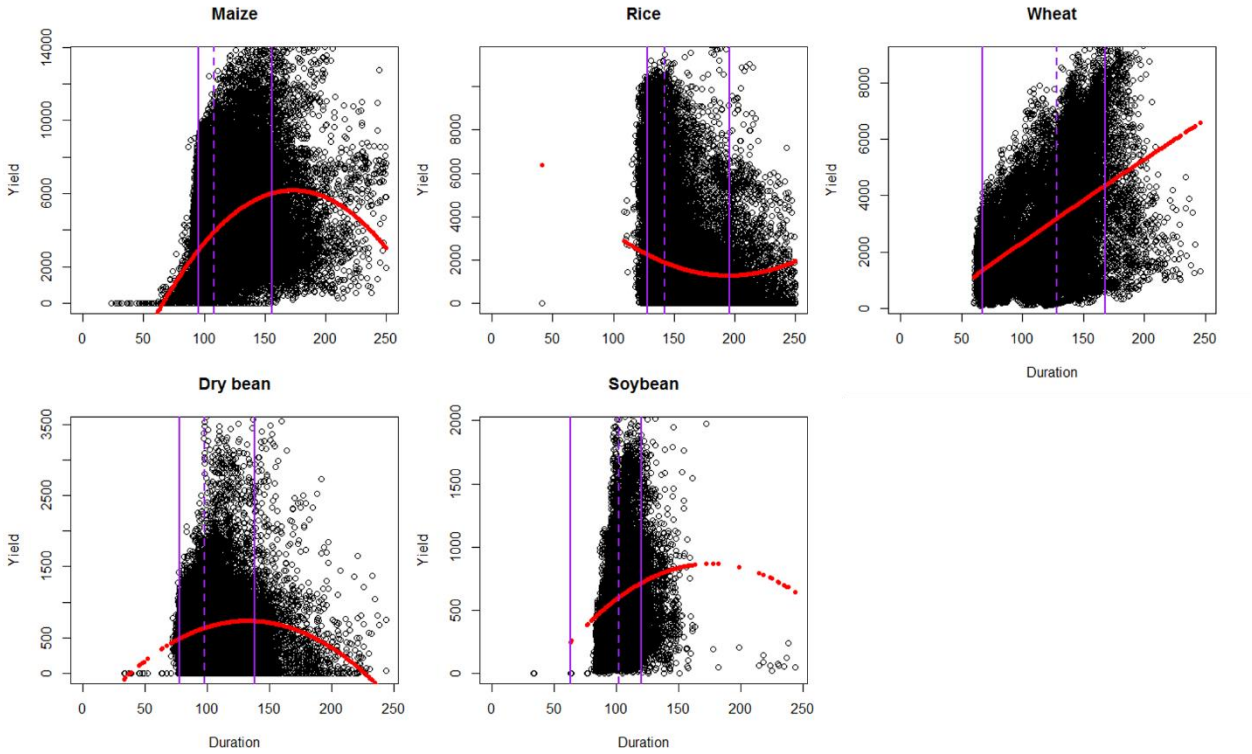

Figure A- 15. Simulated duration vs. yield for rain-fed crops, along with a quadratic curve fit to each cloud of points. The dotted purple line represents the median duration, whereas the two solid purple lines represent the 5th and 95th percentiles.

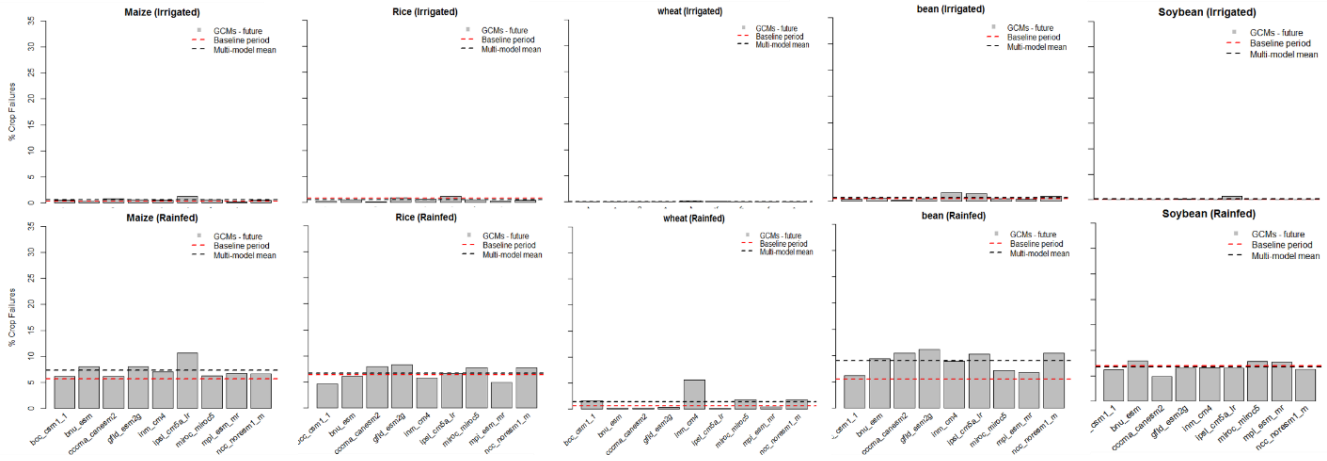

Figure A- 16. Average rates of crop failures across all cultivation areas for each production system. Results are shown for the 9 GCM's (bars), the historical baseline (red dotted line) and the mean across GCM's in the future period (black dotted line).

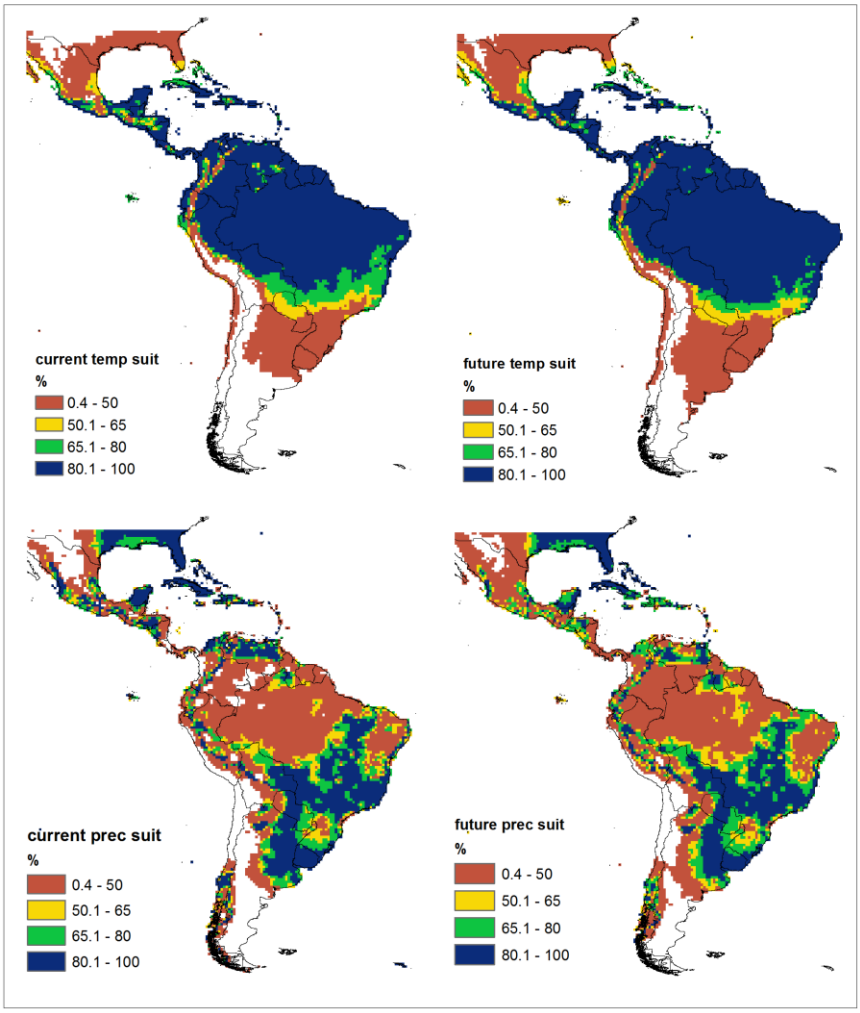

Figure A- 17. Temperature (above) and precipitation (below) suitability for current (left) and future (right) conditions for sugarcane.

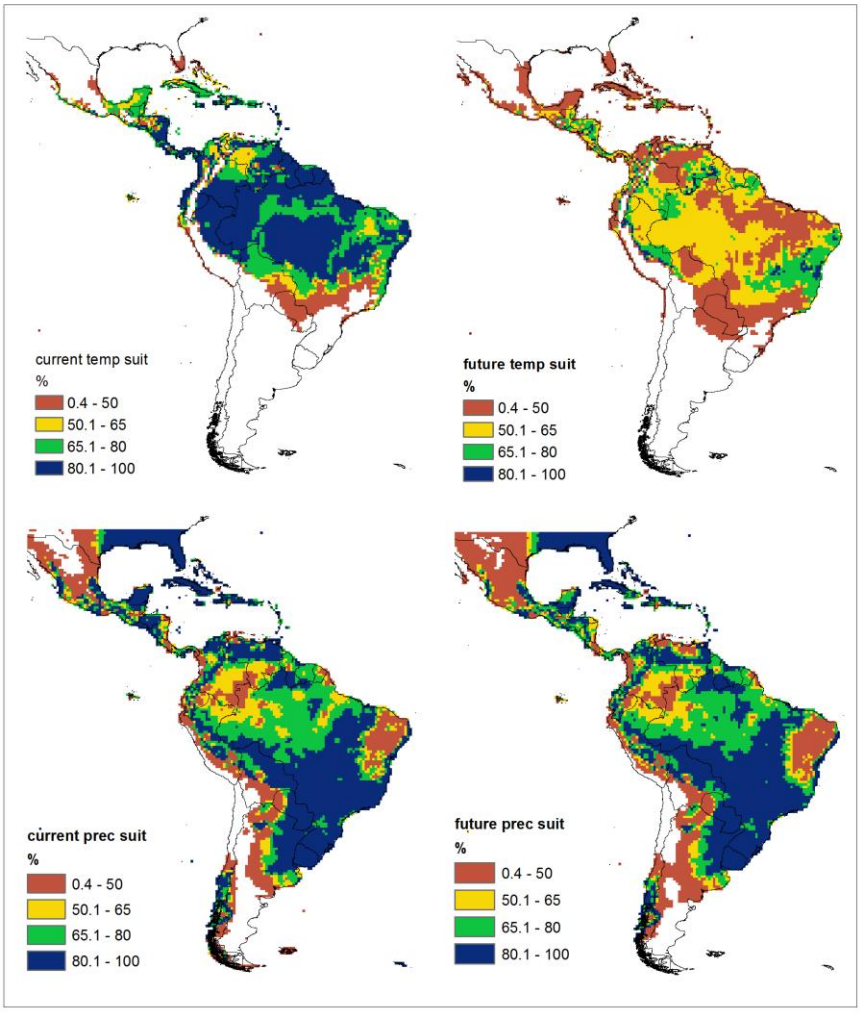

Figure A- 18. Temperature (above) and precipitation (below) suitability for current (left) and future (right) conditions for banana.

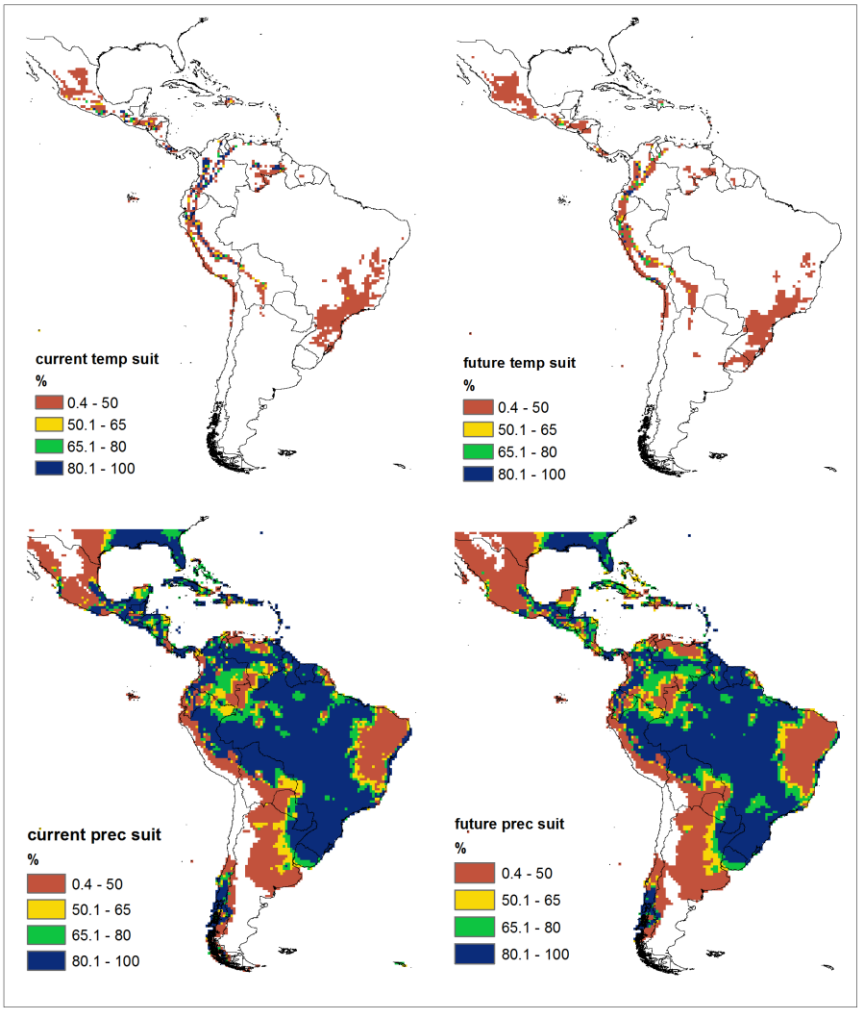

Figure A- 19. Temperature (above) and precipitation (below) suitability for current (left) and future (right) conditions for *Coffea arabica*.

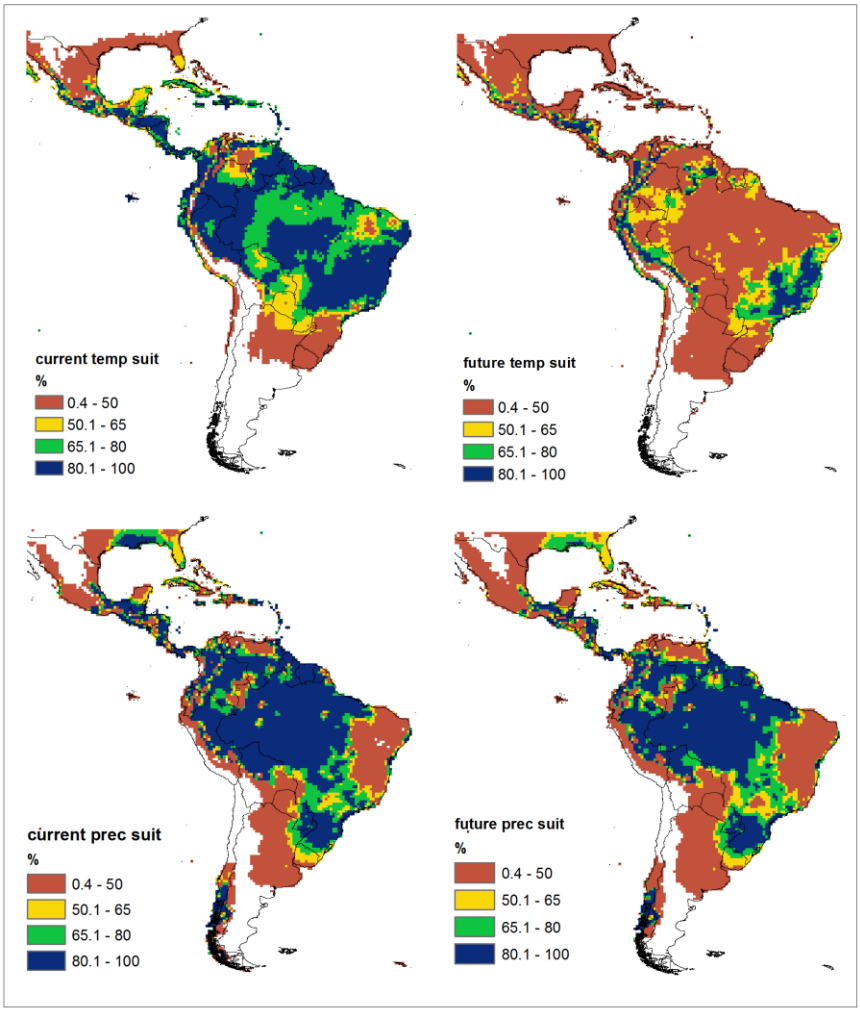

Figure A- 20. Temperature (above) and precipitation (below) suitability for current (left) and future (right) conditions for *Coffea robusta*.

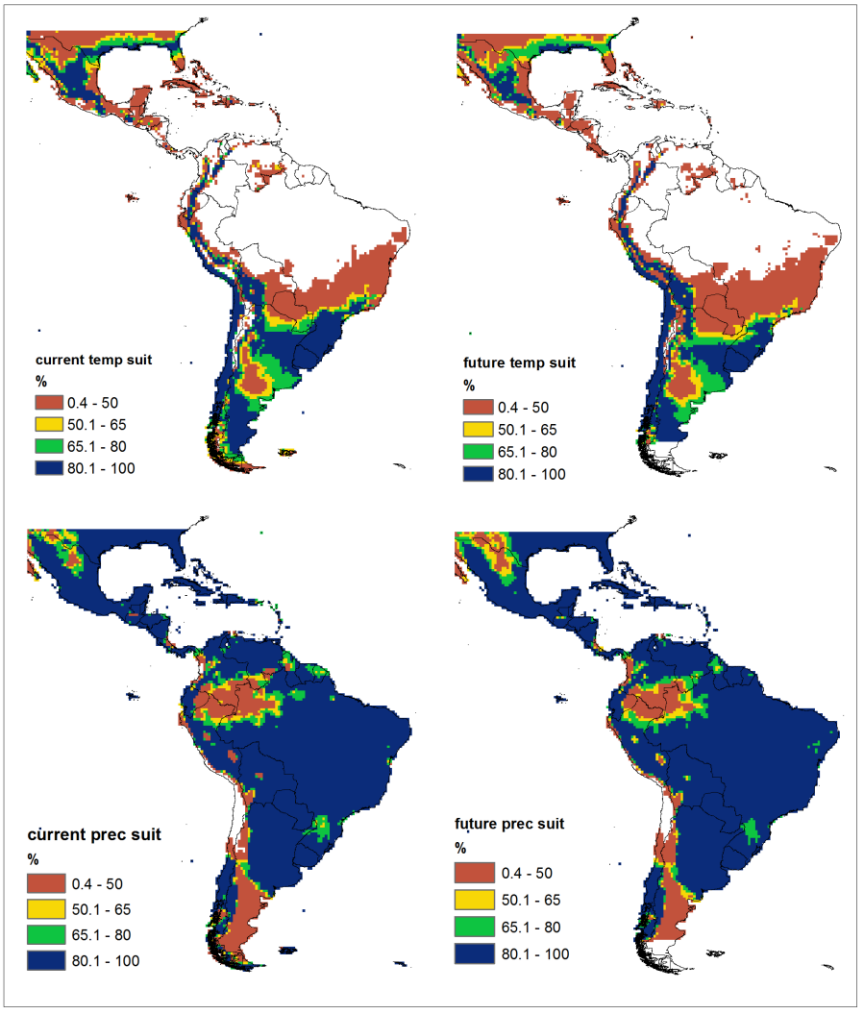

Figure A- 21. Temperature (above) and precipitation (below) suitability for current (left) and future (right) conditions for potato.

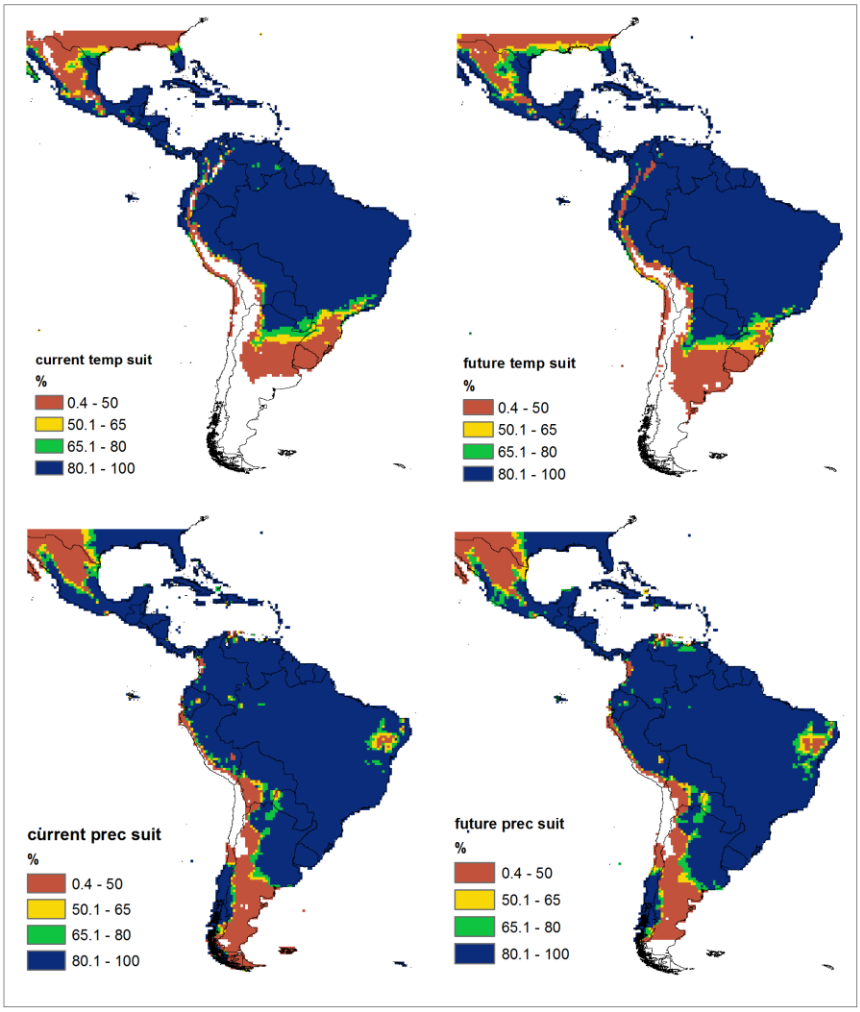

Figure A- 22. Temperature (above) and precipitation (below) suitability for current (left) and future (right) conditions for cassava.

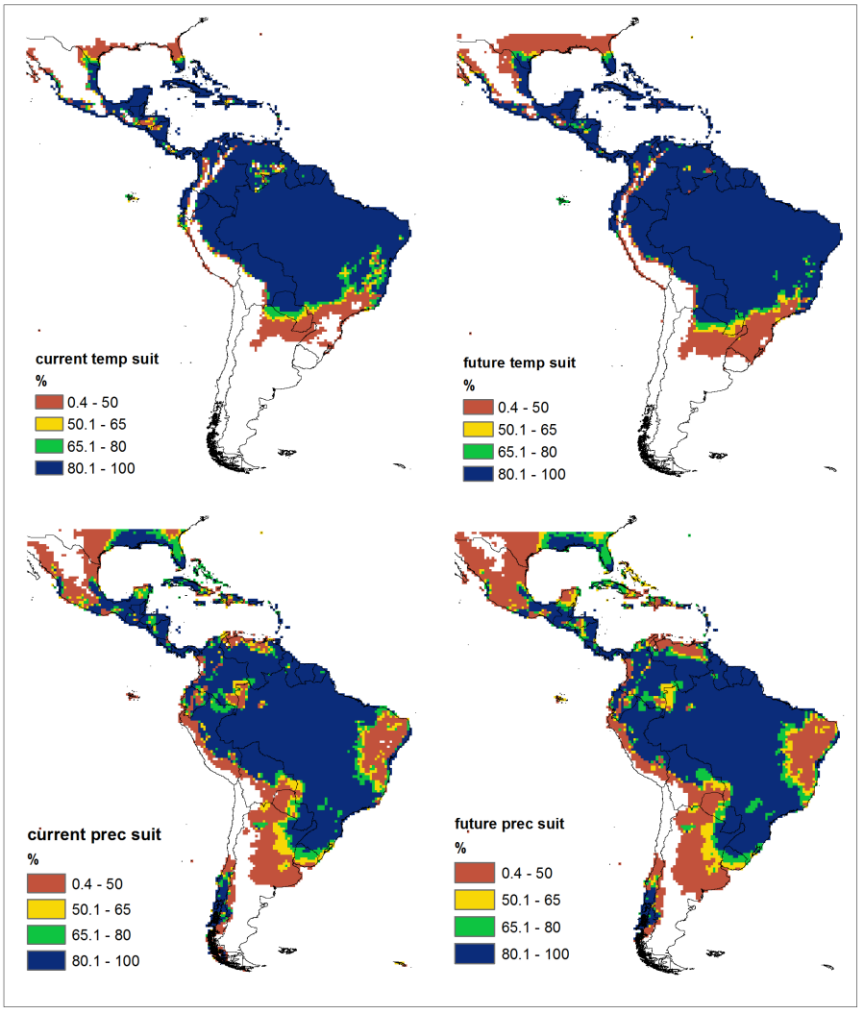

Figure A- 23. Temperature (above) and precipitation (below) suitability for current (left) and future (right) conditions for yam.

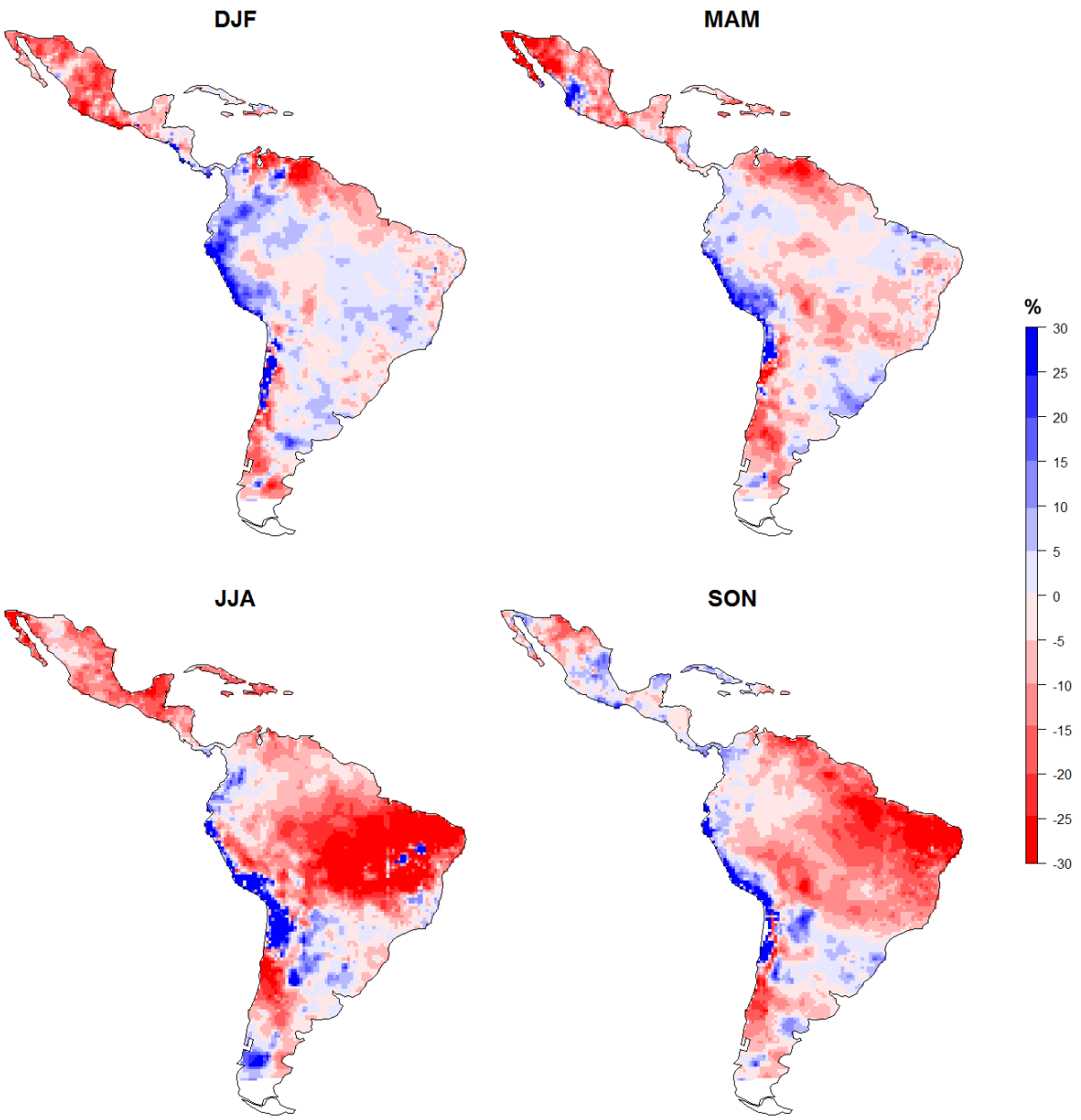

Figure A- 24. Changes in accumulated rainfall (multi-model mean) for four seasons, as follows, December-January-February (DJF), March-April-May (MAM), June-July-August (JJA), and September-October-November (SON).

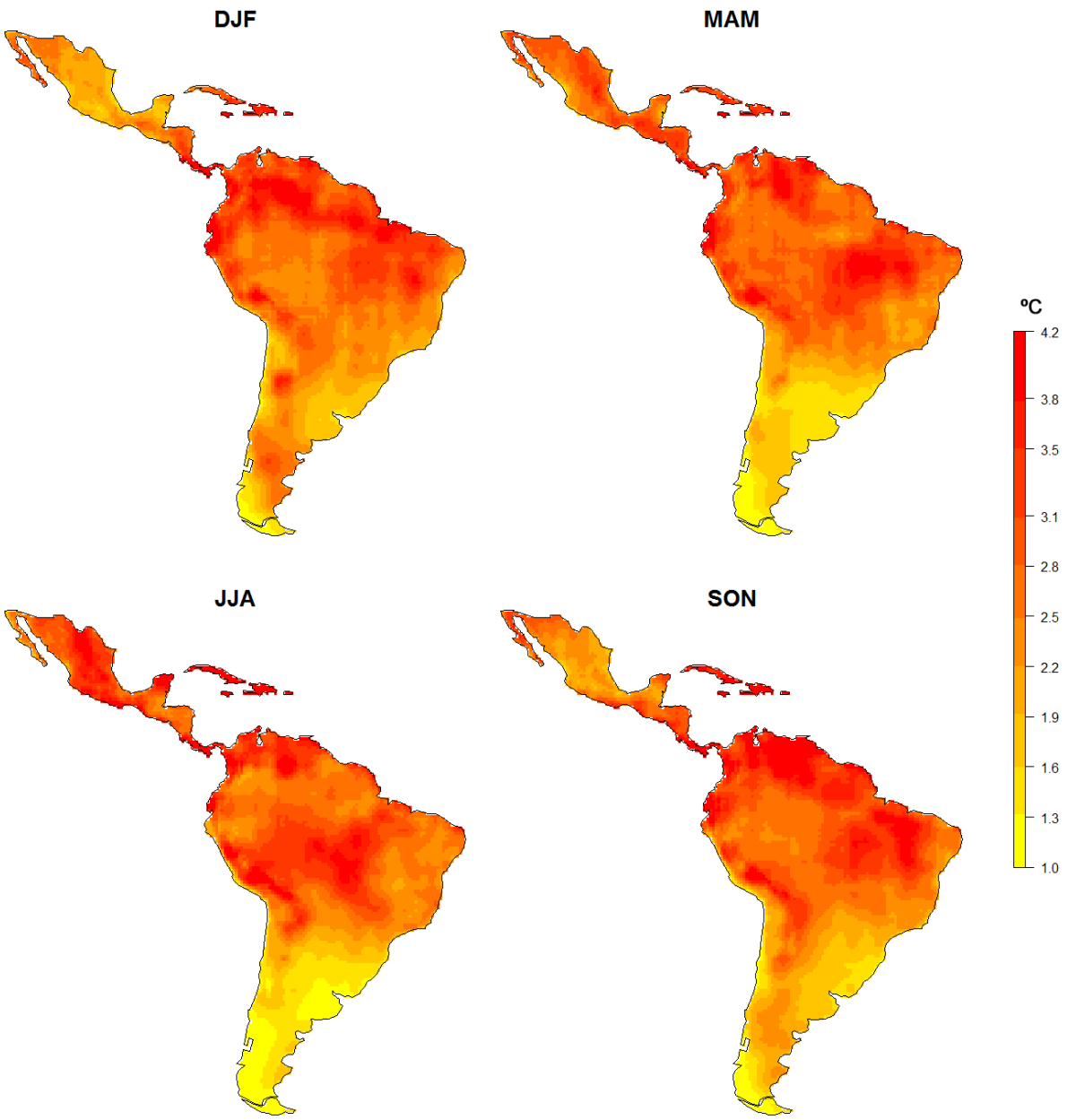

Figure A- 25. Changes in mean maximum temperature (multi-model mean) for four seasons, as follows, December-January-February (DJF), March-April-May (MAM), June-July-August (JJA), and September-October-November (SON).

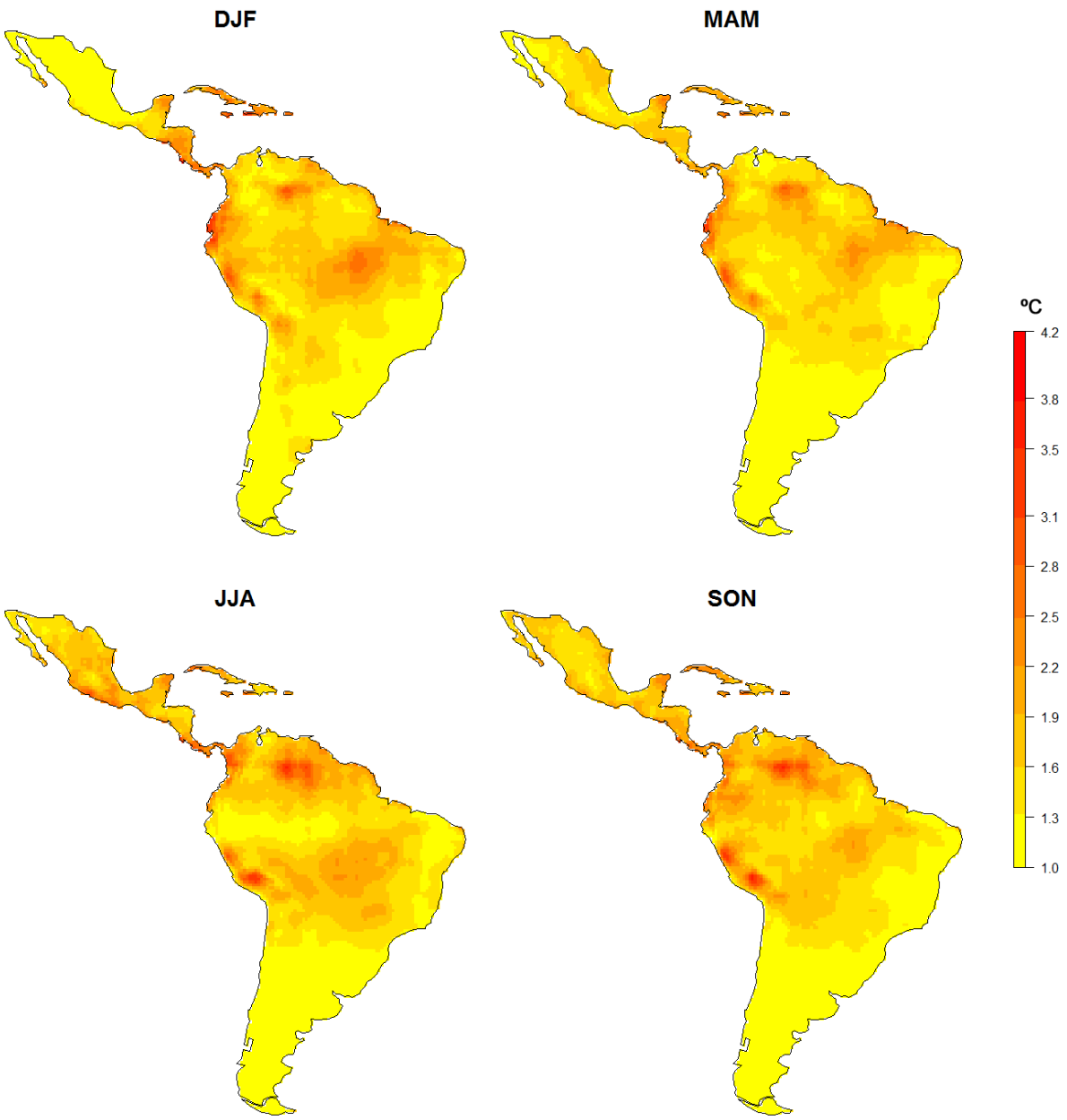

Figure A- 26. Changes in mean minimum temperature (multi-model mean) for four seasons, as follows, December-January-February (DJF), March-April-May (MAM), June-July-August (JJA), and September-October-November (SON).

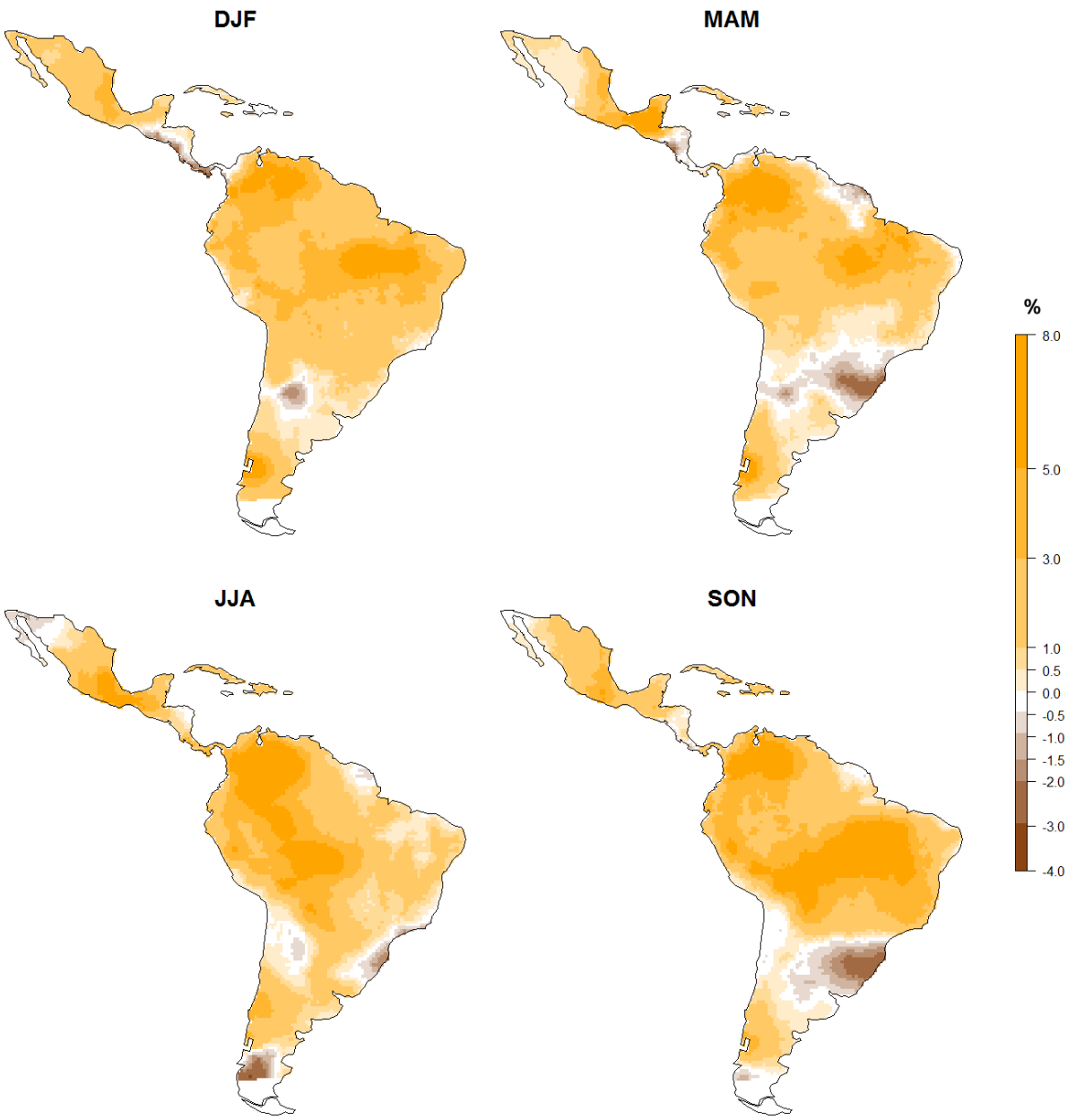

Figure A- 27. Changes in solar radiation (multi-model mean) for four seasons, as follows, December-January-February (DJF), March-April-May (MAM), June-July-August (JJA), and September-October-November (SON).